UNIVERSITY OF PIEMONTE ORIENTALE

“Department of Health Science”

Doctoral course in MEDICAL SCIENCES AND BIOTECHNOLOGY

Cycle XXXI

Three-dimensional oral mucosa models: development and applications

Candidate: Rita Sorrentino

Coordinator: Marisa Gariglio

Supervisor: Lia Rimondini

2019-2020

Index

Abstract

INTRODUCTION: Animal experimentation has been extensively and for a long time applied in several research fields, but since 2011 it has been substantially limited by the Commission of the European Parliament to ensure people/animals safety and reduce research costs. To respond to these directives, many attempts have been focused on the development and validation of new *in vitro* 3D systems, bypassing the traditional 2D cell cultures. In this regard, diverse approaches to tissue-engineered bone and oral mucosa have been developed. Despite the promising premises and the cutting-edge results, the used 3D *in vitro* bone-oral mucosal models still lack interaction between the mucosal and the bone components. Therefore, this project aimed to create 3D models, entirely made with primary human cells (keratinocytes, fibroblasts, and osteoblasts), able to mimic the natural structure and interaction of bone and oral mucosa. A direct future application will be the multi-tissue periodontal regeneration, needing synchronized restoration of the gingival and bone compartments, besides cementum and periodontal ligament.

EXPERIMENTAL METHODS: For the *in vitro* 3D oral mucosa assessment, a collagen-based lamina propria was enriched with a pool of primary human fibroblasts (HGF), freshly obtained from the normal gingiva of young healthy and informed consent donors, put into a culture insert and submerged into defined culture media. A pool of primary human oral keratinocytes (HOK) were seeded upon the gel. When keratinocytes reached confluence, they were grown at the air-liquid interface, stratifying in about two weeks. The oral mucosa model, obtained as above described, was used to evaluate the effect of two mesenchyme cell types, mesenchymal stem cells (hMSC) and osteoblast (hFOB) on keratinocytes stratification. Mesenchyme effect was assessed in 3 different set-ups: paracrine effect (conditioned media, CM), indirect co-culture (transwell system), and direct co-culture (hMSC embedded in the connective tissue substitute). Oral mucosae were, after that, histologically examined. The conditioned media from those experiments were used to growth murine nervous system cells (immortalized ND7/23 and primary dorsal root ganglia DRGs) and quantified the effect on axonal outgrowth.

Regarding the bone compartment, a bovine tendon collagen (BTC) and nano-hydroxyapatite (nHA) sponges developed by Salgado et al., (2015) was synthesized by lyophilization process. The sponge was subsequently implemented with a fibrin coating to increase the stiffness and mechanically characterized by the dynamic mechanical analysis machine. Primary human osteoblasts (hFOB) were integrated into the BTC/nHA sponge diluted directly in the fibrin gel. Oral mucosae, produced as above described, were air-lifted onto the repopulated bone substitute and co-cultivated for others 12 days to allow cell-interaction and keratinocytes stratification. This latter innovative model was histologically and mechanically characterized.

RESULTS AND DISCUSSION: the histological analysis showed an unexpected effect of osteogenically induced hMSC (hMSC-OB) onto keratinocyte stratification. Under the hMSC-OB stimulation, the ratio between the spinosum and the corneum strata resulted impaired due to the increase of the keratinization in treated 3D models. This impairment results correlated to a higher expression of the cytokeratin 10 (typical of keratinized epithelia) with a slight reduction of the cytokeratin 13 (typical on non-keratinized epithelia). These results suggest that hMSC and, in particular, one of their differentiated forms, the osteoblasts (hOB), play a crucial role in mucosal differentiation fate. The proteomic analysis revealed that during osteogenic differentiation, hMSCs increase the production and release of KGF, a factor which

induces keratinocytes proliferation and differentiation. The KGF production (amount increased to 208±36 pg/ml after 14 days of differentiation and to 347±15 pg/ml after 28 days of differentiation), confirmed in ELISA, may explain why, despite the increase in keratin production, most of the keratinocytes retain the nuclei producing a para-keratinized phenotype. At the same time, two 3D hMSC-OM co-cultures was developed. In the first one, hMSC and oral mucosae were kept in contact with a transwell porous system. The histological analysis of 3D culture shows that the crosstalk between oral mucosa and hMSCs improve the keratinocytes behaviour ensuring a complete stratification process. The differentiation analysis of co-cultured hMSC showed that, in the presence of osteogenic factors, oral mucosae halve the time required for hMSC differentiation. In the second model, hMSC were seeded with HGF within the collagen matrix used as *lamina propria* substitute. The histological analysis showed that hMSC speeded up the keratinocyte proliferation and stratification, obtaining the fully epithelium resembling the native one in only 7 days. Once again, the proliferative state induced by hMSCs resulted uncontrolled. Indeed, after another 1 week of direct co-culture, keratinocytes lose their organized structure. The obtained results were used to set-up a mucoperiosteal model composed of an engineered oral mucosa air-lifted and let stratified onto an osteoblast repopulated hard-sponge mimicking the bone counterpart. The mechanical evaluation of this model suggested that mesenchymal cells (hMSC and HGF) and epithelial cells collaborate to remodel the synthetic bone matrix. Moreover, the effect of those models on the nervous system was evaluated by calculating the axonal outgrowth of both immortalized neuronal cells and murine dorsal root ganglia (DRGs). Although the treaded models induce a slight increase of axonal elongation on immortalized neuronal cells, an adverse impact is registered on the ganglia of the back. These recent results suggest that oral mucosae produce pro-innervation factors (i.e., NGF observed by IF analysis) but also specific molecules that inhibit the migration/elongation of unsuitable axons. Finally, the obtained results were used to set-up an innervated mucoperiosteal model composed of an engineered oral mucosa enriched with ND7/23 let stratified at the air/liquid interface directly onto an osteoblast repopulated hard-sponge mimicking the bone counterpart enriched with ND7/23. In the innervated model, it is possible to observe several cells migrating within the bone counterpart; these cells were characterized by immunofluorescence analysis and, at the interface between bone and oral mucosa, several TBR1/β-tubulin type III positive cells identified as ND7/23. However, any axonal prolongations were found despite the presence of secreted NGF within the model.

CONCLUSION: In the present work, the regulatory role of the mesenchymal tissue onto epithelia was evaluated. The main results showed that that during the differentiation hMSC produce and secrete factors that induce the keratinization and the expression of the marker of differentiation CK10; in particular in the middle stage of differentiation (OB14). The proteomic analysis revealed that this effect can be ascribable to KGF secretion. This finding may impact the design of new implantable devices able to induce, alone, the epithelial growth and keratinization to improve implant graft avoiding epithelial graft linked to the morbidity of another zone. Moreover, we also showed that OM might have a pro-innervation effect, at least during the last stages of keratinocytes stratification. Finally, we characterized an innervated mucoperiosteal model that could open new in vitro frontiers for oral biomaterials validation as well as improve knowledge regarding the mesenchymal stem cells roles onto oral mucosa development.

Graphical Abstract

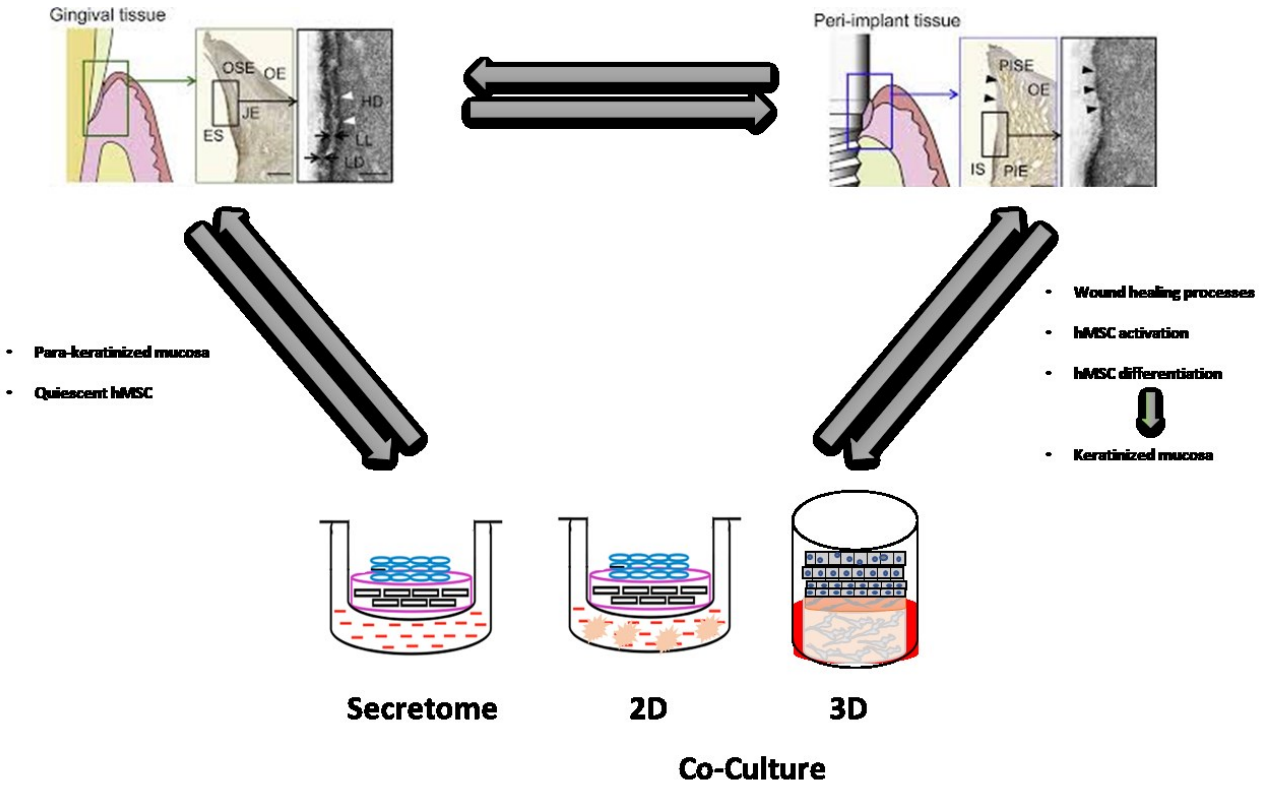

Figure 1 *Graphical Abstract. Assessment of stromal-epithelial crosstalk and mucoperiosteal development. JE: junctional epithelium, OSE: oral sulcular epithelium, OE: oral epithelium, PIE: peri-implant epithelium, PISE: peri-implant sulcular epithelium.*

Chapter 1

Background

I. Introduction

1.1. Tissue engineering (TE)

In 1993, Langer and Vacanti described the tissue engineering (TE) as "an interdisciplinary field that applies the principles of engineering and life sciences toward the development of biological substitutes that restore, maintain, or improve tissue function or a whole organ". This definition still well represents many TE applications and nowadays, even comprises the development of biological substitutes aimed to mimicking the tissue environment and function in vitro (as a tissue model) for being used in the cell biology and embryology fields as a tool to study the cell and tissue response to exterior influences (i.e., drugs, biomaterials, etc.) (Olson et al., 2011; Ikada et al., 2006)

Starting from this background, *in vitro* models have been recently developed to mimic not only the single tissue function but also the complexity of whole organs, including tissue interfaces (Atala et al., 2012). These multi-tissue models have been mainly proposed as tools for analysing the cells-cells interaction within a physiological microenvironment (Gothard et al., 2014) and the fundamental mechanisms involved in cell signaling during tissue repair.

These in vivo models represent valuable tools to speed-up the biocompatibility assessment of implantable materials by reducing the recourse to *in vivo* experimentation.

1.1.1. In vivo models for biocompatibility assessment of implants

The term "*in vivo*" is referred to all the experiments conducted in living organisms. Currently, they still represent a necessary tool to evaluate both the safety and the efficacy issues of new drugs or implantable devices. Indeed, despite several drawbacks mainly related to *i)* ethical dilemmas, *ii)* model handlings complexity, *iii*) long experiments duration, *iv*) limited accessibility, *v*) expensive management of animal facilities and *vi*) inflexible limiting laws (Knight et al., 2011) *in vivo* models use remain irreplaceable.

1.1.1.1. Legislature

In 2015, nine European countries presented a petition to the European Commission (EC) to ban the use of animals in research. The EC reject the petition but stated that ethical justification and adoption of protocol which follow the 3Rs (Replacement, Reduction, and Refinement) must be approved before proceed with each experimental studies (http://ec.europa.eu/environment/chemicals/lab_animals/pdf/vivisection/en.pdf*),* not only for ethical purposes but also because the use of healthy animals growth in adequate animal facility (accordingly to actual European directive and 2Rs statements) allow the production of more robust and reliable results, underlying valid scientific outputs (Hurst

and West, 2010; Singhal et al., 2014). Globally, legislation differs between countries and geographical regions, but in general, the well-being of the animal used in research is protected.

The 3Rs concept was first developed by Russell and Burch (1959) and has become rooted in legislation and guidelines concerning animal experimentation in many Countries (fig. I-1). The 3 Rs stay for "**Replacement**" which stated that, when applicable, alternative methods must be applied to avoid or reduce animal use in research, "**Reduction**" which encourage the use of strategies that enable the obtainment of reliable data starting from as few animals as possible, or, at least, to obtain more information from the same number of animals and "**Refinement**" which impose the use of methods that alleviate or minimize potential pain, suffering or distress, and enhance animal welfare for the animals used.

The directive 2010/63/EU follow the 3D principles and states that "every project proposal in EU member states involving procedures on living non-human vertebrates and cephalopods has to be approved in a review process, including a harm-benefit-analysis (HBA), to assess whether the harm to the animals in terms of suffering, pain, and distress is justified by the expected outcome taking into account ethical consideration and may ultimately benefit human beings, animals or the environment"(Eggel et al., 2018).

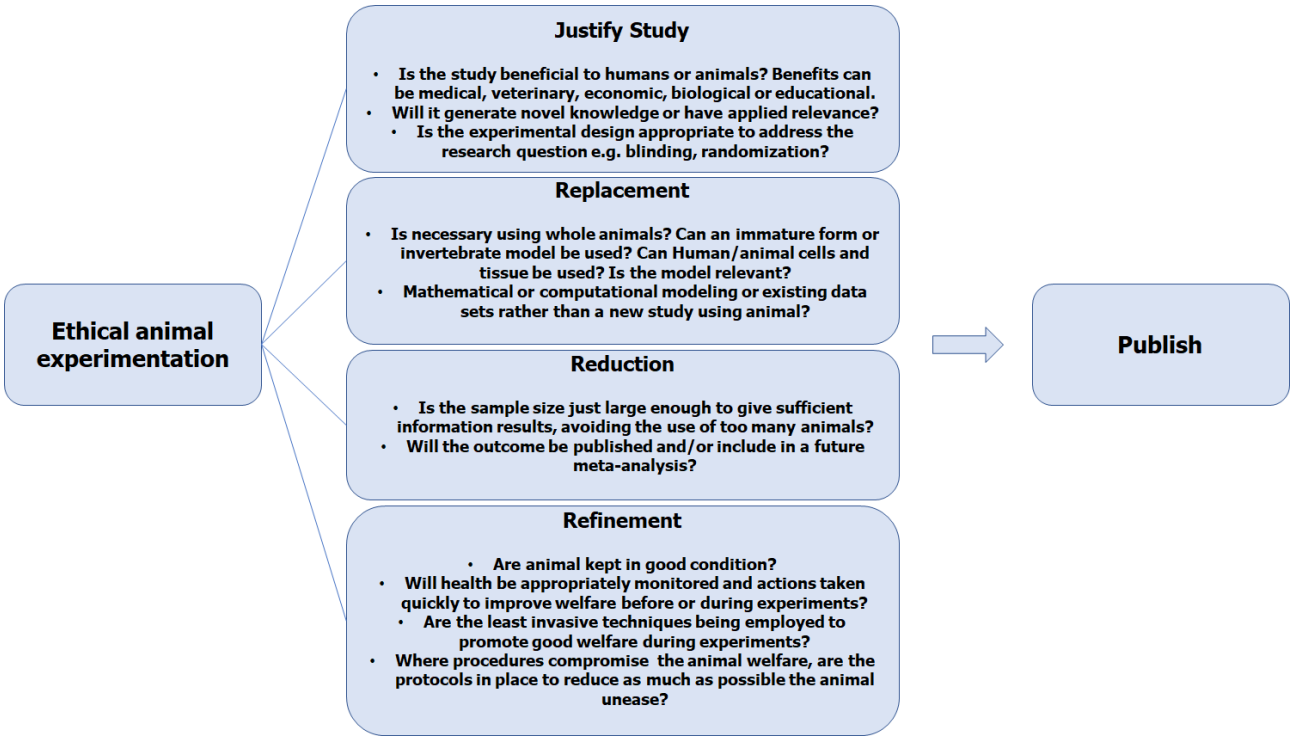

Figure I-1 *Graphical representation of the significant ethical concepts and key questions that scientists must address under the traditional view of the 3Rs – Replacement, Reduction, and Refinement – to justify the use of animals in experimentation, from planning the program of work through to publication. (http://jeb.biologists.org/content/220/17/3007#ref-85)*

1.1.1.1.1. Reduction

'Reduction' requires the limitation in the number of animals used for experimentation in "just enough data and no more". The better strategies to overcome this limitation involve the improvement of the experimental design and the precision of measurement as well as the addition of reliable concomitant measurements (that can be used as internal control) to reduce the variability in the pilot studies (i.e., sex or age). At the same time, it is essential to include, for each experimentation, adequate control groups and to choose the correct animal model (i.e. use aged animal if in the investigation must be considered the senescence) to obtain reliable translational results (McClelland et al., 2000; Eng et al., 2003; de Boo and Hendriksen, 2005). Moreover, the guidelines state that the calculation of statistical power should be included to optimize the sample size.

1.1.1.1.2. Refinement

Refinement is an "integral component of improving laboratory animal welfare, which is vital for healthy biological functioning and a normal behaviour repertoire". This part allows more reliable results since the scarce animal condition can interfere with the measurement. However, for most species, the adequate tools or protocols to assess their health and welfare (i.e., pain assessment is highly developed for mammals compared with other animal groups) were upgraded only in the last few years (Sneddon et al., 2014; Sneddon, 2015). The EC Directive (2010; http://eur-lex.europa.eu/legal-content/EN/TXT/?uri=CELEX:32010L0063) proposes that "all protected animals should have enriched environments in which to live". Indeed, an adequate environment, improve with social housing and apparatus to allow exercise or sensory stimulation reduce the stress in animals reducing the effect of this factor on the experiment outcomes (Singhal et al., 2014).

The term "refinements" is also referred on the experimental procedures; handle animals with proper procedure reduce the stress related to invasive procedures. For instance, to minimize mice anxiety is suggested to avoid collection them by their tail. In general, when applicable, it is recommended the use of painkillers after surgery and non-invasive imaging techniques to collect data (O'Farrell et al., 2013).

1.1.1.1.3. Replacement

According to several regulatory organs, the youngest forms of many species do not suffer. For instance, the UK Animals (Scientific Procedures) Act 1986 (https://www.gov.uk/government/publications/consolidated-version-of-aspa-1986) and European Directive 2010/63/EU (http://eur-lex.europa.eu/legal-content/EN/TXT/?uri=CELEX:32010L0063) allow the use of fish until they acquire the capability of independent feeding and allows the use of embryos (i.e., from chickens) (Tazawa et al., 2002). However, this approach is not valid in several research fields and in particular, it is not valid for biomaterials studies. Due to EU's decision to ban animal testing for cosmetics (EU1223/2009) and the restriction in animal use occurs after 2015, several in vitro models platform including 3D cell cultures have been developed to bridge conventional 2D tissue cultures and animal experimentation Those platforms are often aimed to identify potentially dangerous chemicals and recently, extensive research has gone into *i)* mammalian tissue studies, used to develop *ex vivo* tissue techniques such as the precision-cut tissue slice (Fisher RL and Vickers AE, 2013) and *ii*) stem cell-

derived organoid 3D cultures to improve the translational potency of the studies (Liu et al., 2016; Muthuswamy, 2017). A precision-cut tissue slice is a technique in which an organ, or a part of it, is sectioned in identical portions (usually 0,3 mm thick) and kept in cultures for a limited time. These latter represent an *in vitro* model able to closely mimics the organ complexity since the "slice" maintain the structural and functional features of the whole organ while organoids are *in vitro* derived 3D cell aggregates with organ functionality which offer a comparable structure to primary tissue and a stable system for prolonged cultivation, and that can be easily cryopreserved.

One of the main advantages of 3D cultures is to facilitate the adherence to the 3Rs ethical concepts.

1.1.1.1.3.1. In vitro models – 2-Dimensional vs 3-Dimensional

The term *in vitro* refers to experiments carried out on segments derived from living organisms and cultivated on external support. *In vitro* models are mainly divided in 2 categories, the models growth in 2-"dimension"-D (length and width) that are represented by isolated cells growth as monolayer on synthetic supports (such as coated tissue culture plastic, TCP) and 3-"dimension"-D (length, width, and thickness) that can be referred both to the same cells grown as a multi-layered system on or within heterogenic supports or to tissue sections ex-vivo cultivation (Duval et al., 2017).

Two-dimensional culture techniques have been one of the foremost breakthroughs in the biomedical field. They've been represented, since the early '900, the possibility to carry out experiments with living biological specimens in highly standardized and controlled conditions (Vanderburgh et al., 2017). However, there are several differences between monolayered cells and the natural tissues, and they include tissue-specific substrate stiffness, the spatial cues (such as cell-matrix and cell-cell interaction or receptor topography), and, consequently, the concentration gradients of nutrients, secreted factors and gas (i.e., oxygen). Since the early '90, several researchers focused on the mechanical stimulation of different cell types, and, nowadays, it is well-known that the mechanical stimulus has the same importance of chemical stimuli. Accordingly, the substrate stiffness has a significant effect on cell behaviours such as differentiation and migration process, and substrate morphology severely affects cell appearance via cytoskeleton regulation (Pedersen et al, 2005).

Moreover, the presence of the ECM influences the gene expression; for instance, Mishra et al. (2012) compared metalloproteinase (MMPs) expression in 2D and 3D culture and showed a low or absent expression of some MMPs, indispensable marker for evaluating the pro-metastatic capability of cancer cells, in monolayer condition. Finally, the absence of the third dimension imposes several changes in cellular morphology and receptors topography, and this induces several complications in translate dose/response curve in more complex models (Bradbury et al., 2012).

To overcome these limitations, several 3D models have been developed. Indeed, 3D models have the potential to overcome not only 2D cultures unable to mimic the physiological tissue behaviour but also some animal models because of the lower financial disbursement. The main advantages and disadvantages of 2D and 3D models are summarized in table I-1.

As previously described, the organ complexity influences the difficultness in obtaining reproducible and affordable models. The modern methods in the production of functional tissue and/or organ models entail a multi-disciplinary approach in which engineering, chemical, physical, mathematics, biological, and physiological knowledge are exploited in a trial-and-error tactic (Sharifikia et al., 2017). The development of biological 3D multi-tissue models, intended to mimic physiological tissues, is a complex but promising way to improve the power of biological studies. With these models, the understanding and prediction of human organ response to external stimuli (i.e., xenobiotic molecules roles, mechanical stress, paracrine cross-talk, biomaterials compatibility, drugs safety, etc.) or the cytofunctionality analysis [i.e., the study of the *de novo* production of extracellular matrix (ECM)] could be assessed in a physiological context. This study approach can provide reliable information on cell interaction useful in implant substrate design.

This methodology has so far become a pivotal tool for evaluating necessary processes such as matrix remodelling, cell crosstalk, growth factor secretion, gene expression, regulation, etc. of human cells in their microenvironment. Moreover, as previously described, these models represent a high 3Rs-friendly approach by reducing the use of small animal models (and by lowering the animal-related cost for researchers).

Table I-1 *Principal differences between 2D and 3D cultures*

2D Cell Culture Systems		3D Cell Culture Systems	
Advantages	Disadvantages	Advantages	Issue and Future Prospective
Low-cost	The absence of real cell environments	More relevant cell models	Throughput (the initial study is more expensive and time-consuming; however, results are trustable)
Well established	Lack of predictivity (with increasing cost and failure rate of further studies)	Direct interaction between different types of cells (organotypic models)	Guarantee the right oxygenation to the inner part of the model
A lot of comparative literature	False results caused by the growth media and expansion of cells	Presence of connective/stromal tissue or barrier tissues	Standardize protocols
Easier cell observation and measurement		Better simulation of conditions in a living organism	Increase the complexity
		Reduces the use of animal models	
		Represent a more realistic way to grow and treat cancer cells	

The general approach to design engineering materials is peculiar when the main goal is to obtain implantable tissue instead of tissue models. Implantable tissue required to be safe, fully biomimetic and biocompatible, and the ideal mechanical properties and morphology of the implanted scaffold are studied to guarantee the first phases of the graft and ensure the host tissue migration within both acellular and repopulated implant. On the contrary, tissue models need to resemble, as close as possible, all the features of the mimicked tissue.

Indeed, it is expected that healthy resident cells can invade the free space of the scaffold and interact with implant structure and resident cells to secrete new ECM proteins and structures to re-activate the biological function of the tissue (Antoni et al., 2015). On the contrary, tissue models are designed to mimic, *ex vivo*, all the features and the three-dimensional topography of the single (histotypic model) or the composite (organotypic model) tissue of interest.

When histotypic and organotypic models are considered, the priority is to obtain an easy-handling model suitable for a wide range of tests. These models are mainly developed as platforms for evaluating different biological responses to external stimuli, such as microbial infections, drugs, materials application, or mechanical stress. Above all, these models are addressed to give information regarding gene regulation and expression, macromolecules or vesicles secretion, receptor polarity, and tissue morphology changes in response to certain stimuli. To reach the targets, histotypic and organotypic models must be realized with highly standardized and reproducible protocols and with fully characterized cells (Antoni et al., 2015). This enables to easily and separately identify each variable or cell components offering a considerable advantage in comparison with animal models, where the contributions of some tissue type or cells are often overlapped and hidden by other biological parts.

Besides, another essential advantage of 3D models in comparison with *in vivo* models is found in the study cost, as shown in table I-2.

In both 3D and in vivo models, a key role is played by connective tissue. Indeed, in both pathological and healthy condition, the connective tissue support and regulate the behaviour of all the other tissues. For instance, in tumours, the surrounding fibroblast (nowadays known as tumour-associated fibroblast, TAF) interacts and regulates cancer behaviour. In healthy condition, the connective tissue secretes crucial molecules which regulate and drive the fate of other cells such as the ones which form the lining epithelia. Thus, several studies have been focused on elucidating the interaction between the connective or stromal tissue and the covering epithelia, and in reproducing this interaction in refined 3D models. To pursue this research term, several types of 3D cell culture techniques have been designed to replicate lining epithelia such as gastric epithelium, alveolar epithelium, corneal, skin, or oral mucosa.

Pluristratified squamous epithelia may be resembled by using tissue-specific basal-like keratinocytes on natural or synthetic connective tissue substitutes repopulated by tissue-specific fibroblasts. In this case, keratinocytes stratify at the air-liquid interface, retaining the specific epithelial belongings. Among them, one of the most engineered specialized tissues is the keratinized pluristratified squamous epithelium of the oral cavity (Gibbs et al., 2000).

Table I-2 *Toxicity test costs, in animals and in vitro, as reported by Human Society International (http://www.hsi.org/issues/chemical_product_testing/facts/time_and_cost.html)*

TYPE OF TOXICITY	TEST TYPE	STUDY COST ($ US)
GENE TOXICITY		
CHROMOSOME ABERRATION	*In Vivo*	30000
	In Vitro	20000
SISTER CHROMATID EXCHANGE	*In Vivo*	22000
	In Vitro	8000
UNSCHEDULED DNA SYNTHESIS	*In Vivo*	32000
	In Vitro	11000
EYE IRRITATION/CORROSION		
DRAIZE RABBIT EYE TEST	*In Vivo*	1800
BOVINE CORNEAL OPACITY	*In Vitro*	1400
SKIN CORROSION		
DRAIZE RABBIT SKIN TEST	*In Vivo*	1800
EPIDERM™	*In Vitro*	1600
CORROSITEX®	*In Vitro*	500

1.1.1.2. Animal models for oral implantology: An overview

In the last three decades, several researchers have been focused on their osteointegration and soft tissue integration study of dental implants using several animal models.

Literature reports several papers focused on histological responses to implants in primates (forbidden in Europe) or in dogs with all expected related ethical concerns since no life-saver devices are involved.

Rodents (mice, rats, and rabbits), ovine, and swine have been also used with less restriction; choosing the appropriate animal model for each experimentation allows the production of reliable and reproducible data.

The mouse is the most used animal model in research, and, through the years, several syngeneic and transgenic strains have been established to meet experimental protocols requirements. **Mice** are moderately inexpensive, easy to handle and reproduce quickly in laboratory settings. The mouse genome has high homology with human one and can be easily modified to mimic human disease, included bone defects and age-related disease. However, mice models are not often used to test oral implantable materials or devices mainly because of their reduced size, which requires to scaled-down the devices (Rahal et al., 2000; Beppu et al., 2011) and makes the surgical procedures almost tricky.

Rats, in particular, Wistar and Sprague-Dawley strain, have been extensively used in the implantology field. Wistar rats are variants of the congenital albino rat, whereas Sprague-Dawley rats are of an outbred origin. Due to their bigger size, male rats are more often used than females, and as for mice, extra-oral bones are preferred for dental

material implantation. Some authors, such as Haga et al. (2009), preferred to use mini implants for teeth replacement and evaluating the maxillary bone formation and maturation processes around implants. Following similar strategies, Rinaldi and Arana-Chavez (2010) were able to examine implants in contact with the periodontal ligament of adjacent teeth in the mandible while Hou et al. (2009) shown that the mechanical force of oral environment improves titanium integration. Torricelli et al. (2002) suggested the use of aged rats, instead of young rats, for bone implants evaluation since they showed a reduction in bone formation in aged rats. In the same work, the authors suggest the use of a demineralized bone matrix to improve bone healing and re-mineralization in osteoporotic condition. Genetically-modified rat strains or diseased animals have also been used to mimic human diseases such as diabetes (Biobreeding diabetes-prone rats) or hypertension (Zucker rat); for instance, Hasegawa et al. (2008) showed that the osteointegration and bone volume are reduced in diabetic mice in comparison with non-diabetic rats. Similarly, ovariectomized rats were used to assess the effect of implanted materials onto osteopenic bones. In 2002, Fini et al. compared the osteointegration of titanium (Ti6AI4V) implants in ovariectomized and sham-aged rats and sheep. In their experiments, the author demonstrated that the titanium implants were less osteointegrated in both trabecular and cortical osteopenic bone in comparison with those in normal bone; the authors also observed a decrease of bone microhardness in both trabecular and cortical bone, but this decrease resulted widespread in the osteopenic bone suggesting implant-associated delay in both bone formation and maturation.

Despite the positive results, the bone structure of rodents is poorly representative of human ones and lacks Haversian-type remodelling. Due to this factor, data obtained by those models are not always confirmed in pre-clinical or human models (Li et al., 2015).

Rabbit is one of the most used models in musculoskeletal studies. It is often used in implant dentistry (Neyt et al., 1998) mainly because its knees are large enough to host dental implants designed for humans.

Rabbit has faster bone turnover than human with significant intracortical Haversian remodelling, which corresponds to a quicker osteointegration and to a reduction of time requires for the experimentation (Pearce et al., 2007). For this reason, it is considered as a pre-translational animal model useful to screen new oral implant technologies.

Among all rabbit strains, the New Zealand White with a bodyweight between 2 and 5 kg is the most (Vidigal et al., 2009).

Nowadays, one of the elective models for implant dentistry is represented by **sheep** and/or **goat** since their bone dimension is comparable with the human one despite the higher bone density (around 2-fold) (Rasmusson et al., 1999). Domestic sheep are easy-handling animals that are widely used to study numerous musculoskeletal pathologic conditions or to test different kinds of implants. The use of adult sheep is strongly suggested since the complete bone maturation occurs a long time after puberty (average age: nine months within different breed). The sheep trabecular bone well resembles the human one while the cortical bone presents slight differences in the bone mineral composition and Haversian canals content, lower in sheep than in humans (Ravaglioli et al.,1996; Aerssens et al., 1998). Although, the sheep bone healing and a bone remodeling rate are comparable with that of humans (Pastoureau et al., 1989; Chavassieux et al., 1991; Turner et al., 1993). The critical size defect (CSD) for long sheep bone conventionally corresponds to a 40 mm long segmental defects (Gugala et al., 1999). Moreover, ovariectomized and Vitamin D deficient

sheep under hormone treatments are a suitable model for osteoporosis (Dvorak et al. 2011). Due to those features, sheep is a standard model in the implantology field even if more expensive and time-consuming (the healing and recovering time is higher) then rodents.

Swine is often used for translational purposes in pharmaceutical research. However, for the dental implantology field have been created specific "mini-pig" since the domestic adult one (suitable for dental implants) are too complicated to handle (difficulties in housing because of size and in surgically widening oral tissues) (Pearce et al., 2007). Different strains of mini-pig were developed since the sixties: Yucatan (in its two forms of minipig and micropig), Hanford, Sinclair Hormel (also called Minnesota), Pitman-Moore, Kangaroo Island, Ohmini, Lee Sung, Morini, and Göttingen. Despite small differences in plaque formation and bone structures between minipig strains and in comparison, with human, minipig bone is considered one of the most representative of human bone in terms of bone remodelling processes, density and mineralization (Mosekilde et al., 1987 and 1993; Aerssens et al., 1998; Ma et al., 2009).

Animal model studies enabled a considerable improvement in several research fields. However, the time and financial disbursement required for experimentation with adult and/or diseased animals are higher in comparison with 3D models, and also the reliability for getting reliable results is not 100% (Shanks et al.; 2009). Moreover, these models require highly specialized personnel to be correctly used, and besides, they are subjected to ethical issues and the strict control of national and international regulatory authorities. The regulation regarding *in vivo* model is described in paragraph 1.1.1

1.2. Oral Cavity

1.2.1. Anatomy

The oral cavity is the first segment of the digestive system, bounded externally by the lips and internally by the pharynges. It is formed by different structures composed of hard and soft tissue. The first and outer portion of the oral cavity, named vestibule or *vestibulum oris*, includes the lips and the cheek externally while the inner part is formed by gums and teeth (fig. I-2).

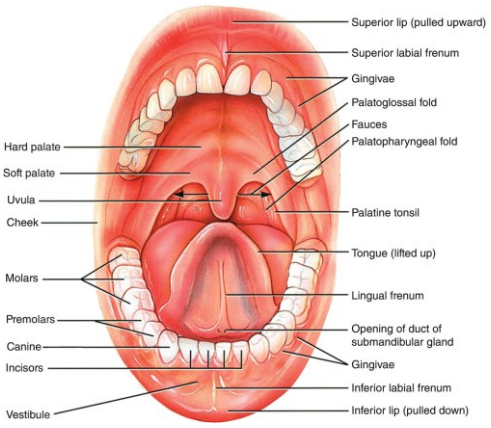

Figure I- 2 *Diagram illustrating the anatomy and central structures of the oral cavity (https://pocketdentistry.com/1-oral-structures-and-tissues/*

The lips, or *vermilion* zone, are lined by a thin keratinized layer balanced out by a prominent *stratum lucidum* and its basal layer results full of melanocytes. The upper lips are innervated by the maxillary (V2) and the mandibular (V3) branches of the trigeminal nerve (V) and the infraorbital branch of the V2 while the lower lips are innervated by V2, V3 and the mental nerve branch of V3, the latter also innerve the oral mucosa (Sadrameli and Mupparapu, 2018).

The teeth are composed of a crown that projects into the mouth, and roots which are connected with the alveolar bone by a flexible but reliable joint called periodontal ligaments. The enamel and the dentin compose the hard and external part of the teeth. In contrast, the soft and inner part, the pulp, is mainly composed of stromal connective tissue supplied by nerve, lymphatics vessel, and blood capillaries. The dental pulp contains fibroblasts (PF) and oral mesenchymal stem cells (O-MSCs) (fig. I-3).

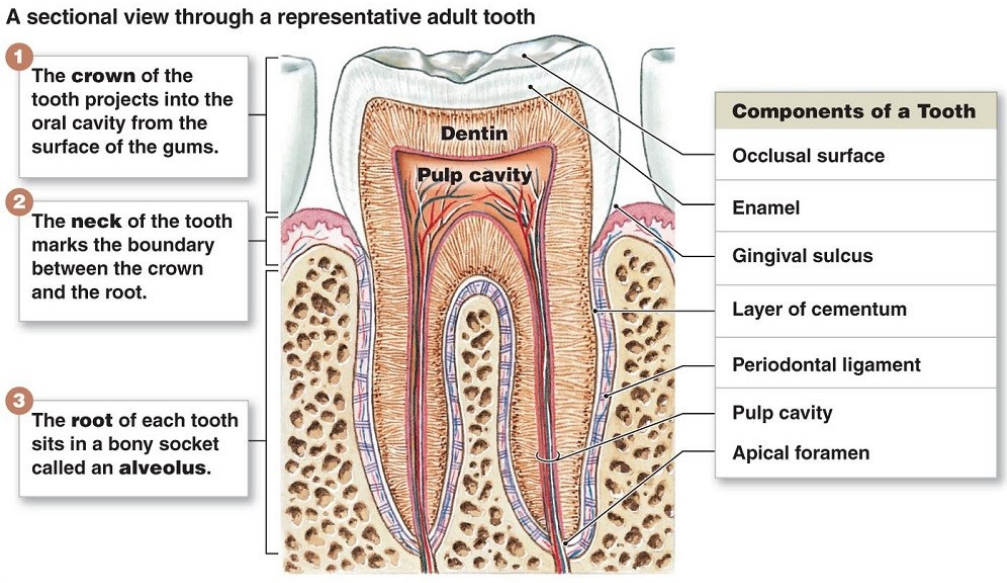

Figure I-3 *Diagram illustrating the anatomy of the tooth and the and foremost function of its components (https://www.printablediagram.com/diagrams-of-teeth-printable/diagram-of-teeth-anatomy/)*

The teeth are surrounded by gingival tissue, which is the only clinically visible component of the periodontium inside the mouth. Gingiva covers, as well, the alveolar bone and other inner structures, and it's firmly attached to them.

The gingival margin has a scalloped-like course across the dentition due to interdental papillae that fill the interdental spaces beneath the tooth contacts. Moreover, the gingiva is histologically divided into two portions:

- The free gingiva, which is characterized by two non-keratinized epithelia in its inner part, known as sulcular epithelium (in the free part) and the junctional epithelium (in direct contact with the teeth). The sulcular epithelium forms the wall of the sulcus and, together with the junctional epithelium, form the dento-gingival junction. The junctional epithelium has two basal lamina, the internal one that faces the tooth and the external one that meets connective tissue; due to this characteristic, it results in the most permeable epithelium and the *lamina propria* underlying the junctional epithelium is characterized by a chronic inflammatory state derived by the filtration of several microbial antigens. On the contrary, the outer surface which is mainly keratinized.

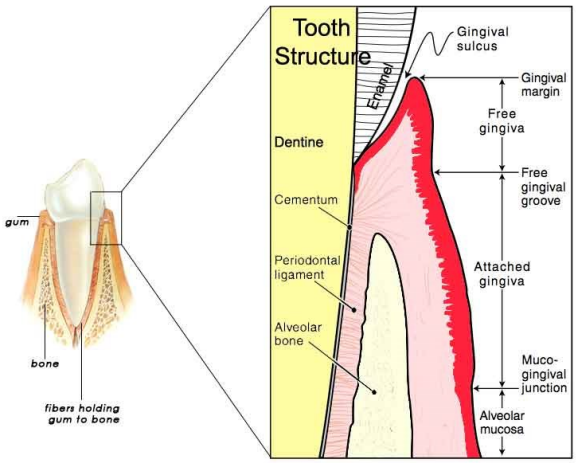

Figure I-4 *Structures of gingival tissues. https://sites.google.com/site/dentalhygieneportfoliofelicia/home)*

- The attached gingiva, which is covered by a keratinized epithelium and extends apically from the free gingiva towards the alveolar mucosa. The latter is defined "attached" because it is firmly adherent to the alveolar bone and in case of bone fenestration to the root cementum.

(Hall and Lundergan, 1993; Garnick and Ringle, 1988).

The *lamina propria* of both free and attached gingiva is rich in nerve, blood, and lymphatic vessels and resident innate immune system cells. Gingival tissues structures are summarised in figure I-4

The second and inner part of the mouth, known as the oral cavity proper, start with the alveolar process of the mandibular and maxillary bone, where teeth are located fixed and enclosed by the periodontium, covered by a soft tissue called mucosa. In the superior zone, the hard and soft palate separates the oral cavity by the nasal cavity while the lower part of the oral cavity is filled by the tongue and the floor of the mouth.

The hard palate is composed of the upper mouth bones lined by a keratinized epithelium while the soft palate is located behind the hard palate and doesn't contain bone but is mainly composed of muscle lined by a non-keratinized epithelium and is innervated by the V3 and the vagus nerve.

The tongue surface is covered by 4 types of lingual papillae named circumvallate, foliate, filiform, and fungiform positioned in different parts of the tongue and assign to taste different savours. Fifth cranial nerve supplies general sensory innervation (not the gustative one) to the anterior 2/3 of the tongue. Finally, the flour of the mouth borders the lower limit of the oral cavity and connect, with the lingual frenum, the gingival tissue with the tongue.

1.2.2. Oral mucosa

The oral mucosa is the linin organ of the oral cavity; from a histological point of view, it shares several characteristics with the skin, the dry lining organ of the human body, and other covering membranes such as the oesophagus. Structurally, both skin and lining membranes are composed of two interconnected tissue: a connective tissue covered by a lining epithelium, mostly a squamous pluristratified epithelium. These two components are strictly interconnected with the epithelial cells that infiltrate within the connective tissue forming the *rete ridge.* The lining epithelia and the connective tissue are attached by a thin but complex structure known as basement membrane.

The principal function of the oral mucosa is to protect the surrounded tissue and glands against external stimuli such as microbial pathogens as well as resident bacteria to avoid the infection and consequent damage of underlying tissue. Physiologically, the oral cavity is daily subject to different mechanical stimuli, such as compression, stretching, and shearing force, towards which the oral mucosa developed a high withstand.

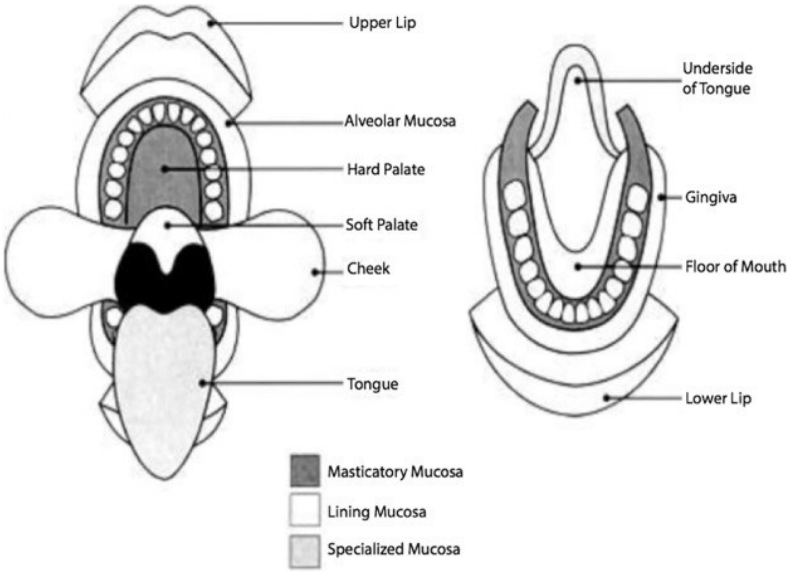

Figure I-5 *Anatomic location of masticatory mucosa (deep gray), lining mucosa (white), and specialized mucosa (light gray). (Squier and Brogden, Human Oral Mucosa: Development, structure and function, 2011)*

As above mentioned, the oral mucosa can be distinguished in three different types of stratified squamous epithelia underlined by a connective tissue named *lamina propria*, accordingly to their structures and function. The lining mucosa is the most broaden type of the oral mucosa and covers the lips, the cheeks, the soft palate, and the floor of the mouth. On the contrary, the specialized mucosa which coats the tongue and the masticatory mucosa that include the hard palate and the gingiva covers less than the 40% or the total area (fig. I-5).

The oral mucosa and the skin shared several features. However, albeit they are composed of the same type of cells, mainly keratinocytes and fibroblast, skin and mucosal membranes are considerably different between each other. The first and microscopical difference notable is the colour. Indeed, the coloration depends on several factors, such as the thickness of the epithelium, the degree of keratinization, the dilatation of underlining capillary, and the quantity of melanin pigment. Moreover, accordingly to the anatomic position, also the structure present in the connective tissue diverges. The connective tissue of the skin, named dermis, contains numerous hair follicles and sweat and sebaceous glands, while the *lamina propria* contains mainly salivary glands that release the salivary trough the duct and within the oral cavity. Within the membranes, the differences depend primarily on their firmness; the masticatory mucosa is a fixed and immobile structure while the lining mucosa is softer and bendable. This difference has an essential application in clinical applications; indeed, injections are easy in loose structures such as the one of lining mucosa, so it is preferable to choose the last one for injecting drugs such as local anaesthetic. This characteristic makes the lining mucosa less

sensible to the inflammation process since the inflammatory fluid can be easily resorbed while in the masticatory mucosa, the provoke pain and swallowing. However, the firm masticatory mucosa is most suitable for biopsy since the lining mucosa requires suturing when surgically incise while masticatory mucosa may not.

Finally, differently by other body structures, oral mucosa misses the musculature structure that bounded the mucosa by underlying tissue. To separate the mucosa lining cheek, lips and a part of the hard palate from the underlying bone or muscle there is a loose stromal tissue full of glands and fat named submucosa while the oral mucosa covering the gingiva and the more significant part of the hard palate are directly attached to the bone. This latter arrangement is called mucoperiosteum and provide a stable and rigid attachment (fig. I-6).

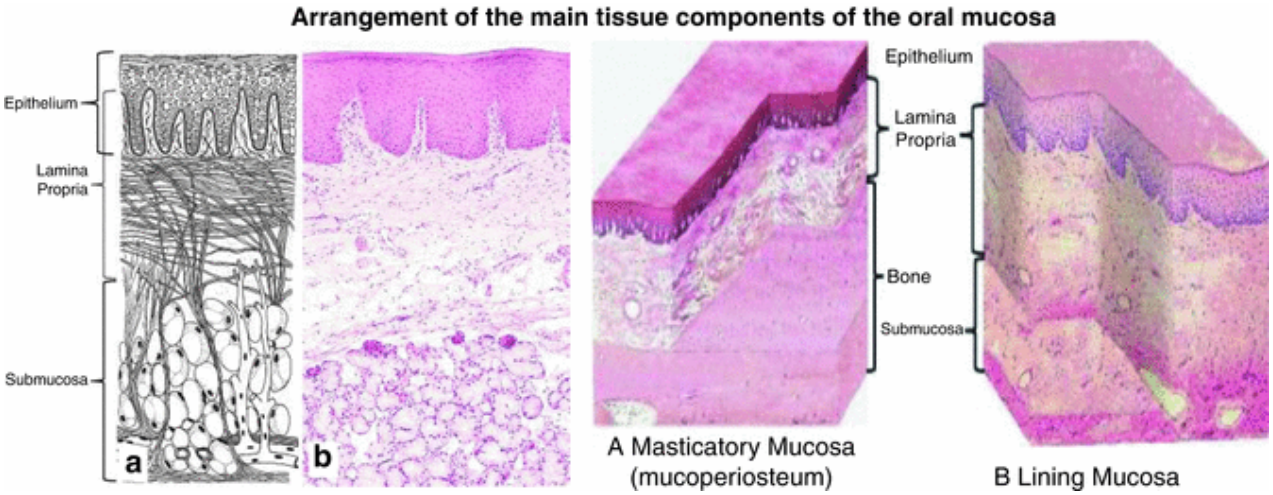

Figure I-6 *Arrangement of the leading tissue components of the oral mucosa. (Squier and Brogden, Human Oral Mucosa: Development, structure and function, 2011)*

1.2.2.1. Oral epithelium

Oral epithelium is a covering and lining epithelium composed of different squamous pluristratified epithelia consisting of cells tightly attached to each other and to the basement membrane which are well organized in distinct layers. Each layer, or stratum, is easily recognized in cross-sectional histological analysis and have a specific role. The main histological difference between the epithelia is the keratinization degree.

Epithelia are classified in keratinized and non-keratinized epithelium; the first is characteristic of the masticatory and the second of the lining mucosa (fig. I-7). The features and differences between oral epithelia are described in Chapter 3.

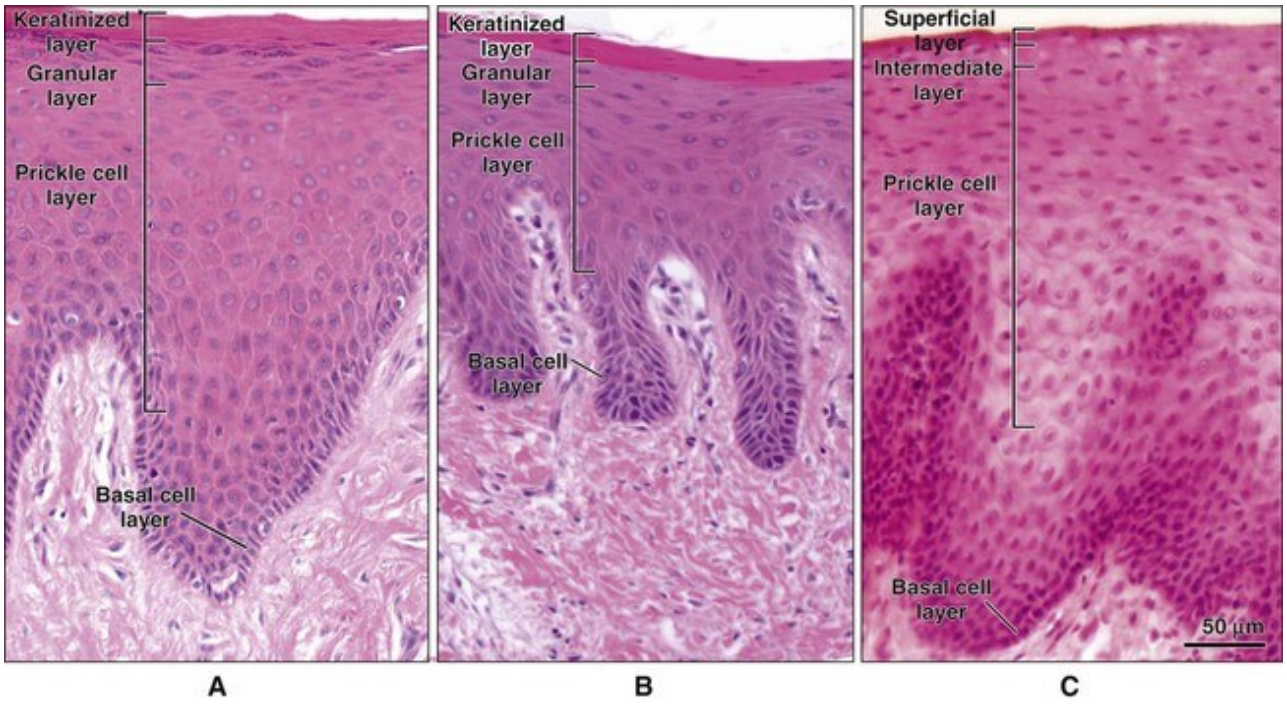

Figure I-7 *Histological features of the leading oral epithelial type. (Squier and Brogden, Human Oral Mucosa: Development, structure and function, 2011)*

1.2.2.2. Basement membrane

The basement membrane is a thin and fibrous layer that connects the epithelial tissue with the underlying connective tissue. It is mainly composed of ECM protein, in direct contact with the epithelial tissue are more prominent the laminin, the type IV collagen and the type XVII collagen (present within the hemidesmosome) while in contact with the connective tissue are mainly present type VII collagen, anchoring fibrils and microfibrils (Kamaguchi et al., 2019). The upper layer is a thin electron-dense membrane in which thick collagen IV fibrils are strongly interconnected and supported by the heparan sulphate-rich proteoglycan perlecan, laminin, integrins, entactin, and dystroglycan. On the contrary, the lower part, which strongly binds the stromal tissue, is rich in substrate adhesion molecules (SAMs). Those protein have also been evaluated as a coating for 2D or 3D cultures. For instance, perlecan is necessary for epithelial formation since it not only supports the collagen structures but also regulates survival and terminal differentiation of 3D keratinocytes (Sher et al., 2006). Laminin, and in particular the sub-unit α-5, is involved in epithelial-mesenchymal signaling and hallow keratinocytes adhesion similarly as a feeder layer (Wegner et al., 2016; Tjin et al., 2018). Glycosaminoglycans improve fibroblast shaping in 3D and increase the number of seeded fibroblasts in S or G2 phases; in this way, an enhanced re-epithelialization process was guaranteed (Belvedere et al., 2018).

The basement membrane is also necessary for several other processes such as the angiogenesis, since basement membrane proteins stimuli endothelial differentiation, or barrier function towards malignant cells invasion.

1.2.2.3. Lamina Propria

The connective tissue which underly the oral epithelia is named "lamina propria" and it is characterized by a huge heterogenicity in terms of cell types, fibres density, and organization. Generally, it is histologically divided into two principal types: the superficial papillary layer (which interval the epithelial ridges) and the deeper reticular layer (characterized by a "net-like" collagen-based structures). The two layers are characterized by an abundant and dense type I collagen fibres that in the papillary layer are thin and loosely arranged while in the reticular layer has collagen fibres arranged in thick bundles that tend to lie parallel to the surface plane.

The lamina propria can be in direct contact with bone, the mucoperiosteal structures (attached gingiva and hard palate) or a looser connective structure of the reticular layer characterized by the presence of type III collagen and others elastic fibres. The lamina propria is also rich in cell types (macrophages, plasma cells, mast cells, and lymphocytes, endothelial cells, and mesenchymal stem cells), blood vessels, and neural elements.

The lamina propria is made of three-dimensional fibres network (mainly collagen, elastin, and fibronectin) and a ground substance composed of water, glycoproteins, and proteoglycans and serum-derived proteins (Mohd at al., 2017).

Currently, at least 28 different collagen subtypes, composed of 46 distinct polypeptide chains have been identified (Shoulders and Raines, 2009). Collagen is typically organized as three parallel α-polypeptide strands coiled in a helical conformation around each other; each triple helix auto-assemble in a complex structure that can be easily observed under the macroscopic. The helix conformation leads the classification of different collagen subtypes; for instance, collagen type I, II, III, and V can be identified with an electron microscope by a characteristic helix arrangement that arises by fibrils with a banding pattern of 64 nm under SEM analysis

The elastic fibres are composed of elastin, which guarantees the elasticity and the support of mature fibres, and microfibrils, which is composed of fibrillin, a glycoprotein, microfibril associated glycoproteins (MAGPs), fibulins and elastin microfibril Interface Located Protein (EMILIN) (Wagenseil and Mecham, 2007). The elastic fibres can be stained by aldehyde fuchsin, orcein, or Weigert's elastic stain and are abundant in the lining mucosa, which needs more flexibility.

The ground substance consists of two heterogeneous protein/ carbohydrate complexes groups: proteoglycans (the polypeptide core with attached glycosaminoglycans chains) and glycoproteins (branched polypeptide chains to which only a few simple hexoses are attached).

The nerve supplying oral mucous membrane is predominantly sensory and arises mainly from the second and third divisions of the trigeminal nerve; afferent fibres of the facial (VII), glossopharyngeal (IX), and vagus (X) nerves are also involved. The myelin sheaths are lost in the reticular layer, where the bare fibres form network terminating in a subepithelial plexus between the epithelial ridges (Basbaum et al., 2009).

Finally, lymphatic and blood vessels are in the *lamina propria while* ducts, arising from different glands, are located in the deeper submucosa.

The main cell type found in *lamina propria* is fibroblast. Fibroblasts play an essential role in several processes, including epithelial morphogenesis (keratinocytes adhesion or integrin expression for the cellular junction formation). Moreover, they can be easily isolated and maintain their ECM secretion capability when cultivated in 3D, and they are essential for keratinocytes proliferation *in vivo* (see chapter 2).

1.2.3. Periodontium

The periodontium is the specialized multi-tissues structures composed by gingiva, periodontal ligament (PDL), cementum, and alveolar bone. The main role of the periodontium is protecting the bordered teeth (fig. I-8). The periodontal ligament, formed by specialized fibroblasts, provides a firm but flexible connection for the teeth, necessary to give the proper withstand towards the mechanical stress. The alveolar bone, the thickened ridge of bone that contains the tooth sockets, forms the alveolar arch and confers stiffness. Like other bones, alveolar bone regularly undergoes a remodelling process regulated by mechanical stimulation. In particular, the tooth pocket is highly subject to this physiologic phenomenon. The bone-forming cells, osteoblast and osteocytes, act on the areas of tension while the bone resorption cells, the osteoclast, line the areas of compression. This process guarantees the "high-quality" of the bone and, consequently, the adequate support to teeth. Periodontium development seems to be regulated mainly by the negative regulation of Sfrp3/Frzb derived from the Wnt pathway (de Jong et al., 2017).

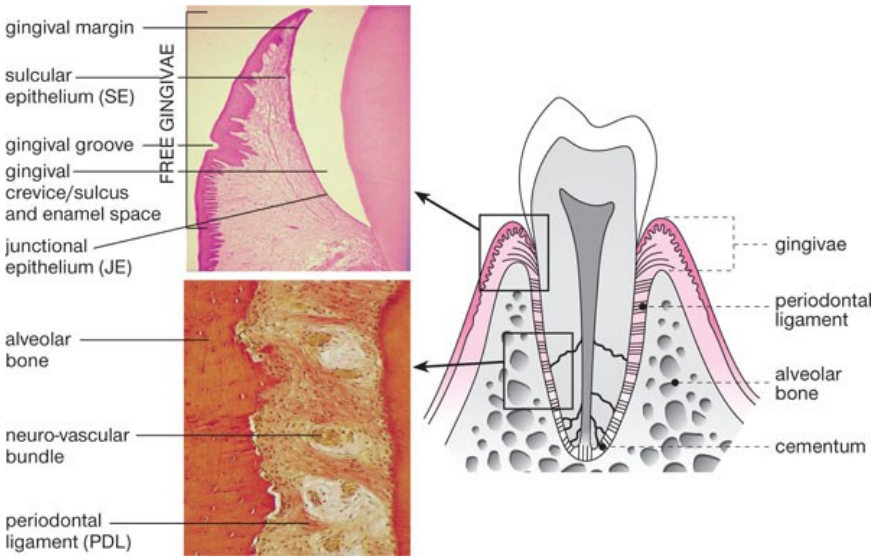

Figure I-8 *Histology and morphology of the periodontium.* https://pocketdentistry.com/1-a-whistle-stop-tour-of-the-periodontium/

Recently, human mesenchymal stem cells (hMSCs) have been found in the periodontium, especially close to the periodontal ligaments and in the gingiva and in dental pulp. That specific dental pulp hMSC (DPMSCs) subpopulation showed an enhanced differentiation potential when compared with bone-marrow-derived hMSC since they can reproduce the entire periodontium but also easily trans-differentiate in neuron-like cells. In the last decades, the secretome of MSCs, isolated from different sources, has acquired interest by researchers involved in tissue regeneration since it has shown impressive potential both in *vivo* and *in vitro* studies.

MSCs secrete several types of soluble factors, such as cytokines, chemokines, or growth factors, which mediate diverse functions and regulates the crosstalk between different cell types.

MSCs are well-known to act a pivotal role in tissue regeneration both locally, with the differentiation in specific cell type to cover defects, and distantly, by secreting several paracrine and trophic molecules which can act directly on the injured cells or indirectly, by inducing other cell type to produce other soluble factor increasing exponentially the

signalling potential. For instance, after injuries, MSCs are reduce the cellular damage by inhibiting the fibrotic tissue formation, promoting angiogenesis to increase the nutrients available to the damaged site, modulating the immune response, and recruiting progenitors and other stem cells to the injured site to start the tissue renewal. The principal involved factors in tissue regeneration are summarized in figure I-9.

MSC features are better described in chapter 2

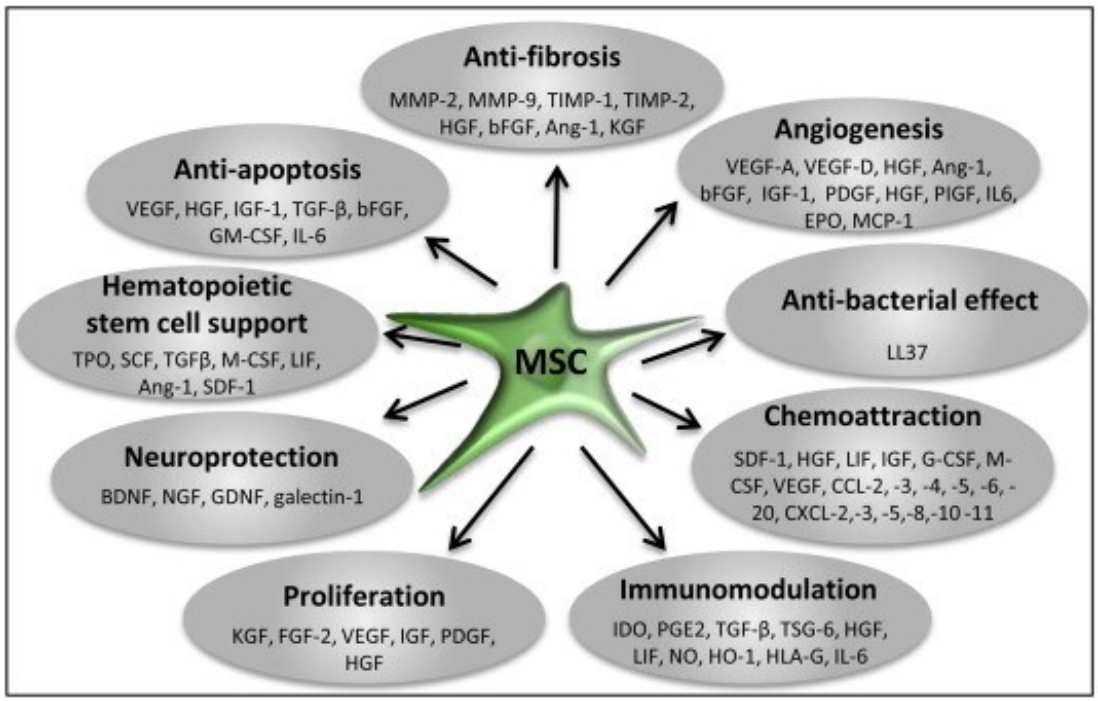

***Figure I-9**. Role of various paracrine factors released by mesenchymal stem cells. Maumus et al. Biocheme 2013*

1.3. Oral mucosa model

1.3.1. Monolayered Keratinocytes cultures

The first successful monolayer culture of keratinocytes was performed in 1975 by Rheinwald and Green; to improve the viability and proliferation of keratinocytes *in vitro* they coated the plastic support with a feeder layer composed of irradiated 3T3 mouse fibroblasts. Keratinocytes were then cultivated in a home-made enriched culture medium named Green's medium.

This method has been lately development to obtain a single-layer epithelial sheet; however, the derived models were often described as challenging to handle due to their fragility. Thus, these monolayer cultures have been improved and used for decades to study the basic biology of oral keratinocytes. For example, several studies showed that oral and skin keratinocytes have different behaviour in terms of differentiation, mitotic ratio, gene expression, and stimuli response. However, those monolayer cultures miss the typical structures and gene expression change to whom keratinocytes undergo *in vivo* during the terminal differentiation process. Thus, the development of a three-dimensional multilayer culture system was a vital innovation in epithelial biology studies, and this innovation will be fully analysed in chapter 3.2.

Nowadays, oral and skin keratinocytes are cultivated in 2D using polarized plastic support coated with collagen and serum and calcium-free media (such as the KGM from Gibco or EpiLife from Thermofisher). Thus, several 2D-based co-culture systems, mainly based on transwell systems, have been used to evaluate keratinocyte interaction with other cell types. As previously described, epithelial cells growth on the top of a stromal tissue mainly repopulated by fibroblast and, although in lower numbers, by mesenchymal stem cells. Due to hMSCs potential in tissue regeneration, several authors tried to establish the relation which intercourse between SCs and keratinocytes. For instance, Sivamani et all. (2015) showed that keratinocytes induce the epithelial trans-differentiation of hMSCs in direct co-culture and myofibroblast differentiation of hMSCs when they are co-cultivated with a transwell model.

Keratinocytes behaviour is severely affected by the growth condition. Alike for other cell types, keratinocytes gene expression, behaviour, proliferation potential, and morphology are deeply related to the three-dimensional stratification. However, differently by other cells, in the 3D histological structure are represented all differentiative stages of keratinocytes. For instance, in the basal layer keratinocytes are characterized by stem capability, which results lost in the spinosum layer. This peculiarity is crucial in the toxicological and pharmaceutical test since the same molecules can have different effects on the fourth layer, which characterizes the epithelium. Despite this intrinsic ability of keratinocytes to differentiate during the stratification, the particularities of each stratum are under the regulation of the closest mesenchyme in both healthy and damaged condition.

3D cell culture endowments the possibility to grow simultaneously different cellular populations in their proper microenvironment; thus, the resulting co-cultures can accurately mimic the cellular functions and the effect of crosstalk in terms of paracrine and autocrine regulation, and cell-cell interaction can be effectively studied. On the contrary, when cells are grown in 2D-based co-cultures, several phenomena cannot be appropriately evaluated. During the years, this statement resulted true in particular for mesenchyme-epithelial interaction.

1.3.2. Histotypic oral epithelial models

In the last three decades, several advances in tissue engineering have provided an alternative approach to *in vivo* studies. Indeed, several three-dimensional models of oral epithelia (keratinocytes alone) or oral mucosa (keratinocytes growth on a fibroblast repopulated scaffold) were established as *in vitro* model aimed to study the developmental or wound healing processes and to evaluate the muco-toxicity and the biocompatibility of new biomaterials and drugs to be used for clinical application Scaffolds and ECM substitutes for connective tissue engineering, and optimization of technique for keratinocytes cultivations are technological key points for three-dimensional model developing.

1.3.2.1. Bilayer cultures

Rosdy et al. (1990), in the first nineties, started to cultivate the keratinocytes from a different source on a permeable cell culture membranes support at the air/liquid interface. This cultivation method allows keratinocytes to arrange multilayer epithelia with different cytokeratin expression accordingly to the layer and the presence of keratin for the keratinized mucosa.

1.3.2.2. Commercial models

Some companies, such as SkinEthic Laboratories (Nice, France) MatTek Corp. (Ashland, MA, USA), developed their own 3D models. The SkinEthic Laboratories model consists of a polycarbonate cell culture inserts on which human TR146 keratinocyte cells or gingival-derived cells are growth at air/liquid interface. However, TR146 are cancer cells derived by a squamous cell carcinoma and miss the capability to differentiate and form the keratin layer.

MatTek Corp developed two specific tools, called EpiOral™ and EpiGingival™, respectively mimicking the lining non-keratinized epithelium and the gingival keratinized epithelium arising, respectively, by buccal and gingival keratinocytes. Both models express the CK13 and produce cytokines, growth factors, and antimicrobial peptide as IL-10, VEGF, and the β-defensins and are made by primary single-donor cells. Both companies also provide models modification such as co-culture with fibroblast or pathological models. However, the media provided are under patent, and models cannot be furtherly developed. Indeed, as shown in table I-3, those models are mainly used for cytocompatibility and genotoxicity tests.

Table I-3 *In this table are summarised the principal application of commercially available oral mucosa*

MODEL	COMPANY	APPLICATION	AUTHOR	JOURNAL	DATE
EPIGINGIVAL	MatTek	Cytomegalovirus infection	Hai et al	Virology Journal	2006
EPIORAL, EPIGINGIVAL	MatTek	Toxicological tests	Klausner et al	Toxicol *in vitro*	2007
EPIORAL	MatTek	Irritancy tests	Delves et al	Toxicology	2008
SKINETHIC RHO	Episkin	Microbial tests and genotoxicity	Challacombe Stephen at al	Microbiology	2008
EPIORAL	MatTek	Mucoadhesive test	Hu et al	Ph.D. Thesis	2010
SKINETHIC RHO	Episkin	Microbial tests and genotoxicity	Challacombe at al	Cell Host & Microbe	2010
EPIORAL	MatTek	Permeability study	Koschier et al	Food Chem Toxicol	2011
EPIGINGIVAL	MatTek	Oral care tests	Yang et al	International dental Journal	2011
SKINETHIC RHE, SKINETHIC RHO	Episkin	Oral care tests	Alonso at al	AAPS Pharm Sci Tech	2011
EPIORAL, EPIGINGIVAL	MatTek	DNA repair evaluation	Mitchell et al	Photochem Photobiol	2012
EPIGINGIVAL	MatTek	UV-radiation tests	Agrawal et al	Photochemistry and Photobiology	2013
EPIORAL	MatTek	Xerogels insulin delivery tests	Boateng et al	Protein pept Lett	2014
EPIORAL, EPIGINGIVAL	MatTek	Toxicology test	Schalge et al	Toxicol Mech Methods	2014
EPIORAL	MatTek	γ-irradiation study	Lambros et al	Evid Based Complement Alternat Med	2015
EPIORAL	MatTek	Mucoahesive test	MucoLox	PCCA	2015
EPIORAL	MatTek	Tobacco tests	Zanetti et al	Chem Res Toxicol	2016
EPIGINGIVAL	MatTek	Tobacco tests	Sundar et al	Virology Journal	2016
EPIORAL, EPIGINGIVAL	MatTek	Ag nanoparticles tests	Pinďáková et al	Int J Pharm.	2017
EPIORAL	MatTek	Mucoahesive test	Song at al	AAPS Pharm Sci Tech	2017

1.3.2.3. Organotypic oral mucosa model

The models named “full thickness engineered oral mucosa” are characterized by a *lamina propria* substitute and an overlying stratified epithelium. The *lamina propria* is represented by a biocompatible scaffold fully repopulated with viable and matrix-secreting oral fibroblasts. This structure has a supporting role in keratinocyte differentiation and

proper behaviour. The appropriate scaffold has, ideally, a withstand but porous structure developed to enable fibroblast infiltration while counteracting the shrinkage that begin with fibroblasts growth. The stratified squamous epithelium, fixed on the *lamina propria* by a self-produced basement membrane, is represented by densely packed keratinocytes with stemness potential. They undergo to differentiation as they migrate to the surface. The positioning to the air/liquid interface of proliferating oral keratinocytes usually induces this phenomenon in a chemically defined medium. The scaffold, the cell source, and culture medium composition could be modified and improved to optimize the full-thickness oral mucosa accordingly to the research purpose.

1.3.2.4. Scaffolds

As mentioned above, the *lamina propria* scaffolds play a crucial role in obtaining adequate oral mucosa. The proper scaffold should have satisfactory biocompatibility, porosity, biostability, and mechanical properties to support both fibroblast and keratinocytes growth. The scaffold developed during the years are numerous and can be divided into the sequent categories: naturally-derived scaffolds, collagen-based scaffolds, gelatin-based scaffolds, fibrin-based materials, synthetic scaffolds, and composite scaffolds.

1.3.2.4.1. Naturally Derived Scaffolds

In the late nineties, Izumi et al. used a commercially available De-epidermalized dermis (DED; AlloDerm™) as *lamina propria* substitute. The AlloDerm™ was chosen since is non-immunogenic but maintain the basal lamina which helps keratinocytes adhesion; on the other side, it presents that have a polarity by which one side has a basal lamina suitable for epithelial cells, and the other hand, it has intact vessel channels which allow for fibroblast infiltration. DED can be prepared by removing the cellular components from the dermis using different chemical procedures and can be preserved in glycerol for extended storage. The main advantages of using DED as *lamina propria* substitute are related to size stability and the low immunogenicity. Both commercial and home-made prepared DED have been used for years to produce oral mucosa since they induce a proper differentiation in epithelial progenitor cells. However, the fibroblasts were unable to migrate toward keratinocytes. Thus, this method has been abandoned because it missed the cellular interaction needed for an appropriate mimic the oral mucosa. De-epithelialized bovine tongue mucosa has been used in the same way.

During the years, several companies have developed their own dermis substitute for skin models that can be adapted to mimic oral mucosa: Dermagraft™, developed by Advanced Tissue Sciences Inc. (Coronado, CA, USA), Apligraf™ (Graft skin), developed by Organogenesis, Inc. (Canton, MA, USA), which is based on a fibroblast-repopulated bovine collagen gel and the Orcel™ (Ortec International Inc., New York, NY, USA), Polyactive™ (HC Implants, Leiden, The Netherlands), and Hyalograft 3D™ (Fidia Advanced Biopolymers, Padua, Italy).

1.3.2.4.2. Collagen-based Scaffolds

The first collagen-based scaffold repopulated by fibroblast was developed by Masuda et al. about 20 years ago. The collagen used was isolated by bovine skin and, ones repopulated with oral fibroblast were allowed contract for one week before being used for culturing keratinocytes. On this base, keratinocytes were able to stratify and to reproduce a tissue histologically resembling the native tissues, but with an extreme presence of invasive epithelial cell within the connective counterpart. To avoid this, Moriyama et al. added a honeycomb structured collagen sponge to improve elasticity and withstand of the *lamina propria* substitute and prevent the epithelial invasion.

Notwithstanding the improvement in the epithelial part, fibroblasts were poorly active in their connective tissue substitute, and they were not able to produce de novo extracellular matrix (ECM). This resulted in a poorly formatted basement membrane, with the total absence of type IV collagen expression and few hemidesmosome-like structures recognizable. In 2002, Rouabhia et al. reproduced a model similar to the Masuda's one, and they showed that stratified keratinocytes were able to express CK14, 19, and 10, proliferation marker Ki-67, integrins (β1 and α2β1) and to secrete laminins in the basement membrane. Moreover, the same Authors detected the interleukins IL-1β, IL-8, TNF-α, and different metalloproteinases, including the gelatinase released into the medium.

During the years, several improvements have proposed starting from this model, including collagen cross-link. However, has shown by Ma et al. these processes enhance calcification process in the *lamina propria* substitute. The collagen-based scaffold has also been improved with the addition of chitosan (a cellulose-like substance which improves the cross-linking efficacy of glutaraldehyde) or glycosaminoglycans (GAG, indispensable components of the ECM) such as chondroitin sulphate and hyaluronic acid to enhance the mechanical properties of the scaffold itself. Those developments improved the ECM secretion by embedded fibroblasts.

1.3.2.4.3. Gelatin-based Scaffolds

Gelatin is the denatured form of collagen, and it has been often used in tissue regeneration because it promotes fibroblast proliferation and the re-epithelialization while the immune system does not recognize it. As collagen-based scaffold, gelatin-based scaffolds have been improved with chitosan and hyaluronic acid which increase the stability and reduced the contraction rate during the experiments. Combination with glucan, an antimicrobial polysaccharide, is reported to promote wound healing and reduce the coagulation process.

1.3.2.4.4. Synthetic and hybrid Scaffolds

In 2004, El-Ghalbzouri successful developed a biodegradable segmented copolymer of poly (ethylene glycol terephthalate)-poly (butylene terephthalate) (PEGT/PBT). Due to its porous nature, the PEGT/PBT scaffold can be repopulated with the injection of fibroblasts embedded in fibrin or collagen to obtain better results, as made by Wang et al. in 2005.

1.3.3. Cell Source and culture medium

Epithelial and stromal cells sources are important for epithelial model engineering. Usually, early passage fibroblasts, isolated by oral mucosal biopsy, are used to repopulate the stromal compartment. They can be maintained with high proliferation potential and ECM secretion capability for 10 to 15 passages. Regarding the epithelial compartment, keratinocytes can be isolated from different oral cavity sites to mimic the corresponding epithelium properly, but they are difficult to expand, and they must be used in the very early passages, between 1 and 2, to enable their adhesion and proper stratification. During the years, several immortalized keratinocytes lines have been proposed to overcome the low availability and the patient-related behaviour of keratinocytes. The most used model is the cancer cell line TR146; the differentiation of this latter transformed keratinocytes is incomplete since neoplastic cells cannot undergo through the terminal differentiation process. Similarly, both home-made and commercially available h-tert immortalized or spontaneously immortalized keratinocytes have been proposed. However, being immortalized, those cells type not always behave differ by primary cells and the resulted models are not suitable for assays such the tumorigenic assay.

The most used medium for oral mucosa reconstruction is Dulbecco's modified Eagle medium (DMEM)-Ham's F-12 medium (3:1), supplemented with foetal calf serum (FCS), glutamine, epidermal growth factor (EGF), hydrocortisone, adenine, insulin, transferrin, tri-iodothyronine, fungizone, penicillin, and streptomycin. This media can be enriched with ascorbic acid, calcium chloride, and glycerol to modulate the keratin production.

1.3.4. Applications and development of engineered oral mucosa

Compared with organotypic skin cultures, full-thickness oral mucosa has not yet been commercialized for clinical applications. In the last decades, several researchers started to evaluate the capability of engineered oral mucosa to drive the tissue regeneration of other squamous based epithelial tissue such as the cornea or the urethra. Still, the use of this technique is forbidden in clinical practice.

1.3.4.1. Oral mucosal toxicity evaluation

Nowadays, the main application of full-thickness oral model is the evaluation of the biocompatibility and immune-tolerance of new biomaterial or compounds such as dentifrices (Mostefaoui et al.2002; Moharamzadeh et al., 2008), implants (Chai et al., 2010; McGinley et al., 2013), mercury chloride (Khawaja et al. 2002) and surfactants (Hagi-palvli et al., 2014). This *in vitro* model is a reliable tool for mucotoxicity evaluation of dental biomaterials since they better reflect the clinical situation than monolayer cell culture. Cytokines released and toxic metabolites generation may be easily and accurately quantified using oral mucosa equivalent. Moreover, the effects of the external stimuli on the outer layer cell morphology and behaviour can be exclusively assessed in 3D model considering that the outer layer is absent in the monolayer cultures.

1.3.4.2. Mucosa model implementation

Recently, literature has reported the development of osteo-mucosa models mimicking the physiological appearance of the hard palate, gingiva, and alveolar mucosa to test biomaterials or compounds in contact with the soft-hard tissue interface. In 2014, Bae et al. proposed a model composed of a mice calvaria bone, used as a bone substitute, and an engineered fully stratified oral mucosa growth on the top of the calvaria bone. From a histological point of view, the model mimics the physiologic appearance of the osteo/mucosa. However, during the model characterization, the interaction between the cellular components, and the role of paracrine signaling were not evaluated. In this work, the authors localized a fluorescently labelled bisphosphonate in their 3D models thanks to an acellularized collagen matrix used to connect the hard and the soft tissue. Another may disadvantage of this model is that the histomorphometry of the calvaria do not represent the one of the alveolar bone.

In 2016 and 2018 Almela et al., developed other bone-mucosa models that are deeper analysed in chapter 4.

1.3.4.3. Infected model development

Full-thickness oral mucosa has been described for assessing host-microbial interaction. In 2004, Andrian et al. mimic a gingivitis model adding *Porphyromonas gingivalis* on an oral mucosa model evaluating the *P. gingivalis* invasion within the epithelial part and toward the *lamina propria* while Pinnock et al., compared the response induced by *P. gingivalis* in 2- and 3-dimensional condition. Among the infected models, the intracellular survival of *P. gingivalis* and the newly formed bacterial units released *by cells* were significantly increased in the oral mucosa model in comparison with monolayer cultures. This phenomenon was accounted to the multi-layered nature and exfoliation of epithelial cells in the organotypic models. Furthermore, since *P. gingivalis* have the capability to degrade host cytokines, the authors quantified the released cytokine in the culture media and found that CXCL8 and IL6 were present in higher concentrations in the 3D cultures.

Similar works were performed by Dongari-Bagtzoglou and her group between 2010 and 2018; their works were mainly focused on evaluating the interaction between different streptococcus strains during co-infection with *Candida albicans*. They showed that *C. albicans* biofilms create hypoxic or anoxic micro-niches via mitochondrial oxygen consumption that allow obligate anaerobic bacteria growth also in the presence of oxygen.

In the last 25 years, the oral mucosa models have been continuously improved to better resemble the native tissue by focusing on the epithelial arrangements and on lamina propria engineering. However, the native oral mucosa is not only composed of keratinocytes and fibroblast but many other components such as Langerhans cells, melanocytes endothelial, macrophages, monocytes, and resident MSC contribute to the complexity of native tissue. For this reason, recently, researchers have advanced the oral mucosal model by incorporating the: *i)* endothelial cells for promoting and evaluating the angiogenetic process, *ii)* immune cells to better assess the immune-tolerance and the host response to microbial infection and *iii)* dysplastic cells to elucidate oral disease pathologies.

Optimization of the scaffold matrix, porosity and biodegradability and improvement of isolation and cultivation techniques of oral keratinocyte subtypes are the gaps to fill. The latter remains one of the main drawbacks when the

oral mucosa models are used because of the huge number of cells needed for a single test. Nowadays, these models, in particular those with primary cells, shown a high batch-depended variability.

1.4. Aims and Thesis structures

Mesenchymal stem cells have a huge potential in regenerative medicine field since the capacity to differentiate into various cell types (such as osteoblast, chondrocytes, adipocytes, neuronal-like cells etc.). MSCs provide paracrine and autocrine effect by secreting cytokines, chemokines and growth factors. MSCs secretome has a huge potential in wound healing by increasing the migration and proliferation of several cell types, improving axonal outgrowth and myelinization, by physically support the vascularization, by suppressing inflammatory process and so forth. Moreover, several studies in which hMSCs were injected into murine model, have showed that the implanted cells migrate towards different tissue and acquire the resident cells' phenotype. In the decades, MSC has been found in mostly all tissues, and even in oral cavity.

As already described, the oral cavity is a complex body site characterized by several organ interactions. The mechanism regulating the epithelial differentiation is intricate and still poorly understood. The widely used *in vivo* models and the retrospective studies often failed to identify the actors involved in keratinocytes differentiation due to the presence of several cell types acting both in a synergic or antagonist way.

However, to elucidate cell crosstalk mechanisms in their specific microenvironment it is crucial to improve the engineering of human-based three-dimensional model.

As previously described, in dental implantology field, the use of animal models is particularly complicated. For instance, rodents can be implanted only with scaled-down scaffolds and, more often, in extra-oral site because of their size while other animal models are considered pre-clinical and rarely can be used as a screening model.

To overcome those limitations, in the present thesis work, a three-dimensional mucoperiosteal model was developed. Indeed, despite the several oral mucosa models already existing, none includes the bone counterpart which is essential to evaluate the materials at the hard-soft tissue interface.

Moreover, in this work, were developed three different set-ups to assess the effect of MSC and nervous system onto mucosal behaviour. They were at the end suitable for both developmental and implantology fields.

To obtain these models, different human primary cell types (keratinocytes, fibroblast, mesenchymal stem cells, and osteoblast) in both 2 and 3-dimensional conditions not only as a single compartment but also in co-culture. The main challenge was to establish suitable protocols to growth all cell types in the same experimental state without losing their specific properties. The results related to this part of the work are described in the second chapter and are divided in:

- The evaluation of serum-added and serum-free media on monolayered cultures
- The optimization of the bone scaffold mechanical properties
- The establishment of a home-made keratinized oral mucosa

In the third chapter, the effect of bone-marrow-derived MSC on the keratinized oral mucosa behaviour was studied. In particular, the following aspects were studied:

- the paracrine effect of hMSC in “stem” condition or under osteogenic induction on keratinocytes differentiation
- the secretome composition
- the crosstalk between the oral keratinized mucosa and hMSC, in the presence or absence of osteoblastic differentiation factor, using both direct and indirect co-cultures condition.

Finally, in the fourth chapter, are described:

- the effect of oral mucosa and MSC-implemented oral mucosa on innervation
- the development of an innovative human-based mucoperiosteal model.

II. Bibliography

- Aaboe M, Pinholt EM, Hjørting-Hansen E. Unicortical critical size defect of rabbit tibia is larger than 8 mm. J Craniofac Surg. 5(3):201-3. (1994)
- Adams D. Keratinization of the oral epithelium. Ann R Coll Surg Engl. 58(5):351-8. Review. (1976)
- Aerssens J, Boonen S, Lowet G, Dequeker J. Interspecies differences in bone composition, density, and quality: potential implications for in vivo bone research. Endocrinology. 1 39 :663-670. (1998)
- Antoni D, Burckel H, Josset E, Noel G. Three-dimensional cell culture: a breakthrough in vivo. Int J Mol Sci. 16(3):5517-27. (2015) doi:10.3390/ijms16035517.
- Artzi Z, Tal H, Moses O, Kozlovsky A. Mucosal considerations for osseointegrated implants J Prosthet Dent. 70(5):427-32. (1993)
- Atala A, Kasper FK, Mikos AG. Engineering complex tissues. Sci Transl Med. 4(160):160rv12. (2012). doi: 10.1126/scitranslmed.3004890.
- Atsuta I, Ayukawa Y, Kondo R, Oshiro W, Matsuura Y, Furuhashi A, Tsukiyama Y, Koyano K. Soft tissue sealing around dental implants based on histological interpretation. J Prosthodont Res. 60(1):3-11. (2015) doi:10.1016/j.jpor.2015.07.001.
- Basbaum AI, Bautista DM, Scherrer G, Julius D. Cellular and molecular mechanisms of pain. Cell. 16;139(2):267-84. (2009) doi: 10.1016/j.cell.2009.09.028. Review.
- Belvedere R, Bizzarro V, Parente L, Petrella F, Petrella A. Effects of Prisma® Skin dermal regeneration device containing glycosaminoglycans on human keratinocytes and fibroblasts. Cell Adh Migr. 4;12(2):168-183. (2018) doi: 10.1080/19336918.2017.1340137.
- Beppu K, Kido H, Watazu A, Teraoka K, Matsuura M. Peri-implant bone density in senile osteoporosis-changes from implant placement to osseointegration. Clin. Implant. Dent. Relat. Res. 15(2):217-26. (2011). doi: 10.1111/j.1708-8208.2011.00350. x.
- Berkovitz BK, Barrett AW. Cytokeratin intermediate filaments in oral and odontogenic epithelia. Bull Group Int Rech Sci Stomatol Odontol. 40(1):4-23. (1998)
- Blumenberg M, Connolly DM, Freedberg IM. Regulation of keratin gene expression: the role of the nuclear receptors for retinoic acid, thyroid hormone,and vitamin D3. J Invest Dermatol. 98(6 Suppl):42S-49S. (1992)
- Blumenberg M, Savtchenko ES. Linkage of human keratin genes. Cytogenet Cell Genet.42(1-2):65-71. 1992;61(2):160. (1986)
- Blumenberg M, Tomić-Canić M. Human epidermal keratinocyte: keratinization processes. EXS. 78:1-29. (1997). Review.
- Boukamp P, Petrussevska RT, Breitkreutz D, Hornung J, Markham A, Fusenig NE. Normal keratinization in a spontaneously immortalized aneuploid human keratinocyte cell line J Cell Biol. 106(3):761-71 (1988)
- Bradbury P, Fabry B, O'Neill GM. Occupy tissue: the movement in cancer metastasis. Cell Adh Migr. 6(5):424-32. (2012) doi: 10.4161/cam.21559.
- Calenic B, Greabu M, Caruntu C, Tanase C, Battino M. Oral keratinocyte stem/progenitor cells: specific markers, molecular signaling pathways and potential uses. Periodontol 2000. 69(1):68-82. (2015) doi: 10.1111/prd.12097.
- Castaneda S, Largo R, Calvo E, Rodriguez-Salvanes F, Marcos ME, Diaz-Curiel M, Herrero-Beaumont G. Bone mineral measurements of subchondral and trabecular bone in healthy and osteoporotic rabbits. Skeletal Radiol. 35: 34-41. (2006)
- Ceccarelli S, Romano F, Angeloni A, Marchese C. Potential dual role of KGF/KGFR as a target option in novel therapeutic strategies for the treatment of cancers and mucosal damages. Expert Opin Ther Targets. 16(4):377-93. (2012) doi: 10.1517/14728222.2012.671813.
- Chavassieux, P, Pastoureau P, Boivin G, Chapuy MC, Delmas PD, Milhaud G, and Meunier PJ. Fluoride-induced bone changes in lambs during and after exposure to sodium fluoride. Osteoporosis Int. 2:26-33. 38. (1991)
- Chen J, Li Y, Hao H, Li C, Du Y, Hu Y, Li J, Liang Z, Li C, Liu J, Chen L. Mesenchymal Stem Cell Conditioned Medium Promotes Proliferation and Migration of Alveolar Epithelial Cells under Septic Conditions In Vitro via the JNK-P38 Signaling Pathway. Cell Physiol Biochem. 37(5):1830-46. (2015) doi: 10.1159/000438545.
- de Boo J and Hendriksen C. Reduction strategies in animal research: a review of scientific approaches at the intra-experimental, supra-experimental and extra-experimental levels. ATLA 33, 369. (2005).

- de Jong T, Bakker AD, Everts V, Smit TH. The intricate anatomy of the periodontal ligament and its development: Lessons for periodontal regeneration. J Periodontal Res. 52(6):965-974. (2017) doi: 10.1111/jre.12477.
- Del Angel-Mosqueda C, Gutiérrez-Puente Y, López-Lozano AP, Romero-Zavaleta RE, Mendiola-Jiménez A, Medina-De la Garza CE, Márquez-M M, De la Garza-Ramos MA. Epidermal growth factor enhances osteogenic differentiation of dental pulp stem cells in vitro. Head Face Med. 3; 11:29. (2015) doi: 10.1186/s13005-015-0086-5.
- Deo PN, Deshmukh R. Pathophysiology of keratinization. J Oral Maxillofac Pathol. 2018 22(1):86-91. (2018) doi: 10.4103/jomfp.JOMFP_195_16.
- Desando G, Cavallo C, Tschon M, Giavaresi G, Martini L, Fini M, Giardino R, Facchini A, Grigolo B. Early-term effect of adult chondrocyte transplantation in an osteoarthritis animal model. Tissue Eng Part A.18(15-16):1617-27. (2012) doi: 10.1089/ten.TEA.2011.0494.
- Donati D, Di Bella C, Gozzi E, Lucarelli E, Beccheroni A, Di Maggio N, Fini M, Giavaresi G, Martini L, Aldini NN, Mercuri M, Giardino R. In vivo study on critical defects using the sheep model. Chir Organi Mov. 90(1):31-9. (2005)
- Dongari-Bagtzoglou A. and Kashleva H. Development of a highly reproducible three-dimensional organotypic model of the oral mucosa. Nat Protoc 1: 20128 (2006)
- Duval K, Grover H, Han LH, Mou Y, Pegoraro AF, Fredberg J, Chen Z. Modeling Physiological Events in 2D vs. 3D Cell Culture. Physiology (Bethesda). 32(4):266-277. (2017) doi: 10.1152/physiol.00036.2016.
- Dvorak G, Reich K, Tangl S, Goldhahn J, Haas R, Gruber R. Cortical porosity of the mandible in an osteoporotic sheep model. Clin. Oral Impl. Res. (2011)
- Edmondson R, Broglie JJ, Adcock AF, Yang L. Three-dimensional cell culture systems and their applications in drug discovery and cell-based biosensors. Assay Drug Dev Technol. 12(4):207-18. (2914) doi: 10.1089/adt.2014.573.
- El-Ghalbzouri A, Lamme EN, van Blitterswijk C, Koopman J, Ponec M. The use of PEGT/PBT as a dermal scaffold for skin tissue engineering. Biomaterials 25:2987-2996. (2004)
- Eng J. Sample size estimation: how many individuals should be studied? Radiol. 227, 309-313. (2003) doi:10.1148/radiol.2272012051
- Ennever G, Noonan T, and H. Rosenkranz H. The predictivity of animal bioassays and short-term genotoxicity tests for carcinogenicity and noncarcinogenicity to humans. Mutagenesis, 2(2):73–78, (1987)
- Evans EW. Treating Scars on the Oral Mucosa. Facial Plast Surg Clin North Am. 25(1):89-97. (2017) doi: 10.1016/j.fsc.2016.08.008.
- Finch PW, Rubin JS. Keratinocyte growth factor/fibroblast growth factor 7, a homeostatic factor with therapeutic potential for epithelial protection and repair. Adv Cancer Res. 91:69-136. (2004)
- Fini M, Giavaresi G, Giardino R, Lenger H, Bernauer J, Rimondini L, Torricelli P, Borsari V, Chiusoli L, Chiesa R, Cigada A. A new austenitic stainless steel with a negligible amount of nickel: an in vitro study in view of its clinical application in osteoporotic bone. J Biomed Mater Res B Appl Biomater.71(1):30-7. (2004)
- Fini M, Giavaresi G, Rimondini L, Giardino R. Titanium alloy osseointegration in cancellous and cortical bone of ovariectomized animals: histomorphometric and bone hardness measurements. Int J Oral Maxillofac Implants. 17(1):28-37. (2002)
- Fini M, Torricelli P, Giavaresi G, Carpi A, Nicolini A, Giardino R. Effect of L-lysine and L-arginine on primary osteoblast cultures from normal and osteopenic rats. Biomed Pharmacother 55:213–220. (2001)
- Fisher RL, Vickers AE. Preparation and culture of precision-cut organ slices from human and animal. Xenobiotica. 43(1):8-14. (2013) doi:10.3109/00498254.2012.728013.
- Freilich M, M Patel C, Wei M, Shafer D, Schleier P, Hortschansky P, Kompali R, Kuhn L. Growth of new bone guided by implants in a murine calvarial model. Bone. 43: 78 1-8. (2008)
- Garnick JJ, Ringle RD. The dento-gingival junction as seen with light microscopy and scanning electron microscopy. Scanning Microsc. (1988)
- Gartner LP. Oral anatomy and tissue types. Semin Dermatol. 13(2):68-73. Review. (1994)
- Gattazzo F, Urciuolo A, Bonaldo P. Extracellular matrix: a dynamic microenvironment for stem cell niche. Biochim Biophys Acta. 1840(8):2506-19. (2014). doi: 10.1016/j.bbagen .2014.01.010.
- Gomes PS, Fernandes MH. Rodent models in bone-related research: the relevance of calvarial defects in the assessment of bone regeneration strategies. Lab Anim 45: 14-24. (2010)
- Gothard D, Smith EL, Kanczler JM, Rashidi H, Qutachi O, Henstock J, Rotherham M, El Haj A, Shakesheff KM, Oreffo RO. Tissue engineered bone using select growth factors: A comprehensive review of animal studies and clinical translation studies in man. Eur Cell Mater.28:166-207. (2014)

- Gugala, Z., and S. Gogolewski. Regeneration of segmental diaphyseal defects in sheep tibia using resorbable polymeric membranes: a preliminary study. J. Orthop. Trauma. 3:187-195. (1999)
- Haga M, Fujii N, Nozawa-Inoue K, Nomura S, Oda K, Uoshima K, et al. Detailed process of bone remodeling after achievement of osseointegration in a rat implantation model. Anat. Rec. (Hoboken). 292:38-47. (2009)
- Hagi-Pavli E, Williams DM, Rowland JL, Thornhill M, Cruchley AT. Characterizing the immunological effects of oral healthcare ingredients using an in vitro reconstructed human epithelial model. Food Chem Toxicol. 74:139-48. (2014) doi: 10.1016/j.fct.2014.09.007.
- Hall WB, Lundergan WP. Free gingival grafts. Current indications and techniques. Dent Clin North Am. 37(2):227-42. (1993) Review.
- Hasegawa H, Ozawa S, Hashimoto K, Takeichi T, Ogawa T. Type 2 diabetes impairs implant osseointegration capacity in rats. Int. J. Oral Maxilloføc. Implants. 23: 231-246 (2008)
- Hassan NT, AbdelAziz NA. Oral Mucosal Stem Cells, Human Immature Dental Pulp Stem Cells and Hair Follicle Bulge Stem Cells as Adult Stem Cells Able to Correct Limbal Stem Cell Deficiency. Curr Stem Cell Res Ther. 13(5):356-361. (2018) doi: 10.2174/1574888X13666180223124936.
- Herson MR, Mathor MB, Altran S, Capelozzi VL, Ferreira MC. In vitro construction of a potential skin substitute through direct human keratinocyte plating onto decellularized glycerol-preserved allodermis. Artif Organs 25:901-906 (2001)
- Hildebrand HC, Hakkinen L, Wiebe CB, Larjava HS. Characterization of organotypic keratinocyte cultures on deepithelialized bovine tongue mucosa. Histol Histopathol 17:151-163. (2002).
- Hou X, Weiler MA, Winger JN, Morris JR, Borke JL. Rat model for studying tissue changes induced by the mechanical environment surrounding loaded titanium implants. Int. J. O ral Maxillofac. Implant s. 24:800-807 (2009)
- Hurst JL and West RS. Taming anxiety in laboratory mice. Nat. Methods 7, 825-826. (2010). doi:10.1038/nmeth.1500
- Ikada Y. Challenges in tissue engineering; J R Soc Interface. 3(10): 589–601. (2006) doi: 10.1098/rsif.2006.0124.
- Izumi K, Feinberg SE, Iida A, Yoshizawa M. Intraoral grafting of an ex vivo produced oral mucosa equivalent: a preliminary report. Int J Oral Maxillofac Surg 32: 188-97 (2003)
- Izumi K, Takacs G, Terashi H, Feinberg SE. Ex vivo development of a composite human oral mucosal equivalent. J Oral Maxillofac Surg 57: 571-7; discussion 577-8 (1999)
- Izumi K, Terashi H, Marcelo CL, Feinberg SE. Development and characterization of a tissue-engineered human oral mucosa equivalent produced in a serum-free culture system. J Dent Res. 79: 798-805. (2000)
- Izumi K, Tobita T, Feinberg SE. Isolation of human oral keratinocyte progenitor/stem cells. J Dent Res. 86(4):341-6. (2007)
- Kamaguchi M, Iwata H, Nishie W, Toyonaga E, Ujiie H, Natsuga K, Kitagawa Y, Shimizu H. The direct binding of collagen XVII and collagen IV is disrupted by pemphigoid autoantibodies. Lab Invest. 99(1):48-57. (2019) doi: 10.1038/s41374-018-0113-9.
- Khawaja RA, Qureshi R, Mansure AH, Yahya ME. Validation of Datascope Accutorr Plus™ using British Hypertension Society (BHS) and Association for the Advancement of Medical Instrumentation (AAMI) protocol guidelines. J Saudi Heart Assoc. 22(1):1-5. (2010) doi: 10.1016/j.jsha.2010.03.001.
- Knight A. The Costs and Benefits of Animal Experiments. Basingstoke, Hampshire, UK: Palgrave Macmillan. (2011)
- Langer R, Vacanti JP. Tissue engineering. Science. 260(5110):920-6. Review. (1993)
- Lee DY, Ahn HT, Cho KH. A new skin equivalent model: dermal substrate that combines de-epidermized dermis with fibroblastpopulated collagen matrix. J Dermatol Sci 23:132-137. (2000)
- Lee KH. Tissue-engineered human living skin substitutes: development and clinical application. Yonsei Med J 41:774-779. (2000).
- Li M, Zhao Y, Hao H, Dai H, Han Q, Tong C, Liu J, Han W, Fu X. Mesenchymal stem cell-conditioned medium improves the proliferation and migration of keratinocytes in a diabetes-like microenvironment. Int J Low Extrem Wounds. 14(1):73-86. (2015) doi: 10.1177/1534734615569053.
- Li Y, Chen SK, Li L, Qin L, Wang XL, and Lai YX. Bone defect animal models for testing efficacy of bone substitute biomaterials. Journal of Orthopaedic Translation. 3(3):95–104, (2015).
- Liebschner MA. Biomechanical considerations of animal models used in tissue engineering of bone. Biomaterials. 25: 1697-1714. (2004)
- Liu F. Huang J, Ning B, Liu Z, Chen S and Zhao W. Drug discovery via human-derived stem cell organoids. Front. Pharmacol. 7, 334. (2016). doi:10.3389/fphar.2016.00334
- Ma JL, Pan JL, Tan BS, Cui FZ. Determination of critical size defect of minipig mandible. J. Tissue Eng. Regen. Med. 3(8):615-22. (2009). doi: 10.1002/term.203.

- Ma L, Gao C, Mao Z, Zhou J, Shen J, Hu X, et al. Collagen/chitosan porous scaffolds with improved biostability for skin tissue engineering. Biomaterials. 24:4833-4841. (2003).
- Martini L, Fini M, Giavaresi G, Giardino R. Sheep model in orthopedic research: a literature review. Comp Med. 51(4):292-9. (2001) Review.
- Masuda I. An in vitro oral mucosal model reconstructed from human normal gingival cells. Kokubyo Gakkai Zasshi. 63(2):334-53. (1996). doi: 10.5357/koubyou.63.334
- McClelland GH. Increasing statistical power without increasing sample size. Am. (2000).
- McGonigle O, Ruggeri B. Animal models of human disease: challenges in enabling translation. Biochem. Pharmacol. 87(1):162-71. (2014). doi: 10.1016/j.bcp.2013.08.006.
- Mishra DK, Sakamoto JH, Thrall MJ, Baird BN, Blackmon SH, Ferrari M, Kurie JM, Kim MP. Human lung cancer cells grown in an ex vivo 3D lung model produce matrix metalloproteinases not produced in 2D culture. PLoS One. 7(9):e45308. (2012) doi: 10.1371/journal.pone.0045308.
- Mohd Nor NH, Berahim Z, Ahmad A, Kannan TP. Properties of Cell Sources in Tissue-Engineered Three-dimensional Oral Mucosa Model: A Review. Curr Stem Cell Res Ther. 12(1):52-60. (2017) Review.
- Moriyama T, Asahina I, Ishii M, Oda M, Ishii Y, Enomoto S. Development of composite cultured oral mucosa utilizing collagen sponge matrix and contracted collagen gel: a preliminary study for clinical applications. Tissue Eng 7:415-427. (2001)
- Mosekilde L, Kragstrup J, Richards A. Compressive strength, ash weight, and volume of vertebral trabecular bone in experimental fluorosis in pigs. Calcif. Tissue Int. 40:318-22. (1987)
- Mosekilde L, Weisbrode S, Safron J, Stills H, Jankowsky M, Ebert D, et al.Calciumrestricted ovariectomized Sinclair S-1 minipigs: an animal model of osteopenia and trabecular pl ate perforation. Bone. 4:37 9 -82. (1993)
- Mostefaoui Y, Claveau I, Ross G, Rouabhia M. Tissue structure, and IL-1beta, IL-8, and TNF-alpha secretions after contact by engineered human oral mucosa with dentifrices. J Clin Periodontol. 29(11):1035-41. (2002)
- Müller T, Bain G, Wang X, Papkoff J. Regulation of epithelial cell migration and tumor formation by beta-catenin signaling. Exp Cell Res. 280(1):119-33. (2002)
- Muthuswamy SK. Bringing together the organoid field: from early beginnings to the road ahead. Development 144, 963-967. (2017) doi:10.1242/dev.144444
- Neupane S, Adhikari N, Jung JK, An CH, Lee S, Jun JH, Kim JY, Lee Y, Sohn WJ, Kim JY. Regulation of mesenchymal signaling in palatal mucosa differentiation. Histochem Cell Biol. 2018 Feb;149(2):143-152. (2018) doi: 10.1007/s00418-017-1620-2.
- Neyt JG, Buckwalter JA, Carroll NC. Use of animal models in musculoskeletal research. Iowa Orthoph J. 18:118-23. (1998)
- O'Loughlin PF, Morr S, Bogunovic L, Kim AD, Park B, Lane JM. Selection and development of preclinical models in fracture-healing research. J Bone Joint Surg Am 90 Suppl 1: 79-84. (2008)
- O'Farrell AC, Shnyder SD, Marston G, Coletta P L and Gill JH. Non-invasive molecular imaging for preclinical cancer therapeutic development. Br. J. Pharmacol. 169, 719-735. (2013) doi:10.1111/bph.12155
- Okazaki M, Yoshimura K, Suzuki Y, Harii K. Effects of subepithelial fibroblasts on epithelial differentiation in human skin and oral mucosa: heterotypically recombined organotypic culture model. Plast Reconstr Surg. 112:784-792. (2003)
- Olson JL, Atala A, Yoo JJ. Tissue Engineering: Current Strategies and Future Directions; Chonnam Med J. 47(1): 1–13. (2011) doi: 10.4068/cmj.2011.47.1.1.
- Pastoureau P, Arlot ME, Caulin F, Barier JP, Meunier PJ, and Delmas PD. Effects of oophorectomy on biochemical and histological indices of bone turnover in ewes. J. Bone Miner. Res. 4:S237. 39. (1989)
- Pearce AI, Richards RG, Milz S, Schneider E, Pearce SG. Animal models for implant biomaterial research in bone: a review. Eur Cell Mater 13: 1-10. (2007)
- Pedersen JA, Swartz MA. Mechanobiology in the third dimension. Ann Biomed Eng.;33(11):1469-90. (2005) Review.
- Peehl DM, Rubin JS. Keratinocyte growth factor: an androgen-regulated mediator of stromal-epithelial interactions in the prostate. World J Urol. 13(5):312-7. (1995)
- Rahal MD, Delorme D, Brånemark PI, Osmond DG. Myelointegration of titanium implants: B lymphopoiesis and hemopoietic cell proliferation in mouse bone marrow sed to titanium implants. Int. J. Oral Maxillofac. Implants. 15(2):175-84. (2000)
- Rakhorst HA, Tra WM, Posthumus-van Sluijs SJ, de Groot E, van Osch GJ, van Neck JW, Hofer SO. Mucosal keratinocyte isolation: a short comparative study on thermolysin and dispase. Int J Oral Maxillofac Surg. 35(10):935-40. (2006).

- Rasmusson L, Meredith N, Kahnberg KE, Sennerby L. Effects of barrier membranes on bone resorption and implant stability in onlay bone grafts. An experimental study. Cljn. Oral Implanls Res. 10(4):267-77. (1999)
- Ravaglioli, A., A. Krajewski, G. C. Celotti, A. Piancastelli, B. Bacchini, L. Montanari, G. Zama, and L. Piombi. Mineral evolution of bone. Biomaterials. 17:617-622. (1996).
- Rinaldi JC, Arana-Chavez VE. Ultrastructure of the interface between periodontal tissues and titanium mini-implants. Angle Orthod. 80(3):459-65. (2010). doi: 10.2319/032509-177.1.
- Rosdy M, Clauss LC. Terminal epidermal differentiation of human keratinocytes grown in chemically defined medium on inert filter substrates at the air-liquid interface. J Invest Dermatol. 95(4):409-14. (1990)
- Rouabhia M, Deslauriers N. Production and characterization of an in vitro engineered human oral mucosa. Biochem Cell Biol. 80:189-195. (2002)
- Sadrameli M, Mupparapu M. Oral and Maxillofacial Anatomy. Radiol Clin North Am. 56(1):13-29. (2018) doi: 10.1016/j.rcl.2017.08.002.
- Saintigny G, Bonnard M, Damour O, Collombel C. Reconstruction of epidermis on a chitosan cross-linked collagen-GAG lattice: effect of fibroblasts. Acta Derm Venereol. 73:175-180 (1993)
- Schroeder HE, Listgarten MA. The gingival tissues: the architecture of periodontal protection. Periodontol 2000. 13:91-120. (1997)
- Sculean A, Gruber R, Bosshardt DD. Soft tissue wound healing around teeth and dental implants. J Clin Periodontol. 41 Suppl 15:S6-22. (2014) doi:10.1111/jcpe.12206.
- Shanks N, Greek R, Greek J. Are animal models predictive for humans? Philos Ethics Humanit Med. 4: 2. (2009) doi: 10.1186/1747-5341-4-2
- Sharifikia D, Salem M, Yafia, Fradet G, Mohammadi H. Design and Fabrication of a 3D Scaffold for the Aortic Root Tissue Engineering Application. Journal of Medical and Biological Engineering, Volume 38, Issue 2, pp 211–221 (2017)
- Sher I, Zisman-Rozen S, Eliahu L, Whitelock JM, Maas-Szabowski N, Yamada Y, Breitkreutz D, Fusenig NE, Arikawa-Hirasawa E, Iozzo RV, Bergman R, Ron D. Targeting perlecan in human keratinocytes reveals novel roles for perlecan in epidermal formation. J Biol Chem. 281(8):5178-87 (2006)
- Shetty S; Gokul S. Keratinization and its disorders. Oman Med J.27(5):348-57. (2012) doi: 10.5001/omj.2012.90.
- Shoulders MD, Raines RT. Collagen structure and stability. Annu Rev Biochem. 78:929-58. (2009) doi: 10.1146/annurev.biochem.77.032207.120833. Review.
- Singhal G, Jaehne EJ, Corrigan F and Baune BT. Cellular and molecular mechanisms of immunomodulation in the brain through environmental enrichment. Front. Cell. Neurosci. 8, 971. (2014) doi:10.3389/fncel.2014.00097
- Sivamani RK, Schwartz MP, Anseth KS, Isseroff RR Keratinocyte proximity and contact can play a significant role in determining mesenchymal stem cell fate in human tissue. FASEB J. 25(1):122-31. (2011) doi: 10.1096/fj.09-148775
- Sneddon LU, Elwood RW, Adamo S and Leach MC. Defining and assessing pain. Anim. Behav. 97, 201-212. (2014) doi:10.1016/j.anbehav.2014.09.007
- Sneddon LU. Pain in aquatic animals. J. Exp. Biol. 218, 967-976. (2015) doi:10.1242/jeb.088823
- Sonkoly E, Wei T, Pavez Loriè E, Suzuki H, Kato M, Törmä H, Ståhle M, Pivarcsi A. Protein kinase C-dependent upregulation of miR-203 induces the differentiation of human keratinocytes. J Invest Dermatol. 130(1):124-34. (2010) doi: 10.1038/jid.2009.294.
- Squier CA. Keratinization of the sulcular epithelium--a pointless pursuit? J Periodontol. 52(8):426-9. (1981)
- Tamama K, Kawasaki H, Wells A. Epidermal growth factor (EGF) treatment on multipotential stromal cells (MSCs). Possible enhancement of therapeutic potential of MSC. J Biomed Biotechnol.795385. (2010) doi: 10.1155/2010/795385
- Tazawa H, Aliyama R, Moriya K. Development of cardiac rhythms in birds. Comp. Biochem. Physiol. 132(4):675-89. (2002). doi:10.1016/S1095-6433(02)00125-3
- Tjin MS, Chua AWC, Moreno-Moral A, Chong LY, Tang PY, Harmston NP, Cai Z, Petretto E, Tan BK, Tryggvason K. Biologically relevant laminin as chemically defined and fully human platform for human epidermal keratinocyte culture. Nat Commun. 9(1):4432. (2018) doi: 10.1038/s41467-018-06934-3.
- Torricelli P, Fini M, Giavaresi G, Rimondini L, Giardino R. Characterization of bone defect repair in young and aged rat femur induced by xenogenic demineralized bone matrix. J Periodontol. 73(9):1003-9. (2002)
- Torricelli P, Fini M, Rocca M, Giavaresi G, Giardino R. In vitro pathological model of osteopenia to test orthopedic biomaterials. Artif Cells, Blood Subs, Immob Biotech. 28:181–192. 18. (2000)
- Turner AS, and Villanueva AR. Histomorphometry of the iliac crest in 9-10 year old ewes. Proc. Vet. Surg. 22:413. (1993)

- Vanderburgh J, Sterling JA, Guelcher SA. 3D Printing of Tissue Engineered Constructs for In Vitro Modeling of Disease Progression and Drug Screening. Ann Biomed Eng. 45(1):164-179. (2017) doi: 10.1007/s10439-016-1640-4.
- Velasco MA, Narváez-Tovar CA, Garzón-Alvarado DA. Design, materials, and mechanobiology of biodegradable scaffolds for bone tissue engineering. Biomed Res Int. 729076.(2015) doi: 10.1155/2015/729076.
- Vidigal GM Jr, Groisman M, Gregório LH, Soares Gde A. Osseointegration of titanium alloy and HA-coated implants in healthy and ovariectomized animals: a histomorphometry study. Clin. Oral Implants. 20(11):1272-7. (2009). doi: 10.1111/j.1600-0501.2009.01739.x.
- Wagenseil JE, Mecham RP. New insights into elastic fiber assembly. Birth Defects Res C Embryo Today. 81(4):229-40. (2007) doi: 10.1002/bdrc.20111.
- Wang H, Pieper J, Peters F, van Blitterswijk CA, Lamme EN. Synthetic scaffold morphology controls human dermal connective tissue formation. J Biomed Mater Res A. 74:523-532. (2005)
- Wegner J, Loser K, Apsite G, Nischt R, Eckes B, Krieg T, Werner S, Sorokin L. Laminin α5 in the keratinocyte basement membrane is required for epidermal-dermal intercommunication. Matrix Biol. 56:24-41. (2016) doi: 10.1016/j.matbio.2016.05.001.
- Westerhof W, Dingemans KP. The morphological details of globular keratohyalin granules. J Cutan Pathol. 13(5):375-82. (1986)
- Westerhof W, Dingemans KP. The morphology of keratohyalin granules in orthokeratotic and parakeratotic skin and oral mucosa. Int J Dermatol. 26(5):308-13. (1987)
- You HL, Eng HL, Hsu SF, Chen CM, Ye TC, Liao WT, Huang MY, Baer R, Cheng JT. A PKC-Sp1 signaling pathway induces early differentiation of human keratinocytes through upregulation of TSG101. Cell Signal. 19(6):1201-11. (2007)
- Yu X, Tang X, Gohil SV, Laurencin CT. Biomaterials for Bone Regenerative Engineering. Adv Healthc Mater. 4(9): 1268–1285. (2015) doi: 10.1002/adhm.201400760
- Zhang L, Peng LP, Wu N, Li LP. Development of bone marrow mesenchymal stem cell culture in vitro. Chin Med J (Engl). 125(9):1650-5. (2002) Review.

Chapter 2

Models setting and optimizations

III. Introduction

Mucoperiosteum is a complex structure composed of three main compartments: epithelium, connective tissue, and bone. These components are strongly interconnected, and their interaction plays a fundamental role in the regenerative and homeostasis processes. In the dental implantology, most of the devices are designed to be integrated even with the mucoperiosteum complex.

The final goal of this thesis project was to develop an interconnected mucoperiosteal model able to mimic all the fundamental interplay. To pursue this aim, the most critical cell types composing the mucoperiosteum were considered: mesenchymal stem cells (MSC), MSC-derived osteoblast (OB), gingival fibroblast and oral keratinocytes.

3.1. Human mesenchymal stem cells (hMSC) and the osteogenic differentiation

Human mesenchymal stem cells (hMSC) are defined as non-hematopoietic multipotent stem cells with the capability to differentiate toward all the mesenchyme cell lineage: osteoblasts, chondrocytes, adipocytes, fibroblast and smooth, cardiac and skeletal myofibroblast. MSCs are mainly found in the stromal tissues such as the bone marrow (the first sources of hMSC identified; Gartner et Kaplan, 1980), the fat tissue, the periosteum, the periodontium, the periosteum and the dental pulp (Klees et al., 2007) and in all tissue close to the perivascular niches (Hass et al., 2011). The different tissue-specific population present similar properties, such as the self-renewal, the regenerative potential, the immunomodulatory properties and some surface markers (necessary for a correct hMSC selection) such as the cluster of differentiation (CD) (CD29, CD44, CD73, CD90, CD105) and they lack the expression of CD14, CD34, CD45 and HLA (human leukocyte antigen)-DR (Hass et al., 2011) as summarized in table III-1.

However, hMSC from difference source present a considerable variance in their trans-differentiation potential, for instance, oral-hMSC can be easily trans-differentiate in the endodermal lineage cells such as neurons in comparison with bone marrow-derived -hMSC (Fawzy El-Sayed et al., 2018) while the latter can be easily trans-differentiate in cardiomyocyte in comparison with O-hMSC (Eisenberg et al., 2006).

Table III- 1 *Specific surface marker expression characteristic of mesenchymal stem cells isolated from adipose tissue, bone marrow, and oral cavity.*

	Adipose hMSC	**Bone-Marrow hMSC**	**Oral hMSC**
Positive Marker	CD9, CD13, CD29, CD44, CD54, CD73, CD90, CD105, CD106, CD146, CD166, HLA I, STRO-1	CD13, CD29, CD44, CD73, CD90, CD105, CD166, STRO-1	CD13, CD29, CD44, CD73, CD90, CD105
Negative Marker	CD11b, CD14, CD19, CD31, CD34, CD45, CD79α, CD133, CD144, HLA-DR	CD14, CD34, CD45	CD34, CD38, CD45, CD54
References	Schaffler et al., 2007 Zulk et al., 2002	Pittenger et al., 1999 De Ugarte et al., 2003	Ponnaiyan et al., 2014 Mitrano et al., 2010

From a microscopical point of view, hMSCs arising from different tissue cannot be morphological distinguished. Within hMSC populations, 3 different subpopulations can be recognized: small rapidly self-renewing cells (the most "stem" subtype), spindle-shaped cells (the most abundant subtype) and large, flattened cells (differentiated cells) (Haasters et al., 2009).

MSCs have a paracrine and immuno-modulatory capability since they secrete several classes of soluble factors, such as cytokines, chemokines, or growth factors, which mediate diverse functions and regulates the crosstalk between different cell types.

The immunomodulatory properties of hMSC have been a stimulating topic, even for clinicians. Recently, adult hMSCs produced by Prochymal (Osiris Therapeutics, Inc.) for the treatment of acute graft versus host disease (GVHD) in paediatric allogeneic transplant has been approved in Canada and New Zealand. Several studies have highlighted the effect of MSCs in the bone marrow microenvironment, where they act both as support for co-transplanted hematopoietic cells and donor stem cell engraftment (Newell et al., 2014).

Locally, MSCs interact with all immune cell types by secreting both anti-inflammatory and pro inflammatory factors influencing the immune cells behaviour (Soleymaninejadian et al., 2012). Above all, MSCs secrete TGF-β and IL-6 and to induct the T regulatory cells (Th17), the chemo-attractants IL-8, MCP-1, CCL8, and prostaglandins E2 and F1 which induce the migration of monocyte and macrophages towards the inflamed site (Bettelli et al., 2006; Hoogduijn et al., 2010).

In addition, MSC membranes express several co-stimulatory and co-inhibitory molecules, such as CD40 and programmed death-ligand 1 (PD-L1), via which MSC directly modulate immune cell activity and proliferation (Augello et al., 2005; Franco et al., 2014) as well cell adhesion molecules (ICAM-1 and VCAM-1), via which MSC recruit activated

immune cells to increase their exposure to anti-inflammatory signals (Ren et al., 2010). Those features might be particularly crucial in the implantology field, where the uncontrolled inflammation may lead to implant failure.

hMSC are well-known to act a pivotal role in tissue regeneration both locally, with the differentiation in specific cell type to cover defects and at a distance, by secreting several paracrine and trophic molecules which act directly on the injured cells or indirectly, by inducing other cell type to produce soluble factor thus increasing exponentially the signaling potential. For instance, after injuries, MSCs reduce the cellular damage by inhibiting the fibrotic tissue formation, promoting angiogenesis to increase the nutrients available to the damaged site, modulating the immune response, and recruiting progenitors and other stem cells to the injured site to start the tissue renewal. The principal factors involved in tissue regeneration are summarized in figure I-9.

MSCs, and in particular the foetal ones, possess a damage-site-homing capacity; several distinctive steps characterize this migration process. The homing starts with the expression of homing receptors (i.e., VLA-4) by circulating MSCs, which bind the corresponding co-receptors presented on endothelium (i.e., VCAM-1). Their interaction leads to the connection of circulating cells to the endothelium and induces a rolling effect on the cell surface and subsequent extravasation (Sohni et al., 2013; Eggenhofer et al., 2014). MSCs express a considerable number of this adhesion/homing molecules, including integrins and selectins, this is particularly interesting in the cell therapy field because MSC can be direct toward specific tissue by regulating this receptor (Marquez-Curtis et al., 2013).

Another important factor involved in the homing process is fibronectin (FN), which binds to the ECM components such as collagen, fibrin, and heparan sulfate, playing a fundamental role within the processes of cell adhesion, growth, migration, differentiation, and wound healing (Valenick et al., 2005). FN binds VLA-4 by exposing the V-region to increase MSC adhesion to the ECM, improving and regulating the homing process. This process is regulated by several growth factors such as PDGF or IGF-1, which binds tyrosine kinase receptors; indeed, the hMSCs expressing the PDGF receptor (PDGFRβ) have a superior migratory capacity (Anderse et al., 2015). Various chemokines (CCR2, CCR3, CCR4, and CCL5) are also involved in the homing process (Honczarenko et al., 2006) with an enhanced effect in presence of TNF-α and IL-1β (which induce the chemotactic cytokine CXCL family); those suggesting that the inflammatory state, both local or systemic, influence the homing process (Sohni et al., 2013; Eggenhofer et al., 2014).

Due to their stemness potential, hMSC easily adhere to different substrates. Indeed, hMSC are widely growth onto common plastic surfaces in basal media such as DMEM or DMEM/F12 enriched with 10% of hMSC certified FBS (which guarantee the stem potential for higher passage numbers [(Pal et al., 2009)]. Another suggestion for prolonged the stem features keeps their confluence between 50 and 80%, since the low confluence may induce an excessive proliferation rate with a faster differentiation and the high confluence induce the osteoblastic phenotype. Finally, Haque et al. (2013) showed that a hypoxic environment (2-9 % O_2) could considerably improve growth kinetics, genetic stability, and expression of chemokine receptors during the in vitro expansion of MSC. In particular, the hypoxia condition allows the maintenance of the homing molecules CXCR4 and CX3CR1 that are physiologically expressed at high levels in the bone marrow and ischemic tissues.

Recently, the role of mechanical forces on MSC differentiation fate has been intensively studied. Indeed, it has been observed that the mechanical stimulation can control MSC differentiation. The cytoskeleton, already known to be

a key component in the mechanotransduction processes, has been recognized as a crucial component in MSC differentiation processes. Indeed, when MSC spread onto stiff materials and several focal adhesion structures are visible, the hMSCs are prone to differentiate towards osteoblast lineage (as happened for hard and porous structures) while the spherical morphology is associated with chondrogenic and adipogenic fate (Mathieu et al., 2012). Finally, MSC can be easily induced toward the osteoblastic fate using the differentiation factors. The most used differentiation cocktail includes of Dexamethasone, Ascorbic acid, and β-glycerol phosphate; however, the use of EGF, recombinant bone morphogenetic proteins (BMPs), Vitamin D and other proteins have been successfully employed (Augello et al. 2010).

3.1.1. Osteoblasts and Bone engineering

Bone is a specialized hard connective tissue that supports and protects the inner organs and provides structural integrity (Brotto et al., 2014; Kang et al., 2016). During human life, bone undergoes numerous remodelling, which guarantees the high quality and stability of bone itself and acts as the calcium reservoir (Saraanan et al., 2018; Arumugam et al., 2018). The bone structure is mainly composed of collagen fibres (organic part), and calcium phosphate (apatite) crystals (the inorganic part) that are infiltrated within the collagen matrix and form the inorganic portion of the bone (Saraanan et al., 2018). Within each bone, two different structures are found: cortical bone (the compact and exterior part) and the trabecular (the internal, flexible and porous portion were calcium ions exchange and other metabolic activities of the bone take part) connected by thin vessels which guarantee the communication between the two components. The cortical bone consists of several osteons (metabolically active column composed of osteoblast and osteoclast, which surround the Haversian canal) and is covered by a periosteum (outer surface), and an endosteum (the inner surface covered by a thinner layer of osteoblast). The endosteum is the boundary between the cortical bone and the trabecular bone. The trabecular bone is composed of trabeculae that are aligned towards the mechanical load distribution that a bone experiences within long bones such as the femur. The bone is actively remodelled throughout life by bone cells to guarantee the optimal quality of the bone itself. This process is activated by the osteocytes, which act as mechanosensory and orchestrate the activities of the other bone cell. In particular, the action of osteoblast (known as bone-forming cells), osteoclast (known as bone resorption cells) that act in equilibrium with osteoblast (Laurin et al., 2011).

Osteoblasts are polarized and cuboidal cells that show morphological characteristics of protein-synthesizing cells, such as the abundant rough endoplasmic reticulum (RER), a prominent Golgi apparatus, and several different secretory vesicles. In particular, osteoblasts secrete the osteoid (the unmineralized organic part that forms before bone maturation) (Marks et al., 1988; Demoulis et al., 1997; Capulli et al., 2014).

As previously showed, hMSC under osteogenic factors stimulation express the following molecules: the bone morphogenetic proteins (BMPs), members of the Wingless (Wnt) pathways, Runt-related transcription factors 2, Distal-less homeobox 5 (Dlx5) osterix (Osx) and *Runx2*; the latter upregulate osteoblast-related genes such as *CollA1* and *ALP* (characteristics of preosteoblast)*, BSP*, *BGLAP*, and *OCN* (characteristic of mature osteoblast*)* (Grigoriadis et al., 1988; Nakashima et al., 2001; Fakhry et al., 2013). Moreover, several authors reported that other factors such as fibroblast

growth factor (FGF), microRNAs, and connexin 43 play essential roles in osteoblast differentiation (Kapinas et al., 2010; Buo et al., 2014).

The synthesis of bone matrix by osteoblasts occurs in two main steps: deposition of an organic matrix (by secretion of ECM proteins such as type I collagen, OCN, osteonectin, BSP II, osteopontin, decorin, and biglycan) and its mineralization. Also, the mineralization itself is divided into two steps; the first step is named the vesicular phase, in which osteoblast release negatively charged matrix vesicles which bind proteoglycans immobilizing calcium ions on the immature bone matrix. Then, calcium is released and, with the phosphate obtained by ALP activity on phosphate-based compounds, form the hydroxyapatite crystals. The second step is named the fibrillar phase and occurs when the supersaturation of calcium and phosphate ions inside the matrix vesicles leads to the rupture of these structures, and the hydroxyapatite crystals spread to the surrounding matrix (Glimcher et al., 1998; Boivin et al., 2002 and 2008).

Currently, osteoblast is a valuable tool in several research fields in particular to investigate *i)* the biochemistry and physiology of bone formation, *ii)* the molecular and cellular basis of human bone disease, *iii)* the mechanisms by which bone resorption is coupled to bone formation, *iv*) the anabolic agents and in general the meatbolosm, *v)* the safety and efficacy of new biomaterials (Dillon et al., 2012).

In the last decades, several porous scaffolds for bone regeneration, design to be repopulated with MSC, have been developed.

A successful bone scaffold should promote cell adhesion, infiltration, and growth associated with suitable mechanical properties. To obtain this, the 3D-structures should possess well-interconnected pores that allow cell infiltration and nutrient exchange. Moreover, the degradation rate should follow the natural bone remodelling process, and the waste product must be non-toxic or non-immune-interactor compounds (Barradas et al., 2010; Gentile et al., 2014; Prasadh et al., 2018)

One of the most updated trends in bone tissue engineering involves the use of the 3D-printer to obtain highly reproducible geometry improving the MSC differentiation even in the absence of differentiation factors (Zhang et al., 2019). Another strategy often employed is the use of sponge materials; the advantages of these materials, characterized by high resistance to the compression and easy handling, is the tuneable resorbability. The literature reports a huge variety of different materials ranging from collagen-based material that can be easily functionalized with pro-regenerative moieties (Kowalczewski et al., 2018) to piezoelectric material which provides the electric stimulation (Tandon et al., 2018).

3.2. Human gingival fibroblast

Fibroblasts are a mesenchymal cell type that drive several functions during development and regeneration processes. Morphologically, fibroblasts have the characteristics of all secretory cells, including numerous mitochondria, the extended RER, the prominent Golgi apparatus, and numerous vesicles.

Physiologically, fibroblasts are involved in the synthesis of extracellular matrix protein of the connective tissue (such as collagen and proteoglycans) and play important roles in wound healing. During wound healing, fibroblast proliferates faster to support the regeneration of the damaged site acting with several strategies: *i*) breaking down the fibrin clot formed during the damage allowing the new ECM and collagen structures formation, *ii*) becoming "contractile" by developing intracytoplasmic actin filaments to participate in wound contraction, *iii*) secreting growth factors and cytokines, such as TGF-β to induce keratinocytes migration. However, sometimes, due to the excess of collagen production during the wound healing process, fibroblasts may lead to chelodids scar formation (Bainbridge, 2013).

Fibroblasts are one of the most available mammalian cell types (small biopsy are enough to obtain a large amount of fibroblast) and one of the most accessible types of cells to grow in culture (being mesenchyme-like cells they easily adhere on the plastic surface). Gingival fibroblasts are the major constituents of gingival tissue and express a wide variety of surface molecules, including CD9, CD26, CD55, CD59, CD63, CD71, CD86 CD95, CD99 and CD117 (Palaiologou et al., 2011).

3.3. Human oral keratinocytes

Oral keratinocytes form the primary barrier to physical, microbial, and chemical agents that cause injury in the mouth. They are involved in the proinflammatory process through the production of cytokines either constitutively or after a variety of stimuli. Indeed, oral keratinocytes also participate in controlling oral infections through an inflammatory process that involves the secretion of different interleukins, such as IL-1β and IL-18, in collaboration with local macrophages. Oral keratinocytes express a variety of differentiation markers highly dependent on their microenvironment and influenced by calcium-induced changes in the transcription of target genes (chapter 3).

The pluristratified squamous epithelia are composed of several layers of keratinocytes at different differentiation stages and monolayer culture conditions cannot mimic this characteristic. In particular, drugs penetration and cytokine secretion and microbial interaction are completely impaired in 2D versus 3D condition. To overcome those limitations, several researchers focused their attention on producing complex and highly organized 3D models of pluristratified squamous epithelia (chapter 1 and 3).

3.4. Crosstalk between mesenchyme and keratinocytes

Squamous pluristratified epithelia are composed of several layers of keratinocytes, organized in 4 groups of keratinocytes at different stages of differentiation. Accordingly, to the body site, keratinocytes are intercalated by other cells type such as melanocytes and Langerhans cells and covers different types of connective tissue. The most common pluristratified epithelia are the epidermis, underlined by the dermis, and the oral epithelia, underlined by the lamina propria. The main components of the connective tissue are the fibroblast, which shown an enormous heterogeneity accordingly to the body site function. Several studies have proved that fibroblasts from lamina propria influence keratinocytes behaviour (Sharpe et al., 1988) in the 3D epithelial model. In particular, the fibroblast density plays a key role in obtaining an optimal epithelial developed (Almeda et al. 2016).

Different epithelia have been developed to provide the optimal support and protection to the underlining structures such as glands, bones, or muscle (Gibbs et al. 2000). In particular, the epithelial thickness and the keratinization varied accordingly to epithelial function. The oral mucosa represents an interesting context to study the epithelial differentiation (Clausen et al., 1986). Indeed, although oral keratinocytes have the same embryological origin, in the oral cavity, they are differently arranged in both keratinized (masticatory mucosa), non-keratinized (lining mucosa) and miscellaneous (tongue and palate) epithelia (Squier, 1991). The explanation of these phenomena cannot be ascribable only to mechanical stress but, accordingly to other studies, the underlining connective tissue plays a vital role (Squier et al., 1981; Neupane et al., 2018).

Although several old studies suggested that the epithelial differentiation is an intrinsic property of keratinocytes which are "programmed" to produce a specific epithelium (de Luca et al., 1990; Gibbs and Ponec, 2000), the most recent and accredited theory is that mesenchymal tissue strongly influences the epithelial cell differentiation. For instance, recombinant study on the palate development showed that, exchanging the stromal counterpart of hard and soft palate, the patterns of keratinization changed (Mackenzie et al., 1979; Neupane et al., 2018), other studies reported changing in in morphogenesis and cytodifferentiation (Schweizer et al., 1984) and in cytokeratin expression in particular when immortalized keratinocytes are used. Merne and Syrjänen, showed, in 2003, that the immortalized HaCaT cells, which usually do not express the terminal differentiation marker such as CK10, can be induced toward terminal differentiation by young primary dermal fibroblast.

The lamina propria contains several mesenchymal stem cells, and in 2015, Sivamani et al. showed that MSC and keratinocytes influence each other. The phenomenon is related to the cultivation methods: when MSC was grown in direct contact with keratinocytes, they acquired epithelial phenotype while when they were grown using a transwell system, they expressed early neuronal or myofibroblast markers. However, the effect on keratinocytes differentiation was not well established since the latter was grown in monolayer.

The primary intent of the first part of the present Ph.D. thesis was the set-up of advanced 3D in-vitro organotypic models, including oral epithelium and the underlined tissues, which is composed of the variety of cells not available in the commercial models.

To do this, we had to deal with several technical issues including the optimization of the protocols to the co-cultivating different cell types in both 2D and 3D. To pursue this aim we:

- assessed and selected the best shared conventional media to co-cultivate mesenchyme and epithelial cells without losing the stem and secretory properties of MSC
- optimized an already available bovine tendon collagen/nano-hydroxyapatite (BTC/nHA) scaffold, developed for in-vivo implantation, as optimal support to mimic bone features in static conditions.
- established a custom made keratinized oral mucosa model, starting by a commercially available primary oral keratinocytes (HOK; CliniScience) and primary gingival fibroblast.

IV. Materials and methods

4.1. Standard Cells culture condition:

4.1.1. Primary cells culture condition

Human Oral Keratinocytes (HOK) were purchased from CliniScience (Rome, Italy) and maintained in EpiLife® Medium (Invitrogen, Milan, Italy) supplemented by HKGS factors. Human Mesenchymal Stem Cells (hMSC) were obtained from Lonza (Milan, Italy) and maintained in DMEM low glucose supplemented with 10% FBS (all provided from Sigma, Milan, Italy). Human Gingival Fibroblasts (HGF) and Dermal Fibroblast (HDF) were isolated from healthy donors and maintained in DMEM high glucose plus 10% heat-inactivated fetal bovine serum (FBS).

Before confluence, all cell types were trypsinized, resuspended, and plated for the experiments 10^4 cells/cm^2.

The primary cells used, and their media, are summarized in table IV-1.

Table IV-1 *Summary of primary cell used and their gold-standard medium*

Cell type	Company	Medium
Oral keratinocytes	CliniScience	Epilife+HKGS
hMSCs	Lonza	DMEM-LG+10% hMSC optimized FBS
Fibroblast	Isolated	DMEM-HG+10% FBS

4.1.2. Cell lines culture condition

H-tert immortalized Human Foreskin Keratinocytes (ATCC® CRL-4048™) Ker CT 1080 were obtained from Lonza (Milan, Italy) and maintained in EpiLife® Medium (Invitrogen, Milan, Italy). ND7/23 (Mouse neuroblastoma x Rat neuron) were purchased from Sigma Aldrich (Milan, Italy) and maintained in DMEM high glucose plus 10% heat-inactivated fetal bovine serum (FBS). Human fetal osteoblasts (HFOB; ATCC® CRL-11372™) were purchased by ATCC (Manassas, Virginia) and maintained in a mixture of 1:1 DMEM/F12 media enriched with 10% FBS. Before confluence, all cell types were trypsinized, resuspended and plated for the experiments 10^4 cells/cm2.

The immortalized cells used, and their media, are summarized in table IV-2.

Table IV-2 *Summary of immortalized cell used and their gold-standard medium*

Cell type	Company	Medium
Ker CT 1080	Lonza	Epilife+HKGS
ND7/23	Sigma Aldrich	DMEM-HG+10% FBS
HFOB	ATCC	DMEM/F12+10% FBS

4.1.3. Optimization of culture media for every cell type

In order to assess the best common culture condition for HOK and hMSC, both cell types were kept in cultured with different culture media: EpiLife, OKM (CliniScience), DMEM low-glucose with 10% FBS and FAD2 medium (70% DMEM, 25% F12, 5% FBS enriched with 1,88 mM CaCl2, 50 mM Glycerol, 10^{-10} mM Cholera Toxin, 10 ng/ml EGF, 5 µg/ml Insulin, 0.4 µg/ml Hydrocortisone, 5 µg/ml, apotransferrin and $2*10^{-3}$ nM Triiodo-thyronine) enriched or not with osteoblast differentiation factors (DF) as summarized in table IV-3.

Table IV-3 *Summarizing of media tested for each cell type.*

	Cell Type	
	hMSC	**HOK**
Media	DMEM 10% FBS	OKM
	OKM	OKM+DF
	EpiLife	EpiLife
	FAD2	EpiLife+DF
		FAD2
		FAD2+DF

4.1.4. Viability assay

The colorimetric AlamarBlue assay was performed after 1 and 7 days of culture to assess the viability HOK and hMSC kept in their respective media, in presence or absence of the corresponding differentiation factors. Following the manufacturer instruction, 50 µL of AlamarBlue™ (Sigma Aldrich, Milan, Italy) solution (0.1% in PBS) were spotted into each well containing 500 µl medium; plates were incubated for 4 hours in the dark in an incubator at 37°C, 5% CO2. The medium was then collected and spotted in 96-well black plate and the fluorescence evaluated by a spectrophotometer (Ex 540, Em 590; Sensibility 75%). Cells growth in their "gold standard" medium were taken as control (100% of viability), and results were expressed as viability percentage according to that control.

4.1.5. Migration assay

Scratch assays were performed to evaluate if hMSCs promote keratinocytes migration and to compare if this effect is different between oral and skin keratinocytes.

Briefly, HOKs and Ker CT 1080 were seeded in 24-well plates and maintained in culture until confluence. Once confluent, a sterile p200 tip was used to scratch the cells that subsequently were washed with pre-warmed DPBS and treated with EpiLife media kept in contact with hMSCs for two days in an incubator. Keratinocytes growth in fresh media were used as control. Images were collected after 0, 6, 18 and 24 hours using a ZOE Fluorescent Cell Imager (Bio-Rad).

4.2. Osteogenic differentiation protocol

Uncommitted hMSCs were seeded at $5x10^4$ cells/cm2 and maintained in culture until 80% confluence. When hMSCs reached the desired confluence, the medium was enriched with 50 µM Ascorbic Acid, 10 mM β-glycerol-phosphate and 100 nM Dexamethasone (osteogenic medium) to induce the differentiation toward osteoblastic (OB) phenotype. The differentiation medium was freshly prepared and changed every third day; cells were fixed every week until complete differentiation was reached. At each medium change, the medium was collected, centrifuged for 5 minutes at 1200 rpm and stored at -20° until use.

4.2.1. Osteogenic differentiation protocol evaluation: Alkaline Phosphatase (ALP), Von Kossa and Alizarin Red staining

In order to verify the differentiation state of hMSCs, Alkaline Phosphatase (ALP) staining was performed every week of culture in osteogenic medium. For each time point, differentiated control and undifferentiated cells were fixed for 15 minutes at 4° C, washed in bi-distilled water, and then stained. ALP stain solution (1:0.04 Fast Violet and Naphthol) was added to dry wells and plates were then incubated for 45' at room temperature. Subsequently, cells were washed several times in PBS and let dry.

Von Kossa and Alizarin Red staining were made after 3 and 4 weeks to check the formation of calcium and phosphate nodules.

To perform Von Kossa staining, cells were incubated with 1% silver nitrate solution and treated for 30' under UV lamp; un-reacted silver was removed with 5% sodium thiosulfate solution. Wells were washed several times in bi-distillate water and let dry at RT.

Alizarin Red solution was prepared by solving 0.2 g of Alizarin Red powder in 10 ml of bi-distilled water and the pH was adjusted to 4.2 before use; then, the solution was applied for 15' at room temperature and the excess stain was washed out and wells were let dry.

Finally, images were collected using a stereomicroscope.

4.3. Bone substitute optimization

4.3.1. Scaffold preparation

The scaffold selected was composed by 50:50 nano Hydroxyapatite (nHA) and Bovine Tendon Collagen (BTC) and prepared following the method from Salgado et al. (2015). Briefly, Type I insoluble collagen was diluted in 100 mM chloride acid solution to a 2% concentration homogenized for 2 hours and kept at 4 °C. After, 0.5 g of nHA were solved in 100 mM chloride acid and mixed with an equivalent volume of collagen solution. Subsequently, 10 mM N-Hydroxysuccinimide (NHS) and 40 mM 1-Ethyl-3-(3-dimethylaminopropyl) carbodiimide (EDC) were added to the collagen/nHA solution and transferred to a cylindric mold with a diameter of 5 mm, then freeze at -18 °C for 24 hours to complete the crosslinking. Afterward, it was thawed at room temperature and the scaffold washed with distilled water. Finally, the scaffold was dried in a vacuum oven at -80° with 0.1 bar for 24 h and stored at 4°. Before use, the scaffold was cut in 0.5 cm length piece and sterilized with at least three passages in EtOH 70% (30 minutes each) and several washes in PBS 1x in sterile conditions.

4.3.2. Scaffold repopulation

In order to improve cells penetration inside the scaffold, the suitability of the fibrin gel drop seeding method was evaluated. Briefly, hMSCs were trypsinized, counted, and resuspend $2x10^6$ cell/ml in fibrinogen (6 mg/ml in complete medium). Next, 1,5 U/ml thrombin were added immediately before seeding for each sample, and a drop containing 10^5 cells was added to each scaffold. Subsequently, the fibrin gel formation was inducted by mechanical stimulation and hMSCs were let adhere in the incubator. After 2 hours of incubation, scaffolds were submerged with 1.5 ml of DMEM 10% FBS and enable to grow for 24 hours. Finally, differentiation factors were added as described in section 4.2, and the viability was evaluated after 1, 3, 7, 14, 21 and 28 days as defined in section 4.1.4.

4.3.3. Dynamical Mechanical Properties (DMA) analysis

Dynamical mechanical analysis. Dynamical mechanical analysis (DMA) was conducted in order to characterize the mechanical behavior of collagen-nanoHA biocomposite scaffolds in the wet state under dynamic compression solicitation. Before any measurements, the specimens (4 mm thick, and 7 mm wide) were immersed in the culture medium until equilibrium swelling. The scaffolds were then subjected to compression cycles of increasing frequencies

ranging from 0.1 to 10 Hz at room temperature for 10 min, using a Tritec2000 dynamic mechanical analyzer (Triton Technology, UK). Three samples were measured for each type of scaffold.

For each sample, the storage modulus and the loss factor were evaluated.

The storage modulus representing the elastic component of a material is an indicator of the capability of the material to store energy during deformation and it is in inverse relation with the material stiffness.

The loss factor is the ratio between the amount of energy dissipated by viscous mechanisms and the energy stored in the elastic component, this formula provides essential information about the viscoelastic properties of the material.

Those properties quantify the stiffness and the resistance of a polymer and allow the prediction of polymer behaviour, in terms of withstanding and elasticity under compression.

4.3.4. Scanning electron microscopy (SEM) imaging

To observe the intracellular localization of the nanohydroxyapatite particles, the same samples of the subcutaneous implants for histological analysis (paraffin blocks) were used for SEM analysis. The tissues were reprocessed, according to Lighezan et al. (2009). Briefly, the tissues were de-waxed with xylene (12 h) and rehydrated (100%, 90%, 80%, 70% of ethanol-water and PBS solution). Afterward, the tissues were post-fixed with 1% OsO4 for 1 h. The samples were dehydrated with increasing concentrations of ethanol-water (50%, 70%, 90%, 95%, and 100%) and embedded in epoxy resin (Epon 812V R, Shell Chemical).

4.3.5. Confocal imaging

To determine cell morphology immunofluorescence assay was performed the samples were fixed with 3.7% paraformaldehyde (Sigma) for 30 min and then washed twice in PBS. Then, the materials were incubated for 5 min with 0.1% Triton X100 solution (Sigma), washed twice with 1% bovine serum albumin solution in PBS (BSA, Sigma) and the cytoplasm was stained with Alexa fluor conjugated phalloidin 594 (1:400, Invitrogen) at 2.5% in 1% BSA solution for 1 hour at room temperature and protected from the light. Samples were washed twice with BSA 1% and nuclei were stained with DAPI (4'-6-diamidine-2phenylindole at 0.2%, Invitrogen) for 5 min. After that, the scaffolds were washed twice with PBS and images were acquired with a Confocal Laser Scanning Microscopy (Leica SP2 AOBS SE camera), using the excitation lasers of 405 and 594 nm. Finally, videos were prepared using ImageJ software.

4.4. Established a custom made keratinized oral mucosa model

3D epithelial cultures were prepared according to the protocol described by Lambert et al. (2005) and Squarzanti et al. (2018). Briefly, a *lamina propria* substitute was prepared by enriching a collagen premix (20 ml Rat tail collagen type I 6.6 mg/ml, 2.5 ml 10x F12, 2.5 ml FBS, 250 µL PEN/Strep 100x, 60 µl NaOH 1 M) with $5x10^6$ HGFs, then allowed to contract to the appropriate shape for 2 days. When ready, $6x10^5$ HOKs were seeded onto each *lamina propria* substitute, let to adhere and become confluent. After four days of submerged culture, the 3D system was positioned at the air/liquid interface by adding cotton pads on the bottom to allow keratinocytes stratification. Culture media were

collected every third day and refreshed. After other 12 days, 3D cultures were formalin-fixed and embedded in paraffin for histological analysis. As control, a previously established dermal substitute composed of 20 ml Rat tail collagen type I 6.6 mg/ml, 2.5 ml 10x F12, 2.5 ml FBS, 250 µL PEN/Strep 100x, 60 µl NaOH 1 M with $5x10^6$ HDFs was used as the mucosal base.

4.4.1. Haematoxylin and eosin staining

HE staining was carried out onto the 4 µm thick tissue sections obtained from formalin-fixed paraffin-embedded 3D tissue cultures (Bio-Separation System, YSD-310, Yoshuda). Briefly, slides were rehydrated and stained with Hematoxylin for 10 minutes at room temperature (RT) and counterstained with Eosin for 5 minutes at RT. Lastly, tissue slides were rapidly dehydrated and mounted. Tissue morphology was finally optically evaluated under a Leica DM750 optical microscope at magnifications ranging between 10x and 20x (Leica Microsystems, Basel, Switzerland).

V. Results

5.1. Establishment of the common media for co-culture

5.1.1. Monolayer growth condition establishment: Viability Assay

Human mesenchymal stem cells (hMSCs) and human oral keratinocytes (HOK) growth in different chemically composite media. In particular, hMSCs growth in basal media enriched with 10% of highly nutrient foetal bovine serum (FBS) while HOK growth is severely affected by serum. Indeed, several types of serum-free media implemented with 5% of growth factor mixture. The most common media used for keratinocytes growth are: KSFM from Gibco, the OKM from CliniScience (both supplemented with the bovine pituitary extract), the Epilife from Gibco (supplemented by a mixture of recombinant protein, in particular, EGF) and the KGM from Lonza (supplemented with several recombinant proteins. Only KSFM has been previously used for hMSC/keratinocytes co-cultivation; a comparison between this medium and the others was impossible due to the presence of valid patents on all the keratinocytes media. Likewise, there were not found any papers in which hMSCs were growth in FAD media (used for the organotypic cultures) or in which keratinocytes were grown in the presence of osteogenic/differentiation factors (DF). Due to the lack of literature on this topic, preliminary experiments were performed to establish the suitability of the different media involved in the experimentation and follow protocol comparable with the previous works. The first experiments were performed to select a suitable common media to use for both hMSC and HOK in 2D and 3D conditions and assure that DFs do not affect HOK viability. To asses that purpose, both cell types were incubated for one week with all the media and their viability monitored by Alamar blue assay. In particular, hMSCs were growth with Epilife, OKM and FAD media, and the viability was compared with the gold standard medium DMEM supplemented with 10% of certified FBS while HOKs were growth in OKM, EpiLife and FAD media with or without differentiation factors. Epilife was selected as gold-standard.

Regarding hMSC, the viability assay shows that keratinocytes media, OKM, and EpiLife, initially increase hMSC metabolic activity but at the last experiment time point (7 days) the viability decreased until values comparable to the control. On the contrary, in FAD medium, hMSCs viability resulted steadily higher in comparison with the controls, but the slope of the growth curve results lower than the others.

Concerning HOK, a massive viability decrease is observed when cells are incubated with FAD; however, after seven days, all the viability levels were comparable and similar to the control. In all conditions tested, the DFs do not alter keratinocytes viability. As expected, for both cell types, cells viability value recorded for incubation with OKM and EpiLife results similar. All those findings are summarized in figure V-1. Considering the data shows, EpiLife was select as a common medium for hMSC and keratinocytes in 2D condition, and FAD medium was selected as the common medium for hMSC and keratinocytes in 3D. This preliminary data demonstrate that the effect showed by hMSC/HOK interaction depends on the cells crosstalk and is not an artificially contrived produced by the chemical composition of different media or the differentiation factors.

a)

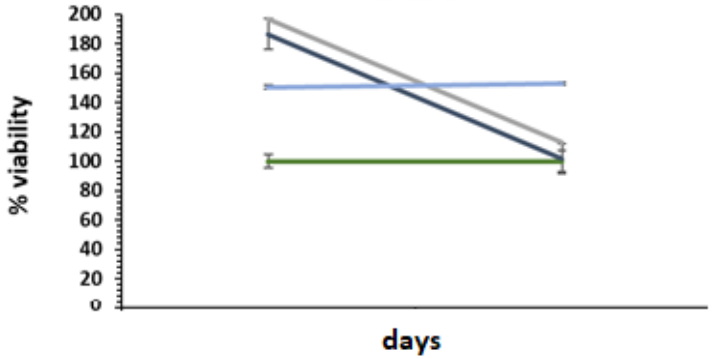

	1	7
DMEM LG 10% FBS	100	100
OKM	186,5955381	101,8494389
EpiLife	196,8878123	112,7096381
FAD2	150,5009472	152,5566391

b)

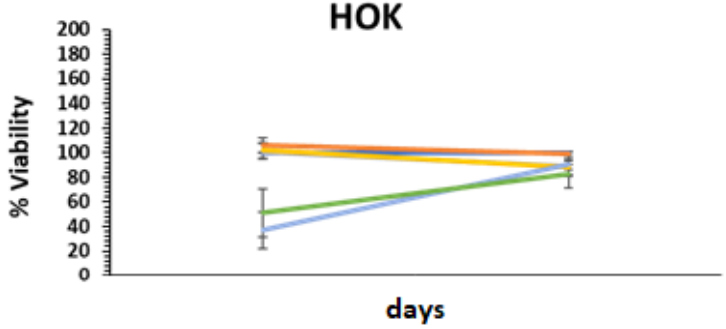

	1d	7d
OKM	100	100
OKM+DF	105,9783915	99,01383372
EpiLife	101,0465267	88,60928142
EpilLife+DF	102,0166286	88,19962396
FAD2	37,06274024	90,80532762
FAD2+DF	51,01293675	82,31666065

Figure V-1 *Graphics represent respectively, hMSC and HOK viability when incubated with each medium or combination of media. Data are presented as viability % percentage calculate on the control average (considered as 100%).*

5.1.2. Evaluation of hMSCs secretory capability into EpiLife medium: Migration assay

As already described in the introduction, hMSCs have an essential role in the wound healing process and in tissue regeneration; in particular, Walter et al. (2010) shown a pro-proliferative effect of hMSC conditioned medium (hMSC_CM) onto both fibroblast and keratinocyte. To confirm that hMSC, growth in EpiLife medium, keeps secreting the molecules that are involved in both skin and oral migration, a similar experiment was performed to evaluate the effect of hMSC_CM on keratinocytes migration and proliferation using a 2D scratch assay. For this assay, hMSCs were growth in EpiLife; the hMSC_CM was collected after two days of cultures, centrifuged to remove the dead cells traces and supplemented with fresh HKGS (EpiLife growth factors) before use. In the meanwhile, skin (ker CT 1080) and oral (HOK) keratinocytes were growth to 95% confluence. Immediately before incubating keratinocytes with hMSC_CM, a scratch was performed for each well on confluent cells.

Compared with Walter et al. (2010) results, both keratinocyte types migrate faster in the presence of hMSC secretome in comparison with the control (fig V-2). Because of the keratinocytes specific doubling time, the wound closure started after 12 hours for HOK and after 24 hours for ker CT 1080. However, HOK showed a faster proliferation and migration rate of ker CT 1080. This data is particularly important to validate the 3D tests described in chapter 3.

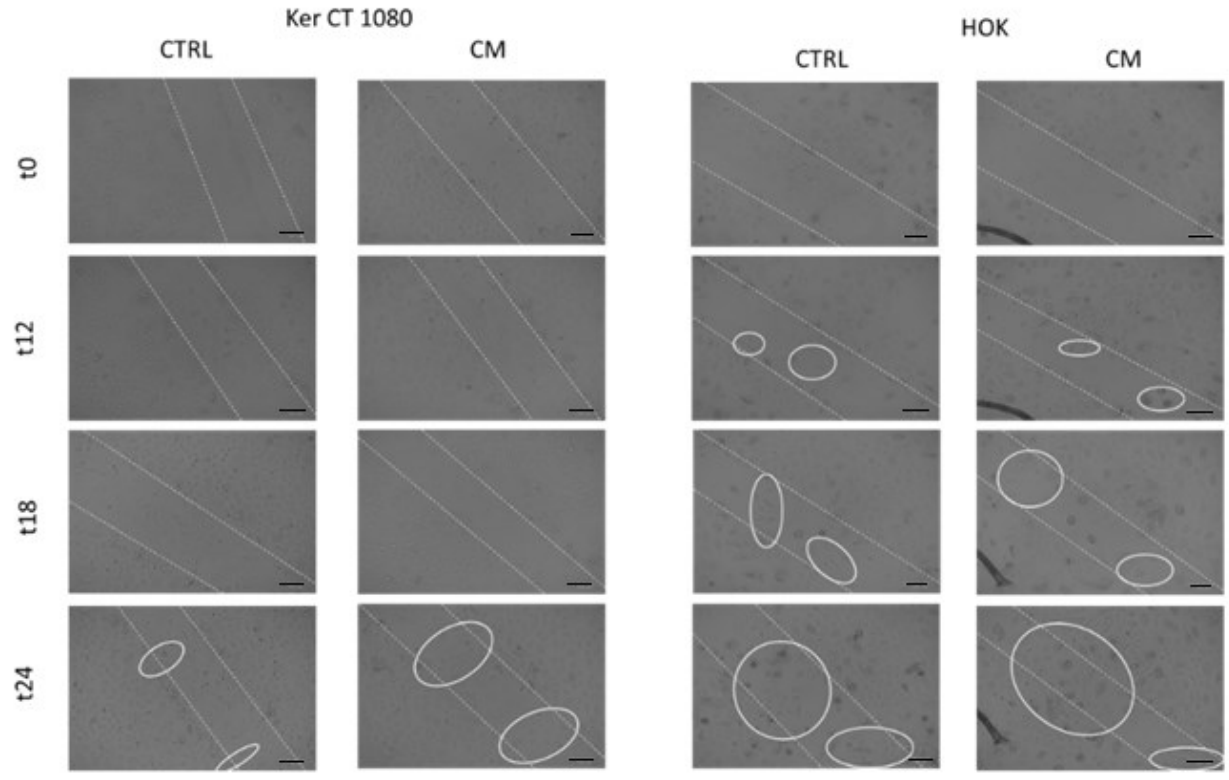

Figure V-2 *Pictures show skin and oral keratinocytes response to hMSC CM. White circle point keratinocytes migration area. In the first row, untreated skin keratinocytes start to migrate within the scratch after 24 hr while, at the same time point, treated skin keratinocytes invaded a larger scratched area. In the third and fourth row, both untreated and treated oral keratinocytes started their migration after 12 hr. Despite, after 24 hr, treated oral keratinocytes covered a larger scratched area. Magnification 10x, bar scale 100 µm.*

5.2. hMSC osteogenic differentiation

Before proceeding with keratinocytes treatments, the correct osteogenic differentiation of hMSC was evaluated. To pursue this aim, hMSCs were treated for one month with the osteogenic factor as described in paragraph 4.2 and every week 4 wells per stain were fixed and stained with alkaline phosphatase (ALP), Von Kossa and Alizarin red staining to follow the differentiative phases.

The phosphatase alkaline is expressed by osteogenic lineage-committee cells and can be detected by ALP stain while Von Kossa and Alizarin red respectively stain the calcium and phosphate deposits characteristic of the mineralization process. The differentiation factors are supposed to induced ALP expression in hMSC within the first two weeks and the mineralization of the matrix after the third week.

In accordance with other authors (Kulterer et al., 2007), between the second and the third week of differentiation, protein expression changes to promote mineralization (here proved by Von Kossa and alizarine Red staining) of the matrix. This switch is related to the downregulation of the proliferation gene such as TGF-β2 or matrix protein genes such as collagen 1 with the consequent up-regulation of mineralization genes such as osteopontin, and osteonectin.

As shown in figure V-3, ALP stain resulted positive already after 1 week of differentiation treatment, the expression of alkaline phosphatase indicates the hMSC gene expression shift toward osteoblastic lineage. Regarding Von Kossa and Alizarin red staining, both resulted negative until the second weeks of differentiation while red and black dots, the respectively characteristic stain of Alizarin Red and Von Kossa, were detected at the mineralization nodules after the third week.

In order to assess the appropriate differentiation, for all experiments in which CM was collected, hMSC were seeded in control wells weakly stained to evaluate the expression of the phosphatase alkaline and the mineralization. To avoid methodological bias, media obtained by incorrectly differentiated cells were discarded.

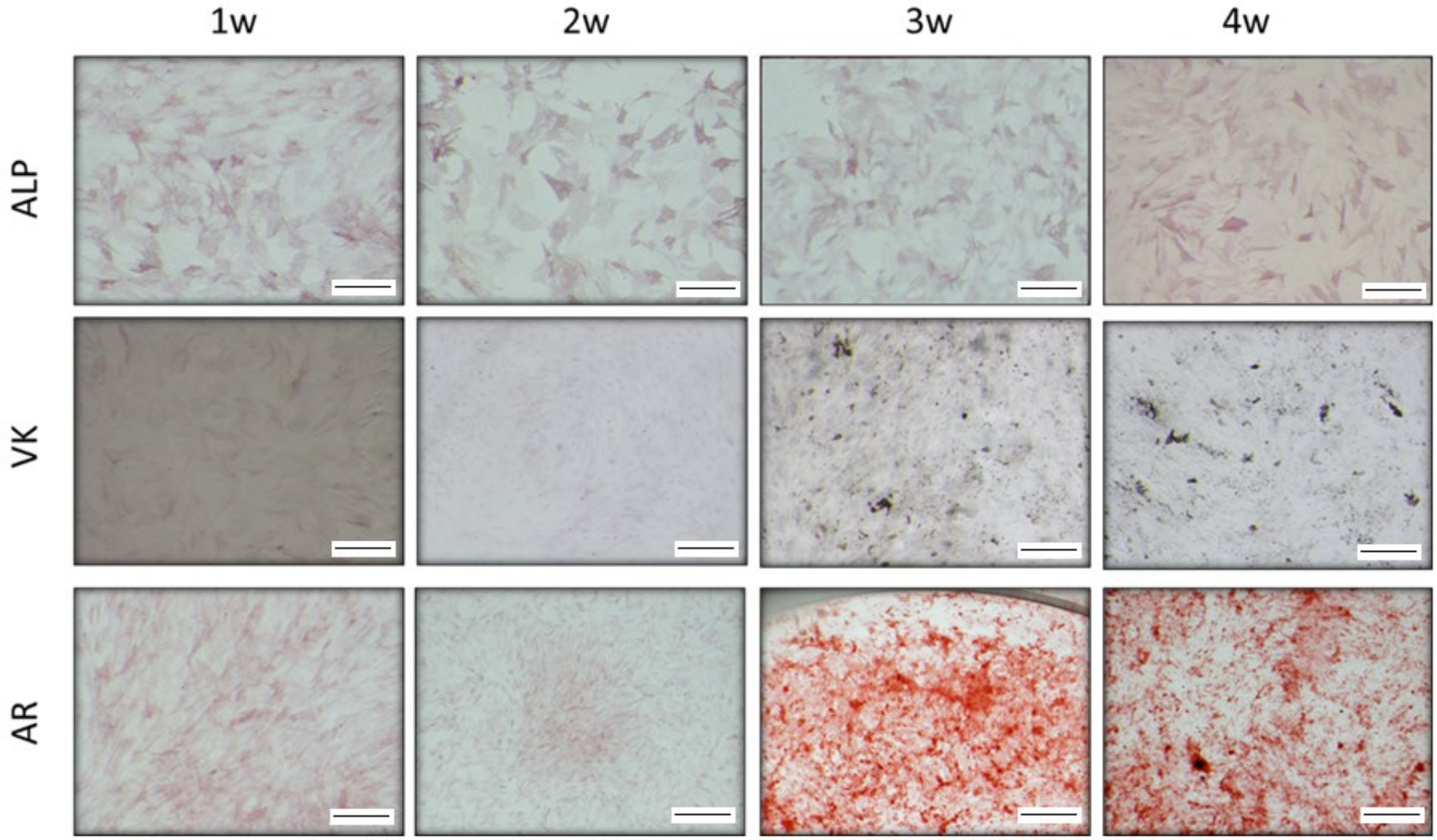

Figure V-3 *hMSC osteogenic differentiation assessment at all time points via ALP: alkaline phosphatase; VK: Von Kossa; AR: Alizarine Red assay. ALP stain (1° raw) resulted positive since the first week as expected. AR and VK resulted positive after three weeks (2° and 3° row; 3° and 4° column). Alizarin red counterstains the negative cells (3° row; 1° and 2° column) in pink. Magnification 6,2x, bar scale 50 µm*

5.3. Scaffold development

5.3.1. Preliminary data

To obtain a composite and functional mucoperiosteum model, the sponge-like bone substitute developed by Salgado et al. (2015) was selected. The nominated sponge is made by a bovine tendon collagen (BTC) hydrogel, supported by nano-hydroxyapatite (nHA), lyophilized to obtain the porous.

In particular, this biological cryogel scaffold was chosen considering the needing of growth keratinocytes to the air-liquid interface, a bone substitute with the capability to mediate the passage of nutrients from the medium.

The development and biological validation of BTC/nHA scaffold were performed by Salgado et al. (2015). They showed by TEM analysis the homogeneous presence of the nHA among the collagen structures and by IF analysis the correct hMSC adhesion and spreading within the materials, as showed in figure V-4.

However, this scaffold was studied for implantation and the stiffness parameter appeared suboptimal to mimic the bone features and the randomise porous structures reduced the cell penetration in the middle of the scaffold. Due to the lower availability of oxygen in the middle of the scaffold, most cells migrate in the upper layer of the structures (as shown by confocal analysis; V-4 b).

To overcome those limitations, the suitability of a fibrin-based gel coating was evaluated as shown in the next two paragraphs.

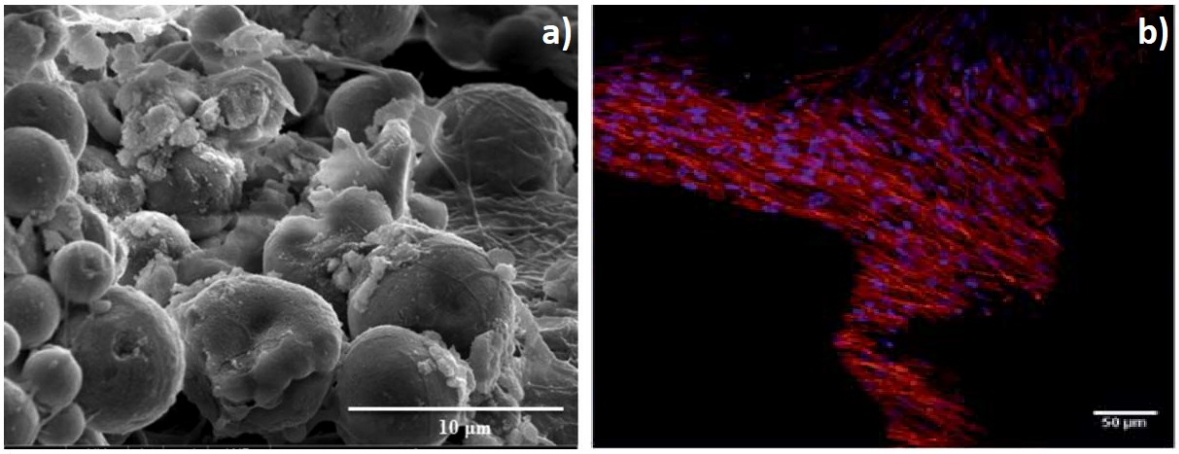

Figure V-4 *(a) Scanning Electron Microscopy (SEM) images show the composite scaffold after 21 days of incubation in SBF solution. (b) CLSM images of HB-MSC cultured for 21 days within the composite scaffold. Image a) bar scale 10 µm; image b) bar scale 50 µm.*

5.3.2. Mechanical properties evaluation

As shown by Kilian et al. (2010), mimicking the physiological microenvironment is crucial to induce the correct phenotype of hMSCs in vitro. In particular, bones are characterized by a high stiff correlated to a withstand to compression stress. In order to improve the stiffness of the BTC/nHA, the effect of a fibrin gel coating was evaluated. The preliminary tests were performed with scaffold swollen in the medium for 24 hours with or without fibrin gel interpenetration. Storage modulus (E') and the loss factor (tan delta) in relation to the frequency are shown in Fig. V-5

As shown in fig. V-5, the fibrin gel increased the scaffold stiffness of 4 times but induced a peculiar viscoelastic behaviour; indeed, the tan delta modulus increased under low-frequency compression force due to an elastic response of fibrin matrix but, at high frequency, the matrix broke down with a spreading of fibrin gel itself within the scaffold revealed by the tan delta value (figure V-5 b).

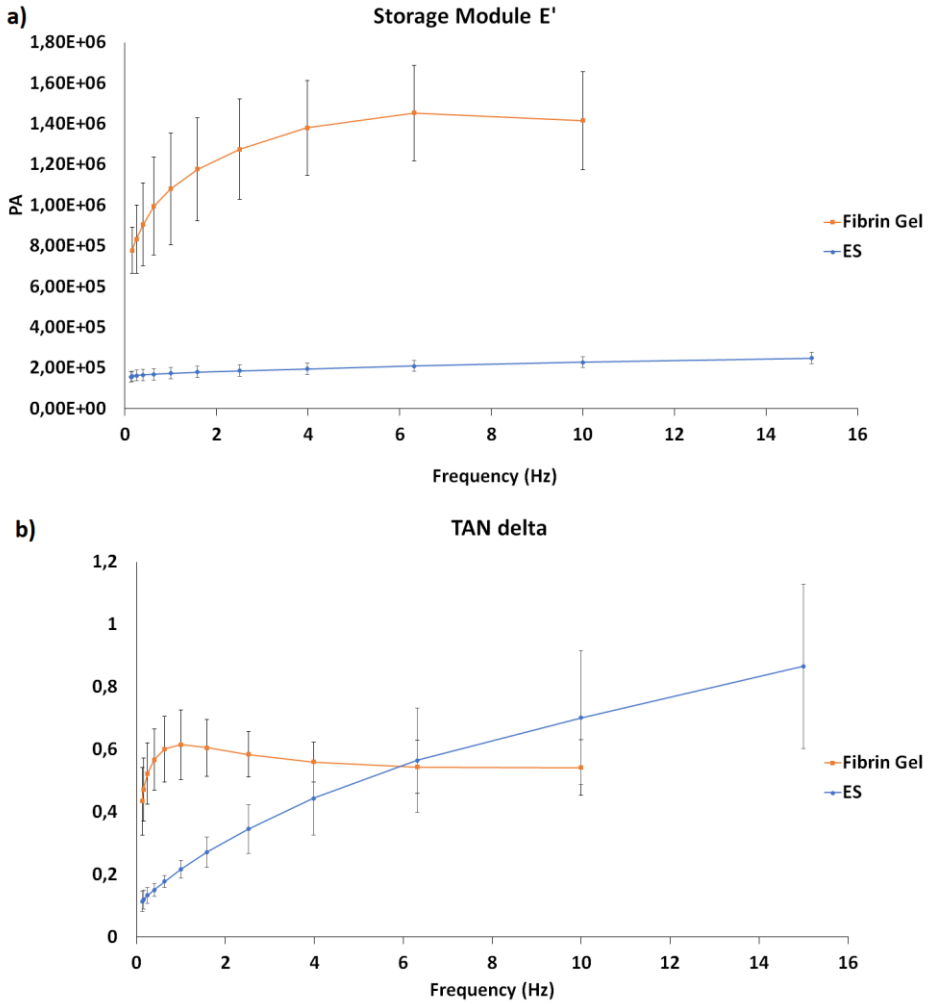

Figure V-5 The graphics represent the viscoelastic behaviour of empty and fibrin gel. In particular, the storage modulus (a) and the tan delta (b) under dynamic compression solicitation of increasing frequencies ranging from 0.1 to 10 Hz after 24 hr of incubation in the medium.

5.3.3. hMSC viability evaluation

The cytocompatibility of interpenetrated scaffold in comparison with empty scaffold and monolayered cultivated hMSCs was evaluated. As shown in figure V-6, the growth curve of hMSCs growth within the interpenetrated scaffold is characterized by a higher slope, which indicates a higher growth in the function of time.

This effect can be ascribable to a better repopulation of the fibrin gel implemented scaffold in comparison with the basal one (as shown in the video in figure V-7 and V-8).

After 14 days, all the curve reached a plateau state induced by the differentiation factor, which promotes the differentiation reducing the self-renewal and the proliferative capability of hMSCs.

Taken together, the mechanical and cytocompatibility results suggested the use of fibrin gel for better mimicking not only the bone alone but also to produce the *mucoperiosteum* model.

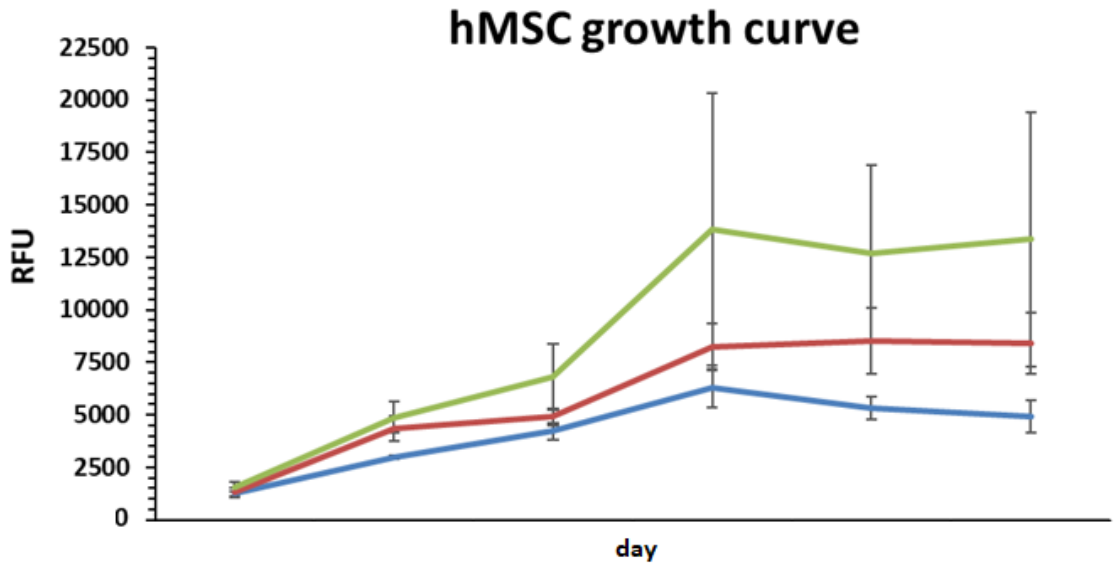

	0	3	7	14	21	28
control (hMSC, monolayer)	1254	2969,666667	4224	6275,666667	5343,666667	4910,666667
Scaffold+cell drop	1314,333333	4351,333333	4894,333333	8228	8500	8402,666667
Scaffold+cell fibrin gel drop	1563	4878,75	6804,75	13846,75	12690,25	13369,75

Figure V--6 The graphic represents the time-depending growth ratio of hMSC seeded insight the scaffold with or without fibrin gel. As shown, the viability is consistent with control cells growth constantly and reaches the plateau after 14 days under differentiation stimuli.

Saffold BTCnHA.avi

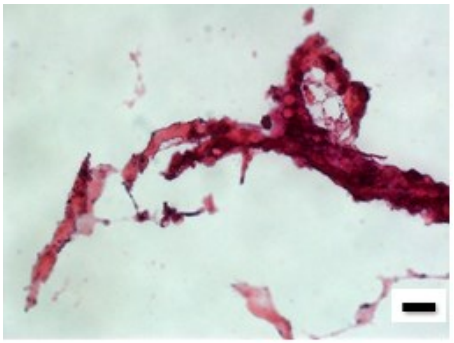

Figure V-7 *Confocal and HE analysis of hMSC repopulated BTC/nHA scaffold. The video shows several layers of the central and inner part of the unfixed and repopulated BTC/nHA scaffold (10x magnification). As showed by nuclear stain (DAPI; blue), cells are few and concentrated in a thin portion. In the HE image (60x magnification) was observed that hMSCs were poorly integrated into the scaffold. Bar scale 20 µm.*

Saffold BTCnHA fibrin gel.avi

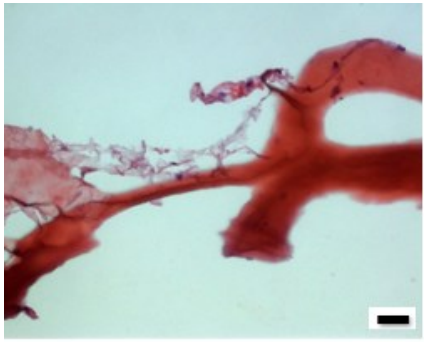

Figure V-8 *Confocal and HE analysis of hMSC repopulated BTC/nHA scaffold implemented with fibrin gel. The video shows several layers of the central and inner part of the unfixed and repopulated BTC/nHA-fibrin gel scaffold (10x magnification). As showed by nuclear stain (DAPI; blue) cells are several and distributed among the entire analysed portion. In the HE image (60x magnification) was observed that hMSCs were poorly integrated into the scaffold. Bar scale 20 µm.*

5.4. Establishment of the 3D parakeratinized (masticatory) epithelium model

Commercially available primary oral keratinocytes HOK (CliniScience) were used to set up a keratinized mucosa model previously described (Squarzanti et al., 2018).

To produce the lamina propria substitute, a buffered rat tail collagen solution was repopulated with human gingival fibroblast (HGF) or human dermal fibroblast (HDF). The latter was used as the control.

To evaluate HOK ability to stratify and set the best culture condition, two different protocols were tested, the **P946 protocol** and the "**standard protocol**". In the P946 protocol, organotypic cultures were grown to the air/liquid interface for 10 days in FAD medium enriched with 4% FBS, 0,9 mM CaCl2 and 25 µM Glycerol. In the "standard protocol", the organotypic cultures were grown to the air/liquid interface for 12 days in FAD medium enriched with 5% FBS, 1.88 mM CaCl2 and 50 µM Glycerol. For each condition, $6x10^5$ HOKs were seeded on the top of a collagen matrix enriched with HDF or HGF and let to adhere submerged for 4 days; after that, models were lifted to air-liquid interface and treated with the two protocols. HOKs were able to stratify and, contextually, differentiate under all conditions tested but the epithelia were characterized by different morphology.

In the P946 HDF protocol (fig V-9a), the oral epithelium appears parakeratinized. Following this protocol, keratinocytes shaped a well-formed basal layer, a thick spinosum layer (the thicker in comparison with the other conditions), composed of cells with abundant cytoplasm but without the prickle or elliptical shape and a poorly formed and fragile keratinized layer. The keratin filaments (stained in dark pink filaments) are still observable but appear detached and degraded.

In the standard HDF protocol (fig. V-9 b) the oral epithelium appeared parakeratinized. Following this protocol, keratinocytes shaped a poorly formed basal layer characterized by small and columnar, but loose, keratinocytes, a thin and poorly formed spinosum layer, with an irregular and non-homogeneous structure and a poorly formed keratinized layer (despite few keratin filaments still observable. It is possible to speculate that, the higher amount of differentiation factors which characterize the standard protocol, in addition to the dermal fibroblast stimuli, reduce the HOK capability of self-organization

In the P946_HGF protocol (fig. V-9 c), the oral epithelium appeared as a keratinized epithelium. Following this protocol, keratinocytes shaped a well-formed basal layer, a thin but well-formed spinosum layer, characterized by cells with abundant cytoplasm, a well-formed keratinized layer characterized by few filamentous layers.

In the standard HGF protocol (fig. V-9 d) the oral epithelium appeared as a keratinized epithelium. Following this protocol, keratinocytes shaped a well-formed basal layer and a fully formed spinosum layer characterized by keratinocytes with a large cytoplasm and a prickle appearance. The keratinized layer is presented and characterized by flat cells with most of the nuclei pyknotic, as typical for squamous cells and few filamentous layers. It is possible to speculate that the presence of tissue-specific fibroblasts improved the HOK capability of self-organization independently by the amount of differentiation factors.

Results are summarized in table V-1

In general, the histological observation showed that in all conditions, HOKs mimicked the physiological layer differentiation at the basal layer, characterized by small and columnar shaped cells while the rest of the layer appeared different in both thickness and cell morphology. The spinous was strongly affected both by the applied protocol and fibroblast subtypes (the dermal fibroblasts reduce the self-organization capability of oral keratinocytes). The keratinization appeared improved by gingival fibroblast and proportional to the amount of differentiation factor (Glycerol, $CaCl_2$ and FBS).

Therefore, all further experiments were performed following the standard protocol, which resembled the physiological features better than the other tested protocols.

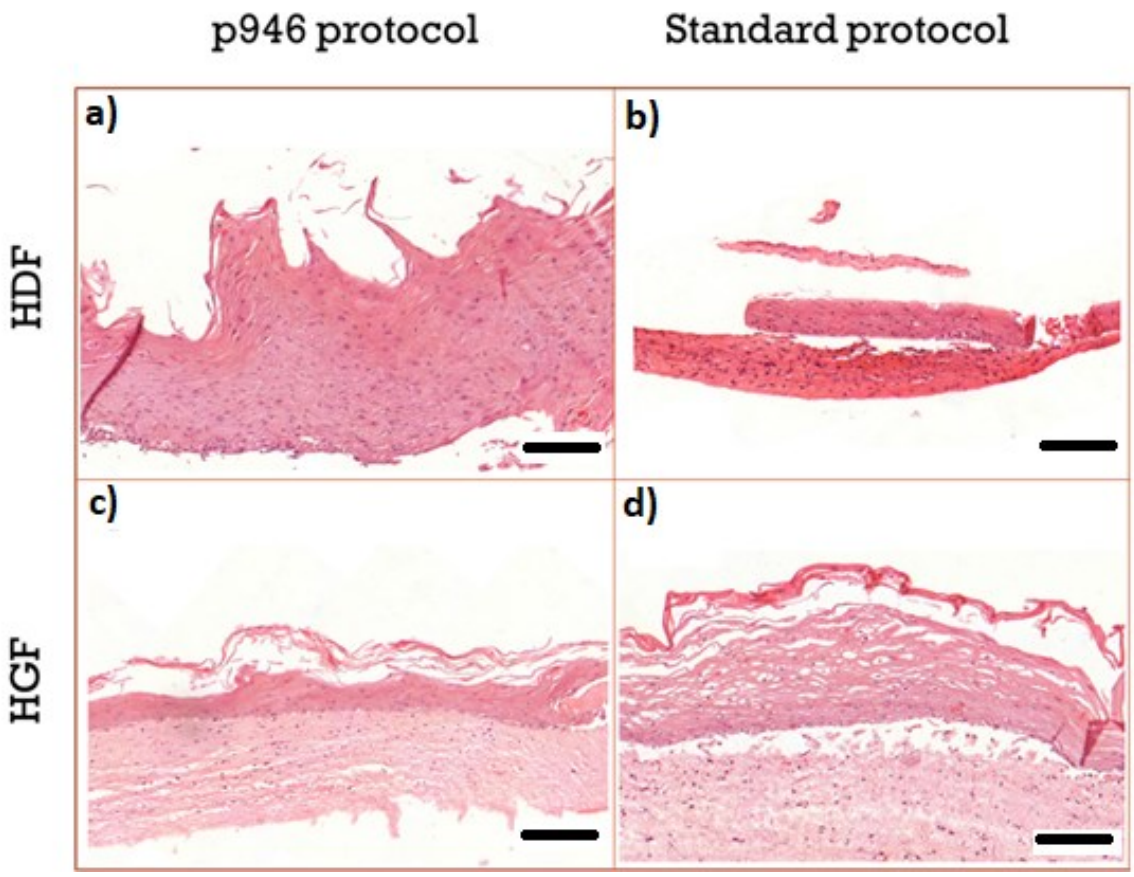

Figure V-9 Haematoxylin and eosin staining show different epithelium features depending on the applied protocol. Magnification 10x; bar scale 200 µm.

Table V-1 *Comparison table of tested condition for oral mucosa 3D model development.*

	Stratum basal	**Stratum Spinosum**	**Stratum corneum**
P946_HDF	*Normally formed* *Small and columnar cells*	*Thick (>20 layers)* *Absence of prickle or pyknotic cells*	*Thin and degraded*
Standard_HDF	Poorly formed Loose cells	Thin (<3 layers) Inhomogeneous Absence of prickle or pyknotic cells	Thin and degraded
P946_HGF	Normally formed Small and columnar cells	Normally formed (>10 layers) Elliptical cells	Well-Formed Visible and intact filaments
Standard_HGF	Normally formed Small and columnar cells	Normally formed (>10 layers) Elliptical and pyknotic cells	Well-Formed Visible and intact filaments Presence of few pyknotic flat cells

VI. Discussion

Nowadays it is well-known that epithelial-mesenchymal interaction plays a key role in the regulation of several processes such as wound healing or epithelial response to external stimuli. However, for many years this crosstalk has been thought of as a binary axis. Fibroblasts have a valuable role of fibroblast in epithelial differentiation and stratification has been proved (Gibbs et al., 2000; Chinnathambi et al., 2003; Dongari-Bagtzoglou et al.; 2006) but, probably, they are not the only cell types involved in epithelial development since the connective tissue is characterized by several cells type. Recently, have been showed that stromal tissues are a suitable source of MSCs that share several characteristics with the most characterized bone marrow derived MSCs (Mushahary et al., 2018). Gingival tissues offer several sources of MSCs: the gingiva itself, the alveolar bone, the ligaments and the dental pulp. Their role mucosa development is still to clarify.

In the present chapter, several technical optimizations were performed to evaluate the MSCs and osteoblasts role in epithelial keratinization better. Monolayered preliminary experiments were performed to evaluate if the commercially available media were suitable to support the growth of the different cell types simultaneously and to check the effect of keratinocytes medium (EpiLife) onto MSC. The viability assay showed that hMSCs growth well in both tested keratinocytes' media. On the contrary, keratinocytes differentiated earlier in media containing FBS than in FBS free media (i.e., Epilife medium), as generally described by the literature. However, in comparison with other works the pro-proliferative effect MSC_CM during the scratch assay showed a delay. In our experimental set-up, the proliferative differences between treated and untreated keratinocytes result clear only after 24 hr (fig. V-2) while other authors (Li et al., 2015; Chen et al., 2015), observed the MSC effect after 6 hours.

This effect can be explained by the enhanced production of chemoattractant and pro-proliferative factors for macrophages and monocytes, such as MCP-1 and GM-CSF, which also improve keratinocytes proliferation, that were over-expressed in the inflammatory microenvironment used by Li et al., (2015) and Chen et al., (2015).

Regarding the 3D model system test, hMSCs were not affected by keratinocytes differentiation factors present in FAD medium, which was subsequentially used for the coculture system (chapter 3). Indeed, during the viability assay, hMSC viability increase (fig. V-1).

Finally, the bone counterpart was evaluated, starting from bone scaffold able to mimic the alveolar bone. As previously shown (Almela et al., 2016) permeable matrix is needed for nutrient passage to support the keratinocytes growth in a pluristratified squamous epithelial at the air-liquid interface (Gibbs et al., 2000). Thus, a scaffold composed of bovine tendon collagen and nano-hydroxyapatite (BTC/nHA) was selected (Salgado et al., 2015) to mimic the bone components.

Because it is well-known that stiff material with rough surface improves hMSC differentiation toward osteoblastic lineage (Olivares-Navarrete et al., 2017; Noori et al., 2017), a BTC/nHA sponge was coated with a fibrin gel (FG). This FG was created with a low amount of thrombin (1,5 U/ml) since, accordingly to Bluteau et al. (2006), low thrombin concentrations (0.5–5 U/mL) should upregulate the expression of the osteoblastic markers improving hMSCs differentiation and, at the same time, allowing both hMSCs and OB migration and proliferation.

From a mechanical point of view, the FG quadruplicates the storage modulus (E') during the formation and increases the stiffens of the sponge (fig V-5).

The modified scaffold was characterized regarding the MSCs cytocompatibility (fig. V-6) and, as shown by the histogram, a continuous increase in the whole metabolic activities of hMSC was noted during the first 2 weeks, suggesting that hMSC proliferated over the time. Remarkably, the growth curve slope was higher for the FG improved BTC/nHA sponge, probably because of bone ECM formation and a better distribution of oxygen and nutrients mediated by the fibrin gel itself. As expected, the growth curve reached a plateau after 2 weeks. Moreover, both confocal and histological analysis, showed an improvement in scaffold repopulation and focal adhesion formation in the presence of the fibrin gel (fig. V-7 and V-8). These results suggested the modified scaffolds are suitable to be used in the mucoperiosteum 3D cell model (see Chapter 4).

VII. Bibliography

- Almela T, Brook IM, Moharamzadeh K. Development of three-dimensional tissue engineered bone-oral mucosal composite models. J Mater Sci Mater Med. 27(4):65. (2016) doi: 10.1007/s10856-016-5676-7.
- Arumugam B, Balagangadharan K, Selvamurugan N. Syringic acid, a phenolic acid, promotes osteoblast differentiation by stimulation of Runx2 expression and targeting of Smad7 by miR-21 in mouse mesenchymal stem cells, J Cell Commun Signal. 1-13. (2018)
- Augello A, De Bari C. The regulation of differentiation in mesenchymal stem cells. Hum Gene Ther. 21(10):1226-38. (2010) doi: 10.1089/hum.2010.173.
- Bluteau G, Pilet P, Bourges X, et al. The modulation of gene expression in osteoblasts by thrombin coated on biphasic calcium phosphate ceramic. Biomaterials. 27(15):2934–2943. (2006)
- Brotto M, Johnson ML. Endocrine crosstalk between muscle and bone, Curr Osteoporos Rep. 12(2)135-141. (2014)
- Chen J, Li Y, Hao H, Li C, Du Y, Hu Y, Li J, Liang Z, Li C, Liu J, Chen L. Mesenchymal Stem Cell Conditioned Medium Promotes Proliferation and Migration of Alveolar Epithelial Cells under Septic Conditions In Vitro via the JNK-P38 Signaling Pathway. Cell Physiol Biochem. 37(5):1830-46. (2015) doi: 10.1159/000438545.
- Chinnathambi S, Tomanek-Chalkley A, Ludwig N, King E, DeWaard R, Johnson G, Wertz PW, Bickenbach JR. Recapitulation of oral mucosal tissues in long-term organotypic culture. Anat Rec A Discov Mol Cell Evol Biol. 270(2):162-74. (2013)
- Clausen H, Vedtofte P, Moe D, Dabelsteen E, Sun TT, Dale B. Differentiation dependent expression of keratins in human oral epithelia. J Invest Dermatol. 86: 249-54. (1986)
- Cunha GR, Fujii H, Neubauer BL, Shannon JM, Sawyer L, Reese BA. Epithelial-mesenchymal interactions in prostatic development morphological observations of prostatic induction by urogenital sinus mesenchyme in epithelium of the adult rodent urinary bladder. J Cell Biol. 96: 1662-70. (1983)
- de Luca M, Albanese E, Megna M, Cancedda R, Mangiante PE, Cadoni A, Franzi AT. Evidence that human oral epithelium reconstituted in vitro and transplanted onto patients with defects in the oral mucosa retains properties of the original donor site. Transplantation. 50: 454-9. (1990)
- De Ugarte DA, Alfonso Z, Zuk PA, Elbarbary A, Zhu M, Ashjian P, Benhaim P, Hedrick MH, Fraser JK. Differential expression of stem cell mobilization-associated molecules on multi-lineage cells from adipose tissue and bone marrow. Immunol Lett. 89:267–270. (2003) doi: 10.1016/S0165-2478(03)00108-1.
- Dillon JP, Waring-Green VJ, Taylor AM, Wilson PJ, Birch M, Gartland A, Gallagher JA. Primary human osteoblast cultures. Methods Mol Biol. 816:3-18. (2012) doi: 10.1007/978-1-61779-415-5_1
- Dongari-Bagtzoglou A. and Kashleva H. Development of a highly reproducible three-dimensional organotypic model of the oral mucosa. Nat Protoc. 1: 20128 (2006)
- Eisenberg CA, Burch JB, Eisenberg LM. Bone marrow cells transdifferentiate to cardiomyocytes when introduced into the embryonic heart. Stem Cells. 24(5):1236-45 (2006). doi: 24(5):1236-45
- Fawzy El-Sayed KM, Elahmady M, Adawi Z, Aboushadi N, Elnaggar A, Eid M, Hamdy N, Sanaa D, Dörfer CE. The periodontal stem/progenitor cell inflammatory-regenerative cross talk: A new perspective. J Periodontal Res. 54(2):81-94. (2019). doi: 10.1111/jre.12616.
- Gibbs S. and Ponec M. Intrinsic regulation of differentiation markers in human epidermis, hard palate and buccal mucosa. Arch Oral Biol. 45: 149-58. (2000)
- Haasters F, Prall WC, Anz D, Bourquin C, Pautke C, Endres S, Mutschler W, Docheva D, Schieker M. Morphological and immunocytochemical characteristics indicate the yield of early progenitors and represent a quality control for human mesenchymal stem cell culturing. J Anat. 214(5): 759–767. (2009) doi: 10.1111/j.1469-7580.2009.01065
- Hass R, Kasper C, Böhm S, Jacobs R. Different populations and sources of human mesenchymal stem cells (MSC): A comparison of adult and neonatal tissue-derived MSC. Cell Commun Signal. 9: 12. (2011). doi: 10.1186/1478-811X-9-12
- Kang HW, Lee SJ, Ko IK, Kengla C, Yoo JJ, Atala A. A 3D bioprinting system to produce human-scale tissue constructs with structural integrity. Nat. Biotechnol. 34(3)-312. (2016)
- Kilian KA, Bugarija B, Lahn BT, Mrksich M, Geometric cues for directing the differentiation of mesenchymal stem cells. Proc Natl Acad Sci. 107:4872. (2010)
- Kinikoglu B., Auxenfans C., Pierrillas P., Justin V., Breton P., Burillon C., Hasirci V., Damour O. Reconstruction of a full-thickness collagen-based human oral mucosal equivalent. Biomaterials. 30: 6418-25 (2009)

- Klees RF, Salasznyk RM, Vandenberg S, Bennett K, Plopper GE. Laminin-5 activates extracellular matrix production and osteogenic gene focusing in human mesenchymal stem cells. Matrix Biol. 26(2): 106–114. (2007). doi: 10.1016/j.matbio.2006.10.001
- Kowalczewski CJ, Saul JM. Biomaterials for the Delivery of Growth Factors and other Therapeutic Agents in Tissue Engineering Approaches to Bone Regeneration. Front Pharmacol. 29; 9:513. (2018) doi: 10.3389/fphar.2018.00513.
- Kulterer B, Friedl G, Jandrositz A, Sanchez-Cabo F, Prokesch A, Paar C, Scheideler M, Windhager R, Preisegger KH, Trajanoski Z. Gene expression profiling of human mesenchymal stem cells derived from bone marrow during expansion and osteoblast differentiation. BMC Genomics. 12;8:70. (2007). doi: 10.1186/1471-2164-8-70
- Lambert PF, Ozbun MA, Collins A, Holmgren S, Lee D, Nakahara T. Using an immortalized cell line to study the HPV life cycle in organotypic "raft" cultures. Methods Mol Med. 119:141-55. (2005)
- Li M, Zhao Y, Hao H, Dai H, Han Q, Tong C, Liu J, Han W, Fu X. Mesenchymal stem cell-conditioned medium improves the proliferation and migration of keratinocytes in a diabetes-like microenvironment. Int J Low Extrem Wounds. 14(1):73-86. (2015) doi: 10.1177/1534734615569053.
- Mackenzie I.C. and Hill M.W. Connective tissue influences on patterns of epithelial architecture and keratinization in skin and oral mucosa of the adult mouse. Cell Tissue Res. 235: 551-9. (1984)
- Mathieu PS, Loboa EG. Cytoskeletal and Focal Adhesion Influences on Mesenchymal Stem Cell Shape, Mechanical Properties, and Differentiation Down Osteogenic, Adipogenic, and Chondrogenic Pathways. Tissue Eng Part B Rev. 18(6):436–444. (2012) doi: 10.1089/ten.teb.2012.0014
- Maumus M, Jorgensen C, Noël D. Mesenchymal stem cells in regenerative medicine applied to rheumatic diseases: role of secretome and exosomes. Biochimie. 95(12):2229-34. (2013) doi: 10.1016/j.biochi.2013.04.017
- Merne M. and Syrjänen S. The mesenchymal substrate influences the epithelial phenotype in a three-dimensional cell culture. Arch Dermatol Res. 295: 190-8 (2003)
- Mitrano TI, Grob MS, Carrión F, Nova-Lamperti E, Luz PA, Fierro FS, Quintero A, Chaparro A, Sanz A. Culture and characterization of mesenchymal stem cells from human gingival tissue. J Periodontol. 81(6):917-25. (2010) doi: 10.1902/jop.2010.090566
- Moharamzadeh K., Brook I.M., Van Noort R., Scutt A.M., Smith K.G., Thornhill M.H. Development, optimization and characterization of a full-thickness tissue engineered human oral mucosal model for biological assessment of dental biomaterials. J Mater Sci Mater Med. 19: 1793-801. (2008)
- Mushahary D, Spittler A, Kasper C, Weber V, Charwat V. Isolation, cultivation, and characterization of human mesenchymal stem cells. Cytometry A. 93(1):19-31. (2018) doi: 10.1002/cyto.a.23242. Review.
- Neupane S, Adhikari N, Jung JK, An CH, Lee S, Jun JH, Kim JY, Lee Y, Sohn WJ, Kim JY. Regulation of mesenchymal signaling in palatal mucosa differentiation. Histochem Cell Biol. 2018 Feb;149(2):143-152. (2018) doi: 10.1007/s00418-017-1620-2.
- Noori A, Ashrafi SJ, Vaez-Ghaemi R, Hatamian-Zaremi A, Webster TJ, A review of fibrin and fibrin composites for bone tissue engineering. Int J Nanomedicine. 12: 4937–4961. (2017). doi: 10.2147/IJN.S124671
- Olivares-Navarrete R, Lee EM, Smith K, Hyzy SL, Doroudi M, Williams JK, Gall K, Boyan BD, Schwartz Z. Substrate Stiffness Controls Osteoblastic and Chondrocytic Differentiation of Mesenchymal Stem Cells without Exogenous Stimuli. PLoS One. 12(1):e0170312. (2017) doi: 10.1371/journal.pone.0170312
- Palaiologou AA, Yukna RA, Moses R, Lallier TE. Gingival, dermal, and periodontal ligament fibroblasts express different extracellular matrix receptors. J Periodontol. 72(6):798-807. (2011)
- Pittenger MF, Mackay AM, Beck SC, Jaiswal RK, Douglas R, Mosca JD, Moorman MA, Simonetti DW, Craig S, Marshak DR. Multilineage potential of adult human mesenchymal stem cells. Science. 284:143–147. (1999). doi: 10.1126/science.284.5411.143.
- Ponnaiyan D, Jegadeesan V. Comparison of phenotype and differentiation marker gene expression profiles in human dental pulp and bone marrow mesenchymal stem cells. Eur J Dent. 8(3): 307–313. (2014) doi: 10.4103/1305-7456.137631
- Salgado CL, Grenho L, Fernandes MH, Colaço BJ, Monteiro FJ. Biodegradation, biocompatibility, and osteoconduction evaluation of collagen-nanohydroxyapatite cryogels for bone tissue regeneration. J Biomed Mater Res A. 104(1):57-70. (2016) doi: 10.1002/jbm.a.35540.
- Saravanan S, Leena RS, Selvamurugan N. Chitosan based biocomposite scaffolds for bone tissue engineering, Int. J. Biol.Macromol. 93;1354-1365. (2016)
- Schaffler A, Buchler C. Concise review: adipose tissue-derived stromal cells-basic and clinical implications for novel cell-based therapies. Stem Cells. 25:818–827. (2007). doi: 10.1634/stemcells.2006-0589.

- Schweizer J, Winter H, Hill MW, Mackenzie IC. The keratin polypeptide patterns in heterotypically recombined epithelia of skin and mucosa of adult mouse. Differentiation. 26: 144-53. (1984)
- Sharpe P.M. and Ferguson M.W. Mesenchymal influences on epithelial differentiation in developing systems. J Cell Sci Suppl. 10: 195-230. (1988)
- Squarzanti DF, Sorrentino R, Landini MM, Chiesa A, Pinato S, Rocchio F, Mattii M, Penengo L, Azzimonti B. Human papillomavirus type 16 E6 and E7 oncoproteins interact with the nuclear p53-binding protein 1 in an in vitro reconstructed 3D epithelium: new insights for the virus-induced DNA damage response. Virol J. 15(1):176. (2018) doi: 10.1186/s12985-018-1086-4.
- Squier C.A. The permeability of oral mucosa. Crit Rev Oral Biol Med. 2: 1332. (1991)
- Squier CA. Keratinization of the sulcular epithelium--a pointless pursuit? J Periodontol. 52(8):426-9. (1981)
- Tandon B, Blaker JJ, Cartmell SH. Piezoelectric materials as stimulatory biomedical materials and scaffolds for bone repair. Acta Biomater. 73:1-20. (2018) doi: 10.1016/j.actbio.2018.04.026.
- Walter MN, Wright KT, Fuller HR, MacNeil S, Johnson WE. Mesenchymal stem cell-conditioned medium accelerates skin wound healing: an in vitro study of fibroblast and keratinocyte scratch assays. Exp Cell Res. (2010) doi: 10.1016/j.yexcr.2010.02.026.
- Zhang L, Yang G, Johnson BN, Jia X. Three-dimensional (3D) printed scaffold and material selection for bone repair. Acta Biomater. 84:16-33. (2019) doi:10.1016/j.actbio.2018.11.039.
- Zuk PA, Zhu M, Ashjian P, De Ugarte DA, Huang JI, Mizuno H, Alfonso ZC, Fraser JK, Benhaim P, Hedrick MH. Human adipose tissue is a source of multipotent stem cells. Mol Biol Cell. 13:4279–4295. (2002) doi: 10.1091/mbc.E02-02-0105.

Chapter 3

Epithelial-Mesenchymal crosstalk

VIII. Introduction

8.1. Oral epithelium

The oral epithelium is a covering and lining epithelium composed of different squamous pluristratified epithelia; it consists of cells tightly attached to each other and to the basement membrane. They are well organized in distinct layers, or stratum, each of them with a specific role and easily recognisable in histological cross-sections.

The main histological difference between the epithelia is the keratinization degree (Schroeder et al., 1997), and therefore, they are classified in keratinized and non-keratinized epithelium; the first is typical of the masticatory mucosa and the second of the lining mucosa (fig. I-7).

8.1.1. Keratinized epithelia

The masticatory mucosa is characterized by a firm and withstands tissue firmly attached to the connective counterpart. This feature is strongly related to the keratin layer, which covers the masticatory mucosa and is formed during the *keratinization* or *cornification* of the epithelium. The keratinized epithelia are divided into 4 distinct layers: basal, spinosum, granular and keratinized (or cornified) (Gartner et al., 1994).

The **basal layer** or *stratum basale* is in direct communication with the basement membrane and it is composed of small and packed cuboidal or columnar cells. This layer contains both keratinocyte progenitor (essential for epithelium renewal) and the maturing population. This latter cellular subtype is characterized by a faster mitotic ration in comparison with the progenitor and a differentiation process (or maturation) essential to produce all the keratinocytes layers (Calenic et al. 2015). The progenitor population is divided into two other subpopulations. The first one is considered a “stem cell” population (or basal epithelial cells) since they retain the self-renewal capability (the asymmetric mitosis) to maintain the proliferative potential of the tissue, and the amplifying cells which have the role of increasing the amount of the cells in the maturing population when necessary. Izumi et al. (1999) showed that the stem progenitors of the oral mucosa are much smaller than the other progenitor cells and that they express a low-affinity neurotrophin receptor, named p75 or NGFR (Nerve growth factor receptor).

P75 contains an extracellular domain composed of 4 chains with 40 aminoacids (AA) repeats each, a single transmembrane domain, and a 155-amino acid cytoplasmic domain. The AA repeats are characterized by 6 cysteine residues at conserved positions, containing the nerve growth factor binding domain, followed by a serine/threonine-rich region. In addition, those cells express the integrin β1 (ITGβ1 or CD29) and the peroxisome proliferator-activated receptor-gamma (PPAR-γ).

ITGβ1 is a membranes receptor encoded by the ITGβ1 gene; integrin receptors are mainly involved in cell adhesion and their intracellular domain is linked to the actin. Integrins are able to mediate bidirectional signals from the extracellular matrix to the cytoplasm. ITGβ1, in particular, work in complex or with the integrins α1 and α2 to form the heterogenic complex that works as collagen receptors or with the isoforms α3 to form the receptors for netrin 1 and reelin. Moreover, ITGβ1 retains the ability to target α-integrins to their cellular localization to allow the formation of focal adhesion. As other integrins, ITGβ1 also mediate the formation of cell-cell junctions known as desmosomes.

PPAR-γ, also known as glitazone receptor, or NR1C3 (nuclear receptor subfamily 1, group C, member 3) is a type II nuclear receptor that in humans is encoded by the PPARG gene. Induce the cell differentiation and the cell-cycle block by a PTEN mediated pathway.

In addition to keratinocytes, in the basal layer are present also other cell types such as melanocytes, Langerhans cells, and Merkel cells (Calenic et al., 2015).

The **spinosum layer** is composed of several rows of large and elliptical cells. The cells of the spinosum layer are known as prickle cells due to the appearance they often acquire after histological processing since they shrink away from each other and remain connected by the desmosomes (the intracellular junction). Physiologically, those two layers represent around two-thirds of the epithelium (Gibbs et al., 2000).

The third layer, knows as **granular layer** or *stratum granulosum*, is the thinnest layer and consists of broad but flattened cells full of keratohyalin granules (KHG). When the KHG of different epithelia are compered, it can be noted that their ultrastructure is an exciting clinical cue; indeed, those features seem to be strictly related to the speed of cell turnover (Westerhof et al., 1986). Westerhof et all. (1987) compared the KHG of oral mucosa and epidermis and showed that globular KHG is typic of quickly dividing epithelia in contrast with the irregular or stellate KHG, mainly found in average but slowly dividing epithelia. However, the KHG patter in not regular; for instance, gingiva has miscellaneous KHG related to its fast-mitotic ratio.

The most superficial layer, the ***stratum corneum***, is characterized by flat (squamous) pyknotic or anucleate cells full of keratin. This latter characteristic is easily visualized during the histological analysis since the squamous cells, or *squames*, are strongly stained by eosin. Among the keratinized epithelia, are present different degrees of keratinization accordingly to the mechanical stress the epithelia them-self endure. This keratinized degree mainly depends from the nuclei retention of squamous cells, when most of the cells lost their nucleus, and the keratinization pattern is completed the epithelium is termed ortho-keratinized, and the cells appear while when the *squames* are mostly pyknotic or shrunken and the keratinization is incomplete, the epithelium is termed parakeratinized (Izumi et al., 2000; Boukamp et al., 1988)

The principal features are summarized in table VIII-1

Table VIII-1 *General characteristic of keratinized oral epithelia*

English layer lame	**Basal layer**	**Spinous (prickle) layer**	**Granular layer**	**Cornified layer**
Latin layer lame	**Stratum basal**	**Stratum spinosum**	**Stratum granulosum**	**Stratum corneum**
Cell layer	2-3	2/3 of the total layers	1-3	
Shape	Cuboidal or columnar	Elliptical cells (larger than the basal cells)	Flat cells with regular & close to each other surfaces (larger & wider than the spinous cells)	Flat Cells (larger & flatter than the granular cells)
Marker	p75, CD29, PPAR-γ, CK5/14	CK1/10, CK6/16, CK2		Acidophilic (dark pink staining with H&E)
Function	Mitotic Function (DNA Synthesis providing new cells)	Mitotic Function and protein synthesis (most active)	Mitotic Function and Protein Synthesis (at a lower rate)	Protection
Characteristics	Contain: Desmosomes Hemidesmosomes Cell capability: Self-renewal	Intercellular space with a prickly appearance	Contains: Keratohyalin granule Pyknotic nuclei	Only a few nuclei are retained in the para-keratinized epithelia

The time needed for the renewal of the epithelium is known as turn over time and it is differently affected by the epithelial anatomical position. For instance, oral epithelia are faster in comparison with skin; this phenomenon explains the higher sensitivity of oral mucosa to the chemotherapeutic drugs, which act on mitotic cells.

The turnover time is regulated and activated by different factors such as cytokines and growth factors. The most critical factors for epithelial proliferation are the epidermal growth factor (EGF), the keratinocytes growth factor (KGF) and the interleukin-1 (IL-1) while the principal inhibitory factors are the transforming growth factors (TGFα and TGFβ) (Peehl et al., 1995; Ceccarelli et al., 2012; Finch et al., 2004). EGF, which is a 6-kDa protein with 53 amino acid residues and three intramolecular disulphide bonds formed within a conserved domain rich in cysteine ($\underline{C}X_7\underline{C}X_{4\text{-}5}\underline{C}X_{10\text{-}13}\underline{C}X\underline{C}X_8\underline{G}X\underline{R}\underline{C}$), stimulates cell growth and differentiation by binding the membrane epidermal growth factor receptor (EGFR). EGF-EGFR binding stimulates the EGFR dimerization with the consequent tyrosine kinase phosphorylation activates the MAP kinase cascade. From a biochemical point of view, this pathway activates several processes: intracellular calcium concentration for cellular mobility, glycolysis, and DNA and protein synthesis to support cell proliferation and metabolism and the upregulation of EGFR itself.

Interestingly, Del Angel-Mosqueda et al. (2015) showed that EGF acts as an enhancer during the osteogenic differentiation of dental pulp stem cells, promoting extracellular matrix mineralization. Besides, Muller et al. (2002) showed that EGF pathway can be amplified by interaction with integrins and inhibits by cadherins (which mediates the cellular-matrix adhesion). Tamana et al. (2010) showed that soluble EGF acts in a similar way also toward bone marrow-derived MSC which were induced to proliferate, migrate and differentiate following the osteogenic fate.

This suggests that EGF acts both as autocrine and paracrine effector for keratinocytes-fibroblast-resident mesenchymal stem cells axis, necessary to both mucoperiosteum development and repair.

8.1.2. Non-Keratinized epithelium

Lining mucosa is the most abundant epithelium in the oral mucosa and it is characterized by a thick non-keratinized epithelium. The first two layers are characterized by the same cells and structural features; however, the ridges of the basal layer are broader in comparison with the ones of keratinized epithelia and the prickle cells are larger. The last two layers are known as intermediate and superficial layer or *stratum intermedium* and *stratum superficialis*, respectively. The latter shows high flexibility in comparison with the keratinized layer and the cells retain the nuclei. Under the histological evaluation with hematoxylin and eosin, this layer usually appears stained. The nonkeratinized epithelium, however, can undergo a keratinization process mechanically induced by shear stress or chemical trauma. From a histological point of view, this hyperkeratinization transmutes a non-keratinized epithelium in an orthokeratinized ones. Although the hyperkeratinization is often a physiological response of epithelia toward exogenous stimuli, not dissimilar to a callous formation in the skin, this phenomenon is sometimes related to a neoplastic transformation (squamous cell carcinoma, SCC) (Gibbs et al., 2000; Izumi et al. 2003)

The principal features are summarized in table VIII-2

Table VIII-2 *General characteristic of non- keratinized oral epithelia*

English Layer Name	**Basal layer**	**Intermedium layer**	**Superficial layer (third and fourth layer) Stratum superficialis**
Latin Layer Name	**Stratum basale**	**Stratum intermedium**	
Cell layer	1	2/3 of the total layers	1-3
Shape	Cuboidal or columnar	Large ovoidal cells without prickly	Slightly flat cells with few pyknotic cells
Marker	p75, CD29, PPAR-γ, CK5/14	CK4/13, CK19	
Function	Mitotic function (DNA synthesis providing new cells)	Mitotic function and protein Synthesis (most active)	
Characteristics	Contain: Desmosomes Hemidesmosomes Cell capability: Self-renewal		Contains: Most of the nuclei Few organelles Dispersed filaments

8.1.3. Cytokeratin

Epithelial cells contain tonofilaments as an intracellular bridge. Tonofilaments, mostly known as cytokeratin (CK), are classified as intermediate filaments and are the most used markers to study epithelial differentiation. Like other proteins, keratin synthesis is strictly regulated (Berkovitz et al., 1988). Each specific cytokeratin is regulated by

transcription factors with specific DNA binding sites. The transcription factor mostly involved in CK expression are Sp1, AP1, and AP2 but also extracellular signals, such as growth factors, can regulate CK expression, driving the epithelial fate. CKs are mostly expressed in pairs; the most critical pair for the basal layer are CK5 and CK14, and they are expressed in both keratinized and non-keratinized epithelia. During the differentiation, specific pairs are expressed in keratinized and non-keratinized, respectively CK1/10 and CK4/13. As above mentioned, CK5 and CK14 are mainly expressed by the undifferentiated keratinocytes of the basal layer. The mechanism which down-regulate the CK5/14 expression in the supra-basal and spinosum layer seems to be related to the expression of POU homeodomain factors Skn-1a and Tst-1. Indeed, the mRNA analysis of a double knockout murine model (Skn-1-/Tst-1-) reveals that CK14 mRNA stays stable in the absence of those two repressor factors. However, the inhibitory effect of POU containing proteins is counteracted by the presence of CBP/p300. Though using a gel-retardation and DNA-mediated cell-transfection assays, Blumenberg (1997) showed that CK5 regulation is complex. CK5 promoter has three binding sites, two with activation properties and one with the inhibitory property; he found that the principal transcription factors are Sp1 and AP2, which act with the other three transcription factors still unknown. Blumenberg also showed that NF-κB families counteract AP1 in CK regulation. AP1 induces the co-expression of CK5/14 by c-Fos and c-Jun, while p65, one of the main components of NF-κB pathways, suppresses the CK5/14 promoters. This suggests that the interplay between AP1 and NF-κB plays a crucial role in driving epithelial gene expression not only during physiological development but also during all processes in which NF-κB physiologically increases, such as during infection or wound healing.

Regarding the regulation of CK 1 and CK10, it has been showed several times that intracellular calcium is a key regulator. In particular, Ca^{2+} acts on a 249-bp region situated near to CK1 promoter, and its activity is mediated by AP1. Another key factor in CK1 and CK10 expression is C/EBPβ. This latter strongly up-regulates the expression of those two early-stage differentiation markers (CK1/10) but seems unable to induce the expression of loricrin and involucrin, two of the late-stage differentiation markers. C/EBPβ is expressed in combination with AP2 in the suprabasal layer, and it regulates only the early events of keratinocyte differentiation. Similar effects are observable when a winged-helix/forkhead transcription factor Whn (Hfh11, Foxn1), is overexpressed. The latter is active only on CK1 promoter and contextually, it down-regulates profilaggrin, loricrin, and involucrin. On the opposite, the transcription factor C/EBPα and AP2 are active only on CK10 promoter, C/EBPα expression is induced in the spinosum layer by the decreased expression of AP2 (fig. VIII-1).

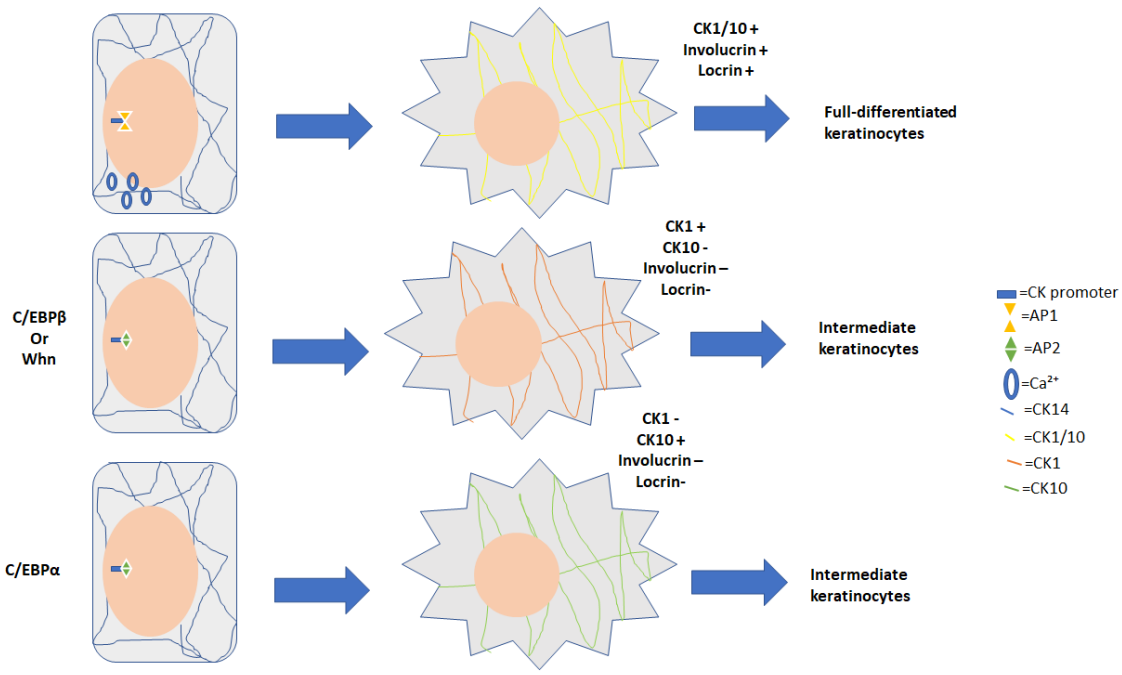

Figure VIII-1 *Schematic representation of CK1/10 induction*

CK13, together with its partner CK4 is expressed in the spinosum layers of non-keratinized epithelia. CK13 promoter contains a TATA box and several other transcription factors binding sites. Moreover, it has two transcription-start sites upstream ATG codon. The overexpression of CK13 is frequently observed in epithelial tumor and it can be upregulated by Ca^{2+} or retinoic acid (Blumenberg et al., 1986, 1988, 1992, 1997; Boukamp et al., 1988; Berkovitz et al., 1998; Adams et al., 1976; Shetty et al., 2012) (fig. VIII-2).

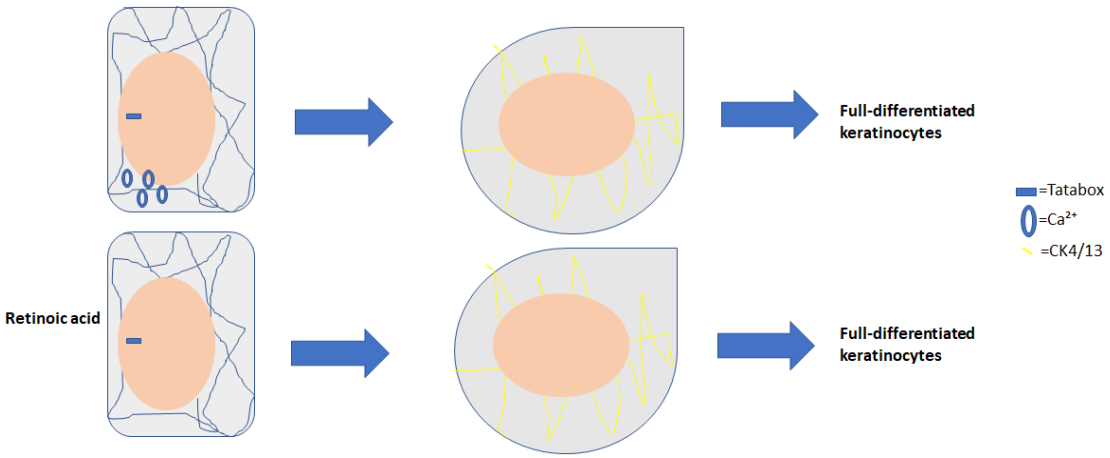

Figure VIII-2 *Schematic representation of CK4/13 induction*

8.2. Gingival mucoperiosteum

Mucoperiosteum is a composite structure composed of the mucous membrane lining the outer part of the alveolar bone known as periosteum. The oral mucosa is characterized by the absence of the submucosa (described in chapter 1) and it is directly connected to the bone. This structure is typically found in the gingival tissue and, in

that contest, takes part in a more complex structure known as the periodontium. The periodontium also includes the periodontal ligaments (PDL) and the cementum and is responsible for protecting the teeth (Atsuta et al., 2016).

The gingival margin follows a scalloped-like course across the dentition due to the interdental papillae, which fill the interdental spaces beneath the tooth contacts. Moreover, the gingiva is histologically divided into two portions:

- The free gingiva, which is characterized by two non-keratinized epithelia in its inner part, known as sulcular epithelium (in the free part) and the junctional epithelium (in direct contact with the teeth). The sulcular epithelium forms the wall of the sulcus and, together with the junctional epithelium, form the dentogingiva junction. The junctional epithelium has two basal lamina, the internal one that faces the tooth and the external one that faces connective tissue; due to this characteristic, it results in the most permeable epithelium and the *lamina propria* underlying the junctional epithelium is characterized by a chronic inflammatory state derived by the filtration of several microbial antigens. On the contrary, the outer surface which is mainly keratinized.
- The attached gingiva, which is covered by a keratinized epithelium, extends apically from the free gingiva towards the alveolar mucosa. The latter is defined as "attached" because it is firmly adherent to the cementum and the alveolar bone.

This structure is interesting because it is encircled by several types of pluripotent stem cells and have the capability to adapt its histological features to protect the regeneration of the underlying tissue. Despite can be easily imagined that mesenchymal stem cells play a key role in epithelial adaptation, the mechanisms which regulate this phenomenon are not well understood.

8.3. Oral mucosa models

The full-thickness engineered oral mucosa is characterized by a *lamina propria* substitute and a stratified epithelium. The *lamina propria* is represented by a biocompatible scaffold fully repopulated with vital and matrix-secreting oral fibroblasts. This structure has a supporting role in keratinocyte differentiation and proper behaviour. The proper scaffold has, ideally, a porous structure to allow fibroblast infiltration but should withstand to the shrinkage began by fibroblast growth. The stratified squamous epithelium, fixed on the *lamina propria* by a self-produced basement membrane, is represented by densely packed keratinocytes with the stem potential to undergo differentiation as they migrate to the surface. This phenomenon is usually induced by the airlifting of proliferating oral keratinocytes in a chemically defined medium. The scaffold, the cells source and culture medium composition could be modified and improved in order to optimize the full-thickness oral mucosa accordingly to the research purpose (Izumi et al., 2000 and 2003; Dongari-Bagtzoglou et al., 2006).

As mentioned above, the *lamina propria* scaffolds play a crucial role in obtaining adequate oral mucosa. The proper scaffold mast has satisfactory biocompatibility, porosity, biostability, and mechanical properties to support both fibroblast ad keratinocytes growth. The scaffold developed during the years are numerous and can be divided into the sequent categories: naturally-derived scaffolds, collagen-based scaffolds, and synthetic scaffolds and composite scaffolds. These models and their applications are fully described in chapter 1.

In general, the gingival tissue is part of a more complex structure characterized by a fine, but not fully understand yet, crosstalk between cell types. In particular, MSCs role, either when in "stem" state or under tissue damaged induced differentiation, is under investigation. In this part of the work, we focused our study on the role of hMSC or osteoblast (OB) on keratinocytes in their three-dimensional physiological environment.

To asses this aim, the engineered 3D organotypic oral mucosa model, described in the previous chapter (2), was employed in 4 different set-ups.

Indeed, this part of the present Ph.D. thesis is aimed to clarify:

- the paracrine effect of mesenchymal stem cells (hMSC) under differentiation condition onto keratinocytes behavior
- the crosstalk between oral epithelia and hMSC in presence or absence of osteoblastic differentiation factor
- the main factor mediating the interaction between the mesenchyme and the oral epithelia

IX. Materials and methods

9. Evaluation of hMSC on Oral Mucosa model

9.1. Paracrine effect of hMSC on Oral Mucosa model

hMSCs were maintained in DMSM 10% FBS and the conditioned medium (CM) was collected every third day, centrifuge at 1200 rpm for 5 minutes and store at -20° until use.

In order to evaluate CM effect onto 3D epithelial cultures, the FAD medium, generally used for growing 3D cultures (¾ DMEM, 5% FBS plus ¼ Ham's-F12 medium enriched with 1.88 mM $CaCl_2$, 50 mM Glycerol, 10^{-10} M Cholera Toxin, 10 ng/ml EGF, 5 µg/ml Insulin, 0.4 µg/ml Hydrocortisone, 5 µg/ml Apotransferrin and $2x10^{-8}$ nM Triiodo-thyronine), was modified by substituting the DMEM 5% FBS part with the conditioned medium produced by differentiating HMSCs.

Freshly produced osteogenic medium mixed with ¼ Ham's-F12 plus the above-listed growth factors was used as the control medium. The experimental procedures are summarized in figure IX-1.

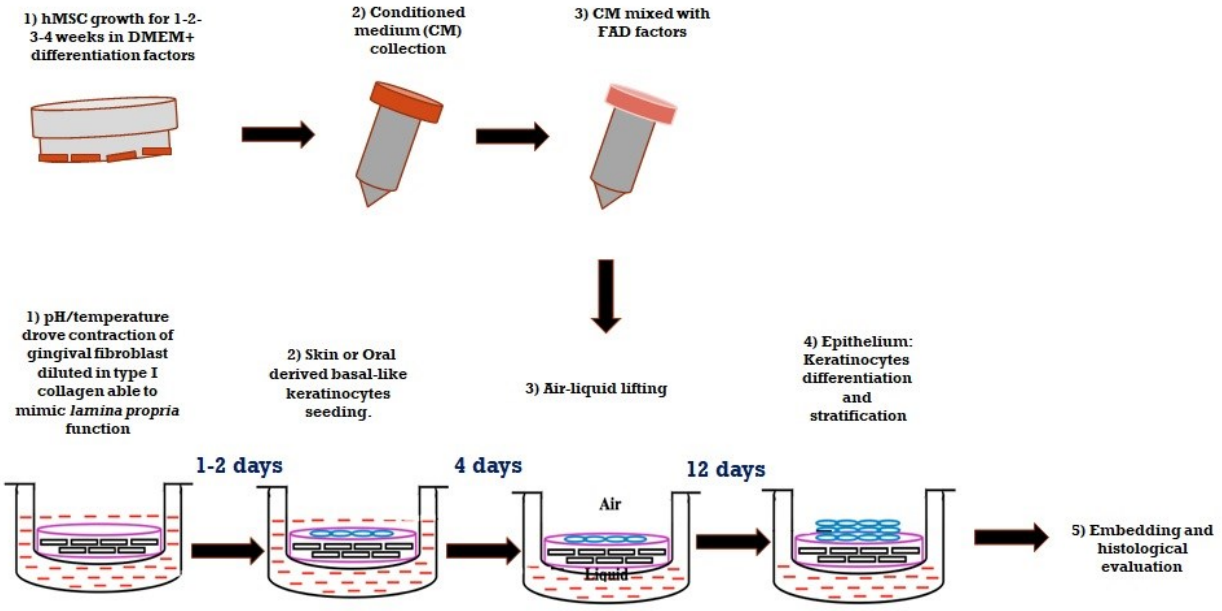

Figure IX-1 *Schematic reproduction of OB conditioned engineered oral mucosa*

9.1.1. hMSC and Oral Mucosa Co-Cultures

Oral Mucosae were prepared as described in paragraph 4.2 in p12 transwell. Briefly, each *lamina propria* substitute was prepared by enriching a collagen premix (1.65 ml Rat tail collagen type I 6.6 mg/ml, 10^5 µL 10x F12, 105 µL FBS, 10.5 µL PEN/Strep 100x, 2.5 µl NaOH 1 M) with $1.25x10^6$ Human Gingival Fibroblasts (HGF), the mixture was left untouched for two days. Following, $1.5x10^5$ HOKs were seed onto each *lamina propria* substitute, let adhere

and growth in submersed condition until confluent. After 4 days, each 3D system was moved on the top of hMSC - populated well and positioned at air/liquid interface by reducing of medium volume to 450 µL. The medium was changed every day for 12 days and then OMs were formalin-fixed and paraffin-embedded for histologic analysis while hMSC were fixed and stained as described in paragraph 4.1.6.

9.2. Evaluation of hMSC derived Osteoblast effect on Oral Mucosa

9.2.1. Paracrine effect of hMSC-derived Osteoblast onto keratinocytes stratification and differentiation

Osteoblast (OB) and OB conditioned media (CM) were obtained as described in paragraph 4.1.5 FAD2_OB_CM was prepared thawing OB7_CM, OB14_CM, OB21_CM and OB28_CM at room temperature and mixing them with ¼ F12, 5% FBS, 1,88 mM $CaCl_2$, 50 mM Glycerol, 10^{-10} Cholera Toxin, 10 ng/ml EGF, 5 µg/ml Insulin, 0.4 µg/ml Hydrocortisone, 5 µg/ml Apotransferrin and $2*10^{-3}$ nM Triiodo-thyronine. Finally, all FAD2_OB_CM were filtrated before use.

Oral Mucosa was prepared as described in paragraph 4.2 but, from the air/liquid interface OM was cultivated in the different FAD2_OB_CM, growth for other 12 days and then formalin-fixed and paraffin-embedded for histologic analysis.

9.2.2. Osteogenic induced hMSC and Oral Mucosa Co-Cultures

Oral Mucosa was prepared as described in paragraph 4.2 in p12 transwell. Briefly, each *lamina propria* substitute was prepared by enriching a collagen premix (1.65 ml Rat tail collagen type I 6.6 mg/ml, 105 µL 10x F12, 105 µL FBS, 10.5 µL PEN/Strep 100x, 2.5 µl NaOH 1 M) with $1.25x10^6$ Human Gingival Fibroblasts (HGF) then allowed to contract to the appropriate shape for 2 days. When ready, $1.5x10^5$ HOKs were seed onto each *lamina propria* substitute, let adhere and growth in submersed condition until confluent. After 4 days, each 3D system was moved on the top of the hMSC-populated wells and positioned at air/liquid interface by reducing of medium volume to 450 µL. Contextually, FAD medium was enriched OB differentiation factors. Medium was changed every day for 12 days and then OMs were formalin-fixed and embedded in paraffin for histologic analysis while hMSCs were fixed and stained as described in paragraph 4.1.6.

9.3. Haematoxylin and eosin stain

HE staining was carried out onto the 4 µm thick tissue sections obtained from formalin-fixed paraffin-embedded 3D tissue cultures. Briefly, slides were rehydrated and stained with Hematoxylin for 10 minutes at room temperature (RT), then counterstained with Eosin for 5 minutes at RT. Finally, tissue slides were rapidly dehydrated and mounted. Tissue morphology was finally optically evaluated under a Leica DM750 optical microscope (Leica Microsystems, Basel, Switzerland).

9.4. Immunohistochemistry analysis

IHC staining was carried out onto, at least, three tissue sections obtained from formalin-fixed paraffin-embedded 3D epithelial tissue cultures. Briefly, slides were deparaffinized and re-hydrated with sequential passages in xylene and descending concentrations of ethanol (100, 95, 90, 70 and 70%); once rinsed, slides were unmasked in EDTA buffer 0,1 M pH 8 (Sigma Aldrich; Milano, Italy) for 20' at 100°C, saturated for 1 hour in PBG (0,5% BSA and 0,2% gelatin in PBS) and incubated overnight with the respective primary rabbit antibodies against CK10 (1:200), CK13 (1:300) and CK5 (1:300) (Abcam; Cambridge, UK). Signals were developed by using a universal ABC kit and DAB substrate (both from Vectastain). Finally, nuclei were counterstained with Hematoxylin for 1 minute at room temperature and mounted in an aqueous mounting medium. Tissue morphology was finally optically evaluated, as above described. Three randomly selected pictures from each slide were collected at 40x magnification. Nuclei and positive cells were manually counted using the cell counter plugin of ImageJ softener. The degree of CK5, CK10 and CK13 expressions were categorized and scored on a scale of 0-3+, as follows: 0: immune-negativity, +: 1-15% positive cells, +: 16-49% positive cells and +++: 50-100% positive cells (the most intense staining visualized).

Statistical analysis was performed using Friedmann' s ANOVA followed by Dunn's post-hoc test.

9.5. Proteomic Array

Protein array (Proteome Profiler™ Human Angiogenesis Array Kit, R&D, Minneapolis, MN, USA; ARY007) charted 55 proteins in conditioned media from hMSCs, OB14 and OB28. The proteomic array was performed according to manufacturer's instructions. Briefly, pre-coated membranes were blocked with the blocking buffer number 7 for 1 hr on a rocking shaker; after that, CMs diluted in Array Buffer 4, were used to incubate the membraned overnight. The second day, the adherent proteins were retrieved by sub-sequential addition of the Detection Antibody Cocktail conjugated with biotin (1 hr), the Streptavidin-HRP solution (30 minutes) and Chemi Reagent Mix (1 minute). Finally, images were collected with a ChemiDoc (Bio-Rad) and profiles of mean spot pixel density were measured using ImageLab Software. A mix of 3 to 4 independently collected CM for each condition were used to perform the analysis.

9.6. Elisa

ELISA (Quantikine® ELISA Human KGF/FGF-7 Immunoassay, R&D, Minneapolis, MN, USA; DKG00) was performed to quantified KGF amount in CM derived by hMSCs, OB14 and OB28 cultivated both in 2D and 3D conditions. The ELISA was performed according to the manufacturer's instructions. Briefly, selected wells were activated with Assay Diluent RD1-25 and samples were added in triplicate. After 3 hr of incubation, the Human KGF Conjugate was used to detect the adherent protein amount. After that, the substrate solution was added to develop the signal. Finally, the absorbance was quantified with the Spectrophotometer UltroSpec 100 set to 450 nm with a correction wavelength set to 570 nm. Three to 4 independently collected CM were used to perform the analysis. After that, the absorbance values were converted in pg/ml with the standard curve equation. Finally, the unpaired t-student test, as statistical analysis, was performed using GraphPad Prism 6.

9.7. Mucoperiosteum model

The mucoperiosteum model was prepared following the scheme below (fig. IX-2). Briefly, hMSCs were trypsinized, count by trypan blue stain, and resuspend $2x10^6$ cell/ml in 1:1 fibrinogen (12 mg/ml) and complete medium. Next, 30 mU/ml thrombin were added immediately before seeding, and 10^5 cells were seeded for in each scaffold. Subsequently, the fibrin gel formation was fastened by mechanical stimulation, and hMSCs were let adhere in the incubator. After 2 hours of incubation, scaffolds were submersed with 1.5 ml of DMEM 10% FBS and let it grow for one week before preparing the connective tissue substitute. The connective substitute solution (1.65 ml Rat tail collagen type I 6.6 mg/ml, 105 µL 10x F12, 105 µL FBS, 10.5 µL PEN/Strep 100x, 2.5 µl NaOH 1 M) was prepared, filled with $3,3x10^5$ HGF/ml, pour in 48 well plate and let solidify for 2 days in incubator. Then, 50 µl of fibrin glue (10 mg/ml fibrin mixed with 0,5 NIH U thrombin and activated with 2,4 mM $CaCl_2$) were used to coat the upper surface of the repopulated BTC/nHA scaffold and the connective layer was moved with a sterile spoon-like spatula on the top of the fibrin glue and left untouched for 30 minutes. Later, $2,5x10^5$ HOKs were seeded in 20 µl on each model, left adhere for 2 hours in the incubator and submerged in FAD medium for 4 days. Finally, the system was cultivated for 12 days with the bone part submerged and the mucosa counterpart at the air-liquid interface. And formalin-fixed and paraffine embedded (paragraph 4.2) for histological analysis (paragraph 9.7.1) or used for mechanical analysis (paragraph 4.3.3)

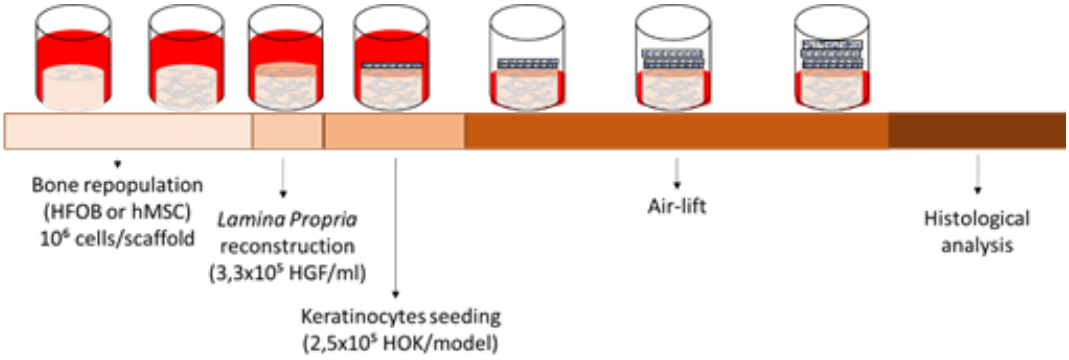

Figure IX-2 *Schematic representation of the mucoperiosteum setting methods*

9.7.1. Masson Trichrome assay

The histological analysis was carried out on, at least, three tissue sections obtained from formalin-fixed paraffin-embedded 3D epithelial tissue cultures. Briefly, slides were deparaffinized and re-hydrated with sequential passages in xylene and descending concentrations of ethanol (100, 95, 90, 70, and 50%). Once rinsed, slides were stained with the Bio-Optica kit 04-010802 and following the manufacturer instructions. Briefly, slides were incubated for 10 minutes with the Weigert's iron hematoxylin, drained out and re-incubated with the Picric acid alcoholic solution; after that, slides were rapidly washed and incubated for other 4 minutes in the Mallory's Ponceau acid fuchsin, washed and reintubated in a Phosphomolybdic acid solution for other 10 minutes. Finally, slides were counterstain for 5 minutes in Masson aniline blue and mounted with a water-based mounting media (Bio-Optica).

X.Results

10.1. Paracrine effect evaluation

10.1.1. hMSCs paracrine effect on keratinocytes stratification and differentiation

Hematoxylin and eosin staining of the treated 3D oral mucosa (fig. X-1) shows that hMSC derived CM (X-1 c) strongly affects the normal stratification; both spinosum and cornified layers are absent or poorly organised, while basal layer cells appear loose and flat in comparison with the untreated control mucosa. On the opposite, control mucosa (b) well resembles the normal mucosal structure (a). The finding is particularly interesting if compared with the monolayer experiment presented in chapter 2. Indeed, when the hMSC CM is applied on the monolayer, keratinocytes metabolism is speeded up while in the three-dimensional structures, the excessive amount of growth factors umpired the correct stratification.

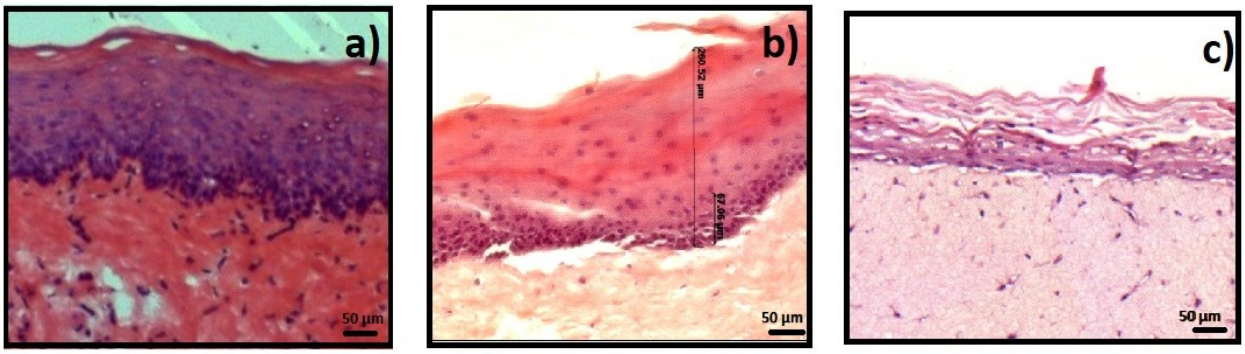

Figure X-1 *a) oral mucosa b)* 3D reconstructed oral mucosa, c) 3D reconstructed oral mucosa after treatment with hMSC derived CM and an untreated one. H&E staining, Magnification 30X, bar scale 50 µm.

10.1.2. Paracrine effect of hMSCs-derived osteoblast effect on keratinocytes stratification and differentiation

To evaluate the effect of osteoblast secretome onto the keratinocyte differentiation, conditioned media (CM), produced by hMSCs under differentiating conditions and collected at the above described time points (7, 14, 21 and 28 days), were mixed with ¼ Ham's-F12 and FAD2 growth factors and used to growth an oral mucosa at the air-liquid interface and follow its differentiation and keratinization.

A control mucosa was also produced by growing it in a freshly produced osteogenic medium mixed with ¼ Ham's-F12 plus the above listed FAD2 factors.

It was observed that the stratification process was affected by OB secretomes. As shown by the HE stainings (fig. X-2) of the control mucosa, despite osteogenic factors fostered the development of the cornified layer (which appeared like a para-keratinized-masticatory mucosa), the cytokeratin pattern expression was not alternated and

the high presence of the specific CK13 was observed in all conditions as well as the expression of CK5 in the basal layer (fig. X-3).

However, the IHC analysis reveals that OB secretome impairs the development of the spinosum layer by interfering with the balance between CK10 and CK13. The MSCs addressed towards osteogenic differentiation increased the CK10 expression in the engineered mucosa with a contextual impairment of the CK13 expression (table X-1), usually expressed homogeneously among the oral mucosa. In particular, we observed that the effect induced by OB14_CM correspond to a statistically significant increase in the keratinization status and in the expression of CK10 differentiation marker in comparison with others condition in both spinosum ($p<0,05$) ad keratinized layer ($p<0,01$).

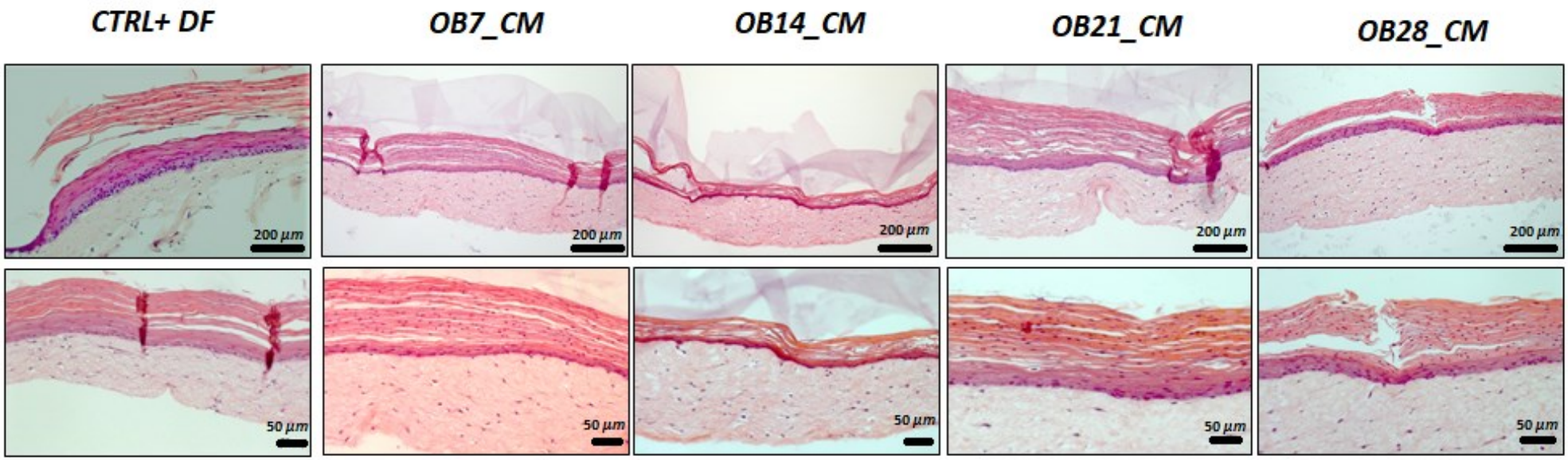

Figure X-2 *Hematoxylin and eosin staining of 3D reconstructed oral mucosa treated with osteogenic factor (DF) or conditioned medium (CM) collected by osteoblast (OB) in different stages of differentiation (OB7, OB14, OB21, OB28). Upper Images magnification 10X, bar scale, 50 µm. Lower images magnification 20x, bar scale 200 µm.*

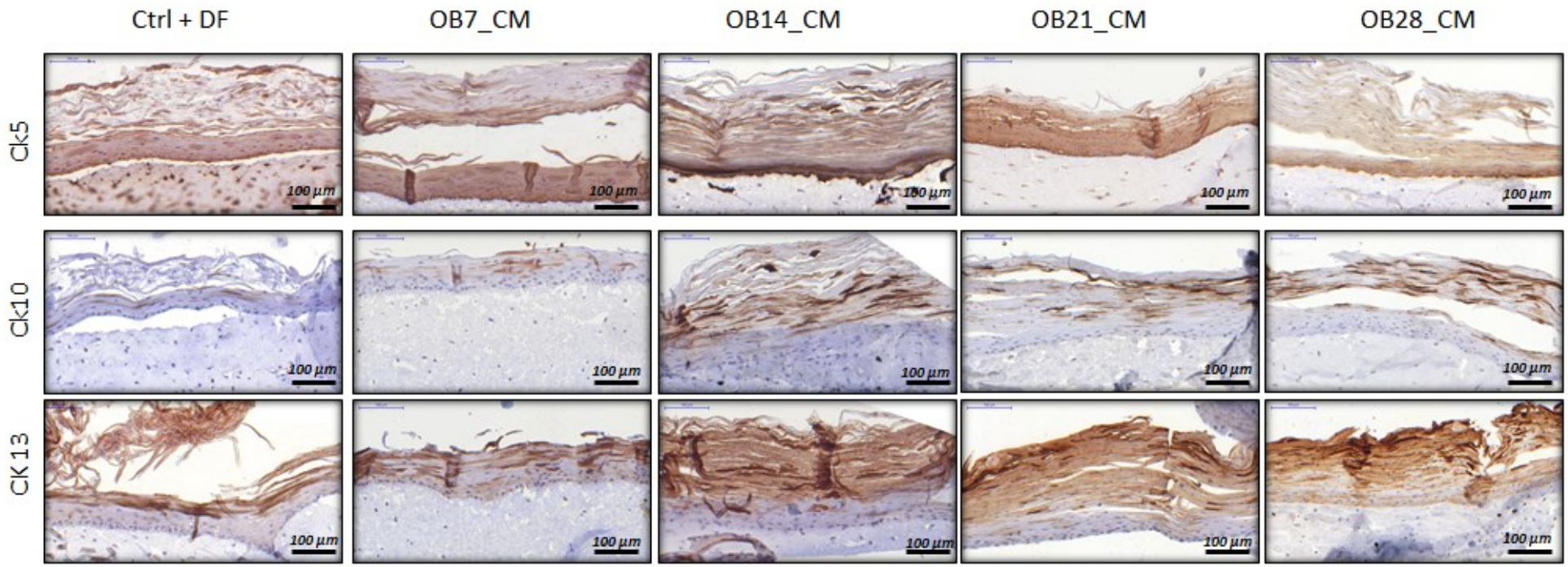

Figure X-3 CK5, CK10 and CK13 immunolocalization in 3D reconstructed oral mucosa treated with osteogenic factor (DF) or conditioned medium (CM) collected by osteoblast (OB) in different stages of differentiation (OB7, OB14, OB21, OB28). Magnification 15X, bar scale 100 µm

Table X-1 *CKs intensity scores.*

Marker	*Layer*	*Control*	*OB7_CM*	*OB14_CM*	*OB21_CM*	*OB28_CM*
	Basal	*+++; H*	*+++; H*	*+++; H*	*+++; H*	*+++; H*
Ck5	*Suprabasal/Spinosum*	*++; H*	*++; H*	*++; H*	*++; H*	*++; H*
	Cornified	-	-	-	-	-
	Basal	-	-	-	-	-
Ck10	*Suprabasal/Spinosum*	*+; E*	*++; E*	*++; E*	*+; E*	*+; E*
	Cornified	-	*++; E*	*+++; E*	*++; H*	*++; E*
	Basal	-	*+; E*	-	*+; H*	*+; H*
Ck13	*Suprabasal/Spinosum*	*+++; H*	*+++; E*	*+++; E*	*+++; E*	*+++; E*
	Cornified	*+; H*	*+; H*	*+; H*	*+; H*	*+; H*

Note: Stainings were scored from 0 (no staining) to 3+ [for the most intense staining the expression pattern was classified as homogeneous (H) or heterogeneous (E)]

10.1.3. Proteomic array and ELISA

In order to detect which factors affected the epithelium proliferation and stratification, media protein profiles were analysed using a 55-proteins-profiler kit. Among the selected proteins, 15 (Serpin E1, Serpin F1, VEGF, FGF-1, IGFBP-3, Pentraxin-3, Persephin, CD26, Angiopoietin-2, TIMP-1, Thrombospindin-1, Thrombospindin-2, Coagulation Factor 3, uPA and Vasohibin) resulted down-regulated, 8 (CXCL16, IGFBP-1, Angiopoientin-1, Angiogenin, PK-1, TIMP-4, KGF and EG-VEGF) up-regulated, 8 (Amphiregulin, Artemin, GDNF, IGFBP-2, CXCL8, MCP-1, MMP-9 and PIGF) showed an irregular trend during the hMSC differentiation in vitro, 5 (VEGF-C, IL-1β, HGF, GM-CSF, CD105 and ADAMTS-1) were expressed only by hMSCs, 4 (CXCL4, Leptin, TGF-β1 and HB-EGF) were expressed only during the differentiation and the basic FGF was expressed only by OB14. The results are summarized in figure X-4 and in table X-2. Among these factors, several have been proven to be involved in wound healing process (ADAMTS-1, Angiogenin, GM-CSF, Angiopoietin and MCP-1) and keratinocytes growth and migration (FGF, IGFBP and TIMP families, MMP-9, Amphiregulin, HGF and KGF). Since we were interested in a factor which directly interact with keratinocytes, we selected KGF as candidate gene and quantified its production with ELISA technique.

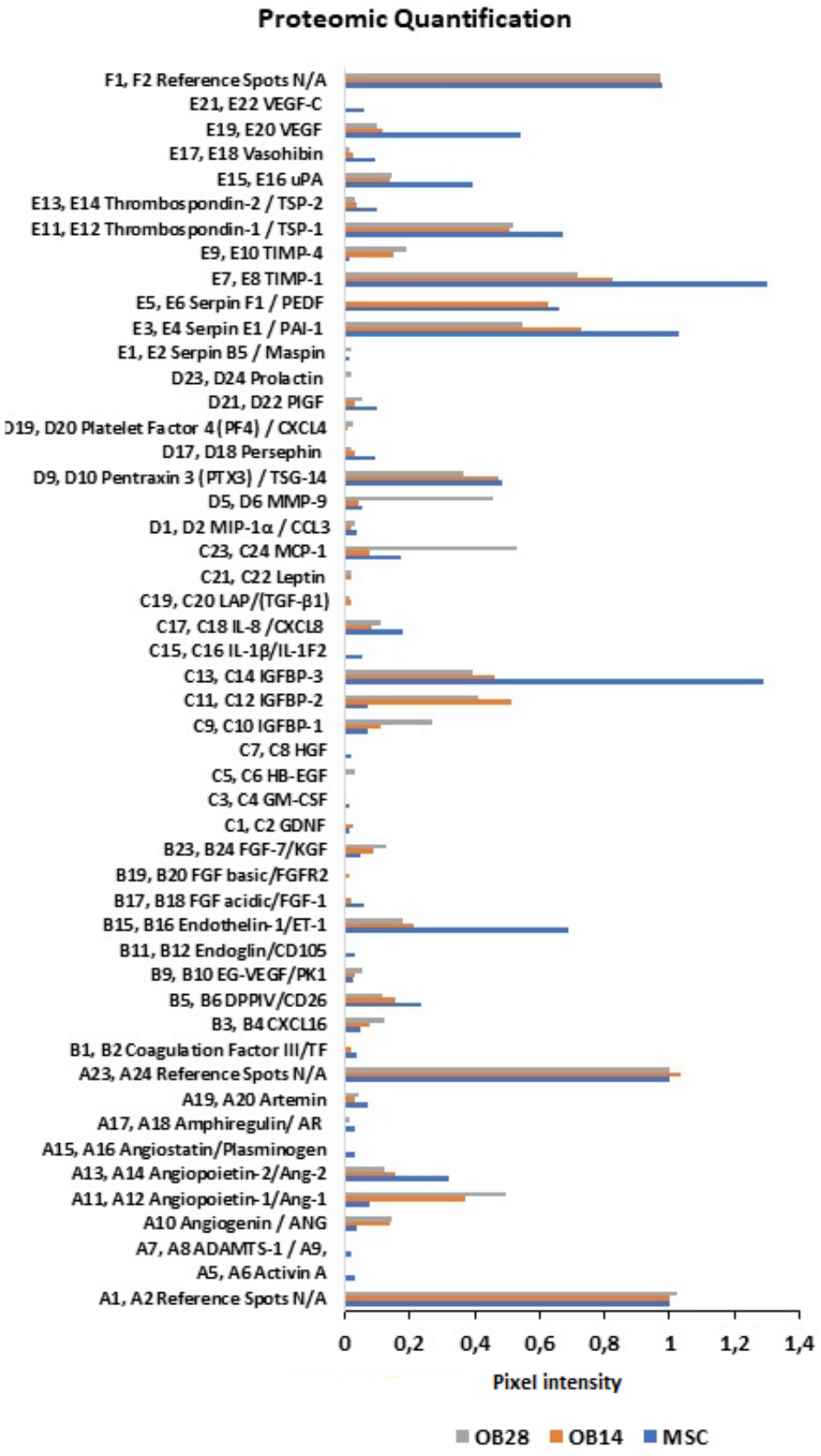

Figure X-4 The histogram represents the amounts of proteins expressed during hMSCs differentiation. Bars represents relative pixel intensity.

Table X-2 *Protein* over, under or irregularly expressed among MSC osteogenic differentiation

DOWN-REGULATED	***UP-REGULATED***	***IRREGULAR TREND***
Serpin E1/PAI-1	CXCL16	Amphiregulin
Serpin F1/PEDF	IGFBP-1	Artemin
VEGF	Angiopoietin-1	GDNF
FGF-1	Angiogenin	IGFBP-2
IGFBP-3	PK-1	CXCL8
Pentraxin-3	TIMP-4	MCP-1
Persephin	KGF	MMP-9
DPPIV/CD26	EG-VEGF	PIGF
Angiopoietin-2		
TIMP-1		
Thrombospondin-1		
Coagulation Factor 3		
Vasohibin		
Thrombospondin-2		
uPA		

ELISA assay highlighted a statistically significant difference ($p<0,05$) between the KGF produced during the hMSC differentiation and that produced by the undifferentiated hMSCs. KGF amount increased to 208±36 pg/ml after 14 days of differentiation and to 347±15 pg/ml after 28 days of differentiation (fig. X-5 a) The low or absent presence of KGF among the different OM-CMs tested suggests that all the KGF produced is metabolized by oral keratinocytes.

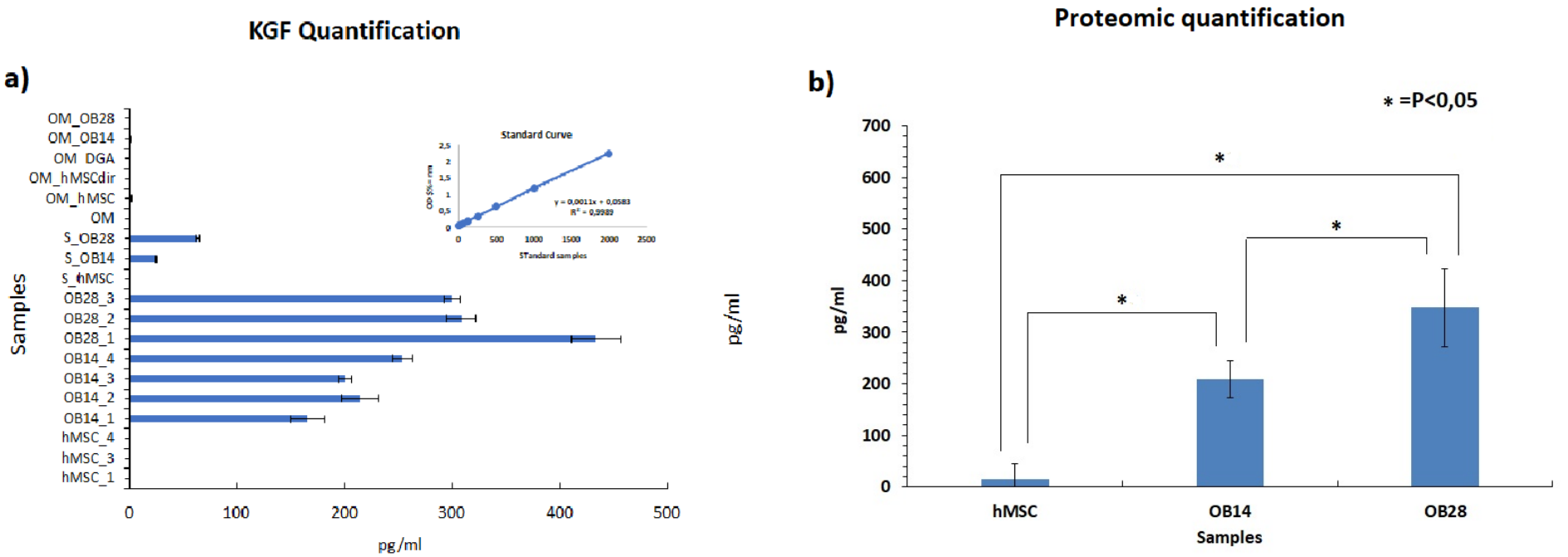

Figure X-5 KGF quantification by ELISA assay. The absorbance values were converted in pg/ml with the formula obtained with the standard curve. a) KGF amounts for each independent replicate; b) KGF amounts calculated for each condition. Bars indicate means and standard deviations, * p<0.05

10.2. Co-Culture of the oral mucosa and hMSCs with or without differentiation factors: crosstalk effects

10.2.1. hMSCs affects keratinocytes stratification and differentiation

To evaluate if the hMSCs secretome affects oral mucosa differentiation, a 3D hMSC-OM co-cultures was developed. Histological analysis of the control 3D culture shows that the crosstalk between oral mucosa and hMSCs improve the keratinocytes behaviour ensuring a complete stratification process, both in the presence and absence of differentiating factors (fig. X-6 a).

In particular, hMSCs seem to induce a stratification well-resembling the masticatory epithelium; above all the co-cultured oral mucosae growth without differentiation factors are characterized by 2 to 4 columnar-shaped and small cells which form a dense layers characteristic of the basal stratum, by a thick spinosum layer with some squamous cells and few pyknotic nuclei, a granulosum stratum and a thin keratinized layer with few nuclei retained. When the oral mucosa is co-cultured with hMSC in the presence of the differentiation factors, despite the basal layer appears similar to that formed in absence of differentiation factors, the spinous layer appears thicker and denser of nuclei. CK10 expression was enhanced by the presence of hMSC differentiating a toward osteoblast lineage, indicating a role of this latter in fostering parakeratinized differentiation of the engineered mucosa.

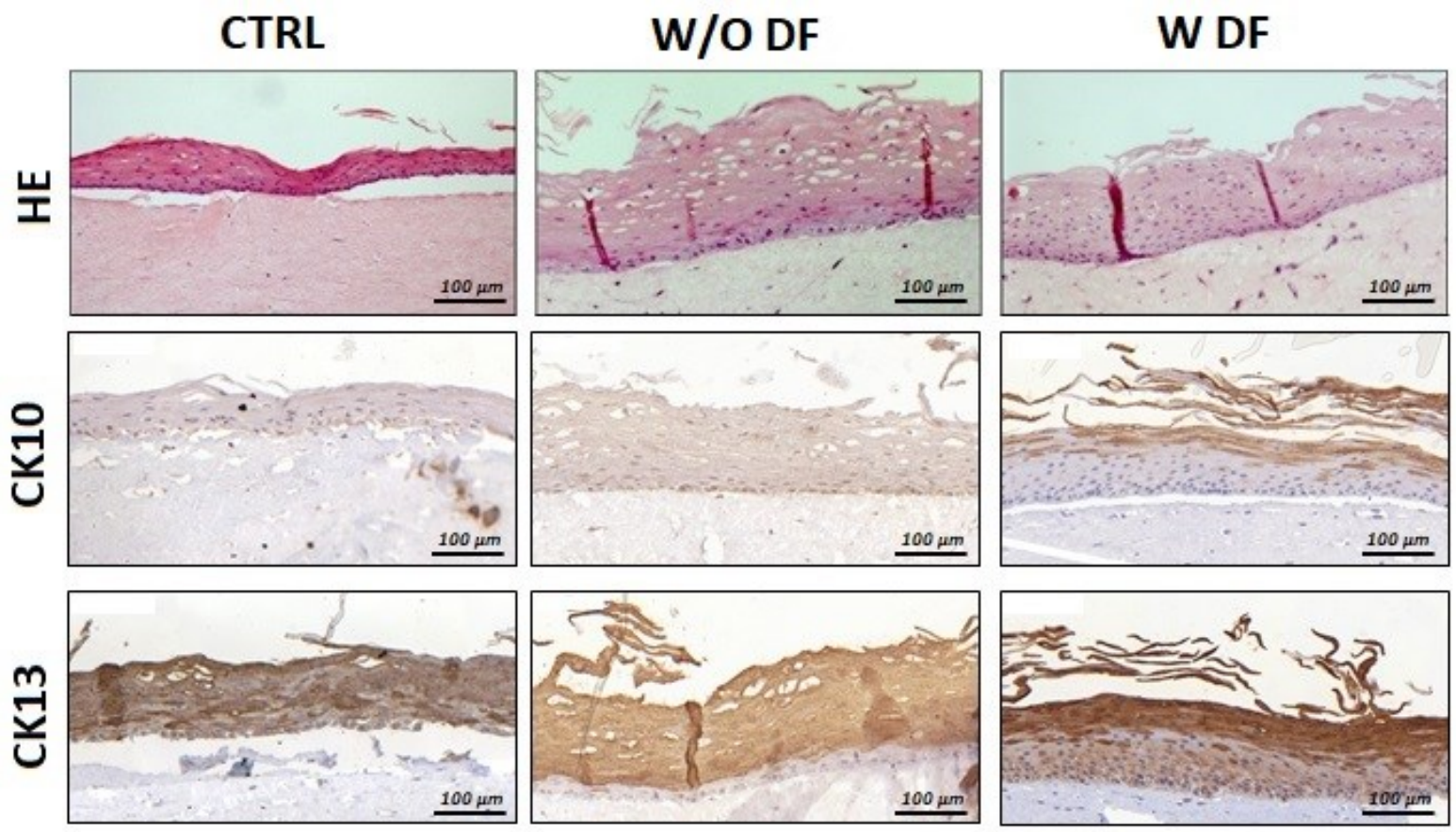

Figure X-6 *HOK differentiation patterns in response to the undifferentiated and differentiated hMSC secretome. Immunohistochemical staining of CK10 and CK13 shows the effect of the hMSC co-cultivation with or without differentiation factors. Magnification 20x, bar scale 100 µm*

10.2.2. Mucosa model affects hMSC osteogenic differentiation

To evaluate the effect of oral mucosae models onto hMSC differentiation, the hMSC, growth in co-cultures with oral mucosae, were fixed and stained. As previously shown, hMSCs need 3 to 4 weeks under differentiation stimuli to fully differentiate into osteoblasts and produce the deposits of calcium/phosphate that can be successfully stained. Nevertheless, as shown in figure X-7, both Von Kossa and Alizarin Red stains, specific for calcium and phosphate deposits respectively, gave positivity strongly already after 12 days co-culture in the presence of differentiation factors. All the other tested conditions used as controls (monocultured hMSCs in DMEM and FAD2 media with or without differentiation factors and co-culture hMSC and oral mucosa in FAD medium without differentiation factors) gave negative signals.

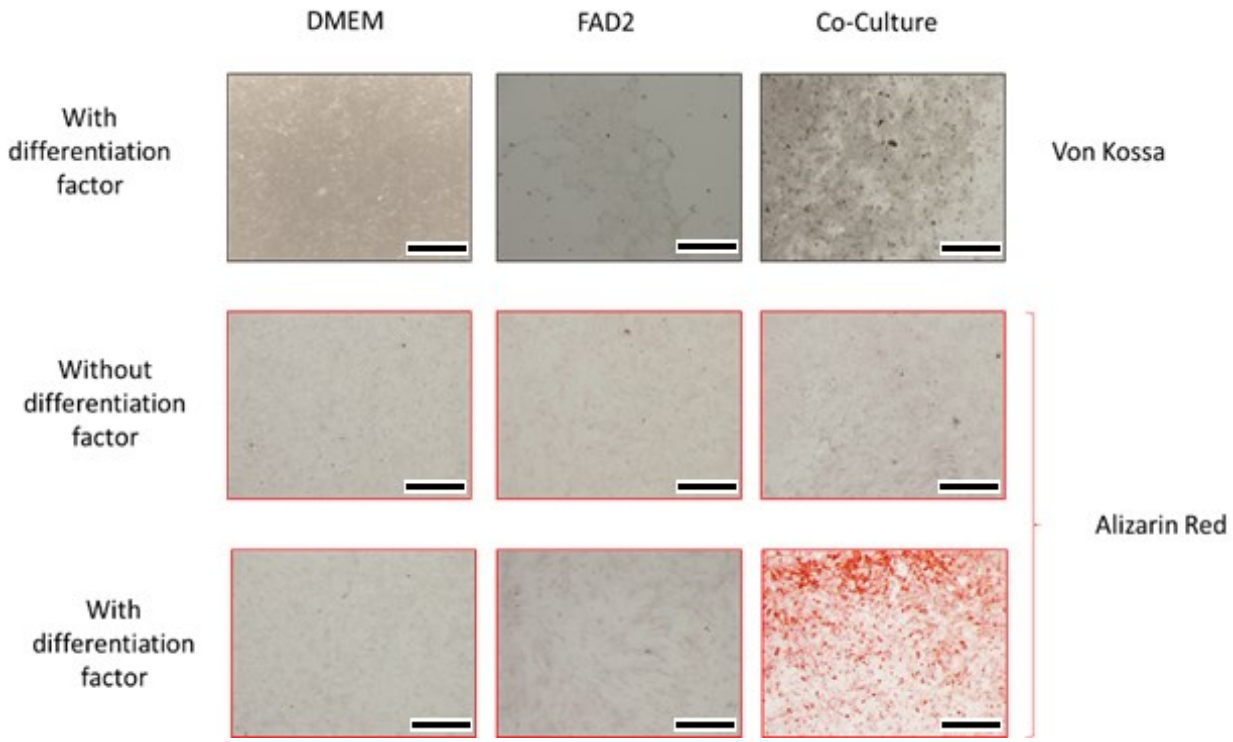

Figure X-7 Von Kossa and Alizarin Red calcium and phosphate deposits staining after 12 days co-cultured hMSC with oral mucosa in FAD medium with or without differentiation factors or monocultured hMSC in DMEM or FAD media with or without differentiation factors. Magnification 4x, bar scale 75 µm

10.3. Connective tissue development: fibroblast-hMSCs interactions effect onto keratinocytes stratification and differentiation.

The effect of hMSCs embedded within the connective tissue, together with HGF was assessed. As shown in figure X-8, hMSCs influenced keratinocytes stratification and differentiation also when embedded in the connective tissue. The histological analysis showed that hMSC speeded up the keratinocyte proliferation and stratification, obtaining the fully epithelium resembling the native one in only 7 days. Once again, the proliferative state induced by hMSCs resulted uncontrolled. Indeed, after another 1 week of direct co-culture, keratinocytes lose their organized structure.

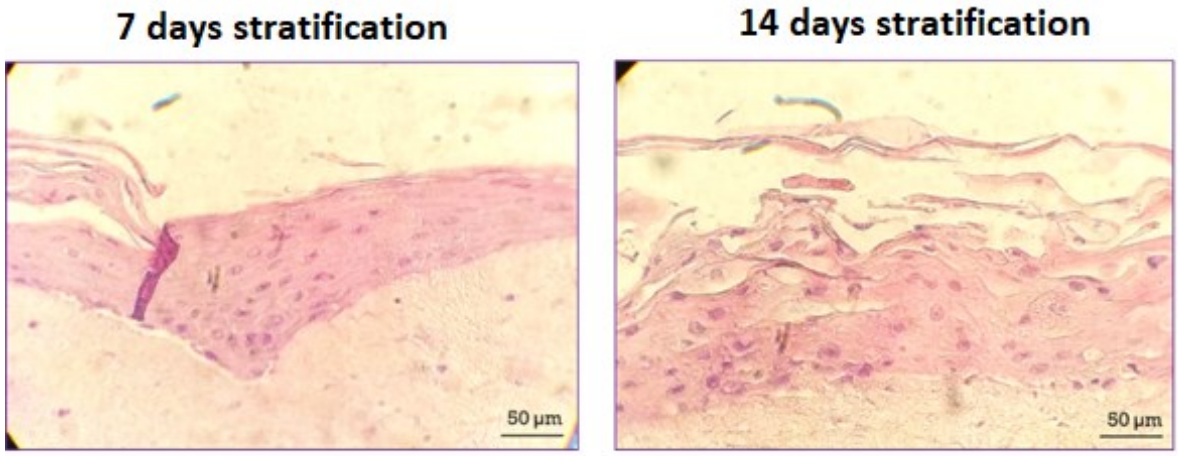

Figure X-8 Haematoxylin and eosin analysis of oral mucosa growth in direct contact with hMSC for, respectively, 7 and 14 days. Magnification 20x, bar scale 50 µm

10.4. 3D composite model

10.4.1. Histological analysis

Masson Trichrome stain was used (fig X-9 a) to evaluate the mucoperiosteum model morphology. As shown by the histological sections, the connective tissue adapts to the scaffold surface following the porous structures of the scaffold itself. The keratinocytes layers are less in comparison with the base models and the basal cells appear flatter than their usual morphology. However, the spinosum layer is well-formed with a sufficient thickness. The keratinization was not observed.

10.4.2. Mechanical properties evaluation

The storage modulus (E') and the variation of loss factor (tan delta) in the meaning of the frequency were evaluated after mucoperiosteum development. The basal scaffold, interpenetrated with the fibrin gel (BTC/nHA_FG) was considered the control for the composite model: *i*) BTC/nHA_FG repopulated with HFOB (BTC/nHA_FG_HFOB), *ii*)

BTC/nHA_FG lined by the oral mucosa (BTC/nHA_OM), and *iii*) the full model composed by BTC/nHA_FG_HFOB lined by the oral mucosa (BTC/nHA_FG_HFOB_OM).

As shown in figure X-9 b the storage modulus showed a similar trend for the pair BTC/nHA_FG (blue line) / BTC/nHA_FG_HFOB_OM (yellow line) and the pair BTC/nHA_FG_HFOB (orange line) / BTC/nHA_FG_OM (gray line). In particular, at high frequency, the first pair present values 3 times higher than the second pair.

E' modulus decrease when the control BTC/nHA_FG is compared with the repopulated scaffold BTC/nHA_FG_HFOB. On the contrary, E' modulus increase when the BTC/nHA_FG_OM is grown in the presence of osteoblasts (BTC/nHA_FG_HFOB_OM).

The E’ modulus variation among the samples indicated a degradation of the fibrin gel actuated or by the HFOB or by the HGF contained within the connective tissue. On the contrary, the storage modulus trend registered for the mucoperiosteum model results similar to the one listed for the control (BTC/nHA_FG). Those data indicated that the interaction between the OM and the HFOB increase the matrix production by osteoblast cells.

The presented results are confirmed by Tan delta curves (fig. X-9 c). The Tan delta value registered highlighted an opposite trend when the full model (BTC/nHA_FG_HFOB_OM) is compared to the others. This attest an increasing of the elastic property in comparison with the viscous one, suggesting the formation of a more physiological matrix within the model.

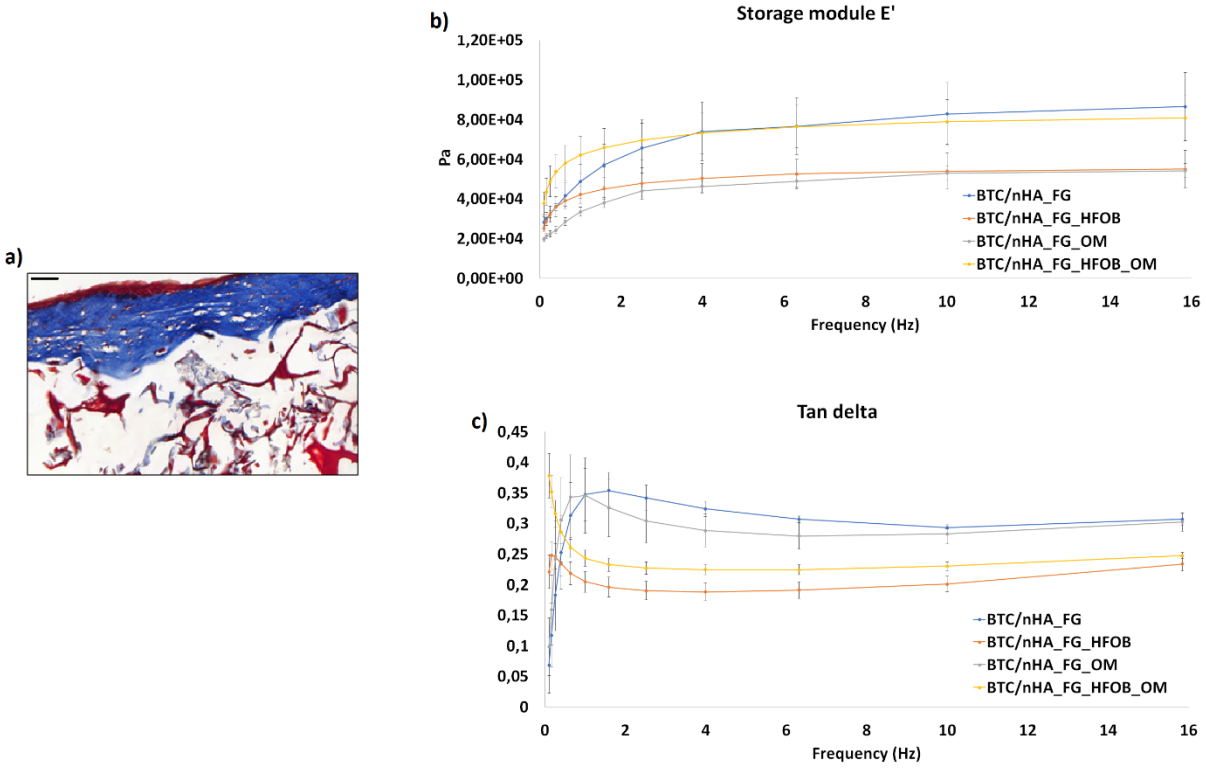

Figure X-9 *a) Histological images show the development of a mucoperiosteum model. 10x magnification; 150 µm bar scale. The curves represent the viscoelastic behaviour of BTC/nHA improved with the fibrin gel used as base for a mucoperiosteum model. In particular, the (b) storage modulus E' and the (c) the loss modulus Tan Delta are expressed in meaning of to the frequency*

XI. Discussion

For the last 4 decades, several researchers have been focused on the development of novel three-dimensional (3D) cultures resembling cells behaviour physiological stimuli response and pathological development. The first examples of such models were developed in oncology to evaluate epithelial-mesenchymal transition (Mishra et al., 2012). Currently, 3D cultures have been largely advanced and employed in several medical-related fields, also including tissue engineering (TE) and regenerative medicine fields. Despite 3D cultures have been applied in TE for evaluating porous scaffold cytocompatibility and effectiveness as implantable tools, the effect of the three-dimensional matrix on cells (both primary and immortalized cancer cells) has not been often well-thought-out. Indeed, the parameters that were usually evaluated for those cultures were limited to the cell adhesion capability onto the newly developed matrix, to the middle-term viability of seeded cells and, eventually, to differentiative potential of progenitor or stem cells was retained (Yu et al., 2015). Consequently, several engineered tissues models have been developed to resemble the physiological microenvironment to be applied in the biomaterial and prosthetic fields (Velasco et al., 2015). Despite the effort, most of them still lack the physiological complexity and the tissue interface connection.

In the dentistry field, several research lines have been focused on the hard-soft tissue interface, especially in dental implantology, where the devices are for hard and soft tissue integration. In particular, the soft tissue of the oral mucosa is composed of a heterogenic group of pluristratified squamous epithelia underlined by a connective tissue layer in direct contact with different deep structures such as bones or muscles (Gibbs et al., 2000). In addition, the soft tissue at the peri-implant interface displays histological properties different from the soft tissue around natural teeth and if not maintained properly, the peri-implant mucosal barrier fails and leads to peri-implant disease.

Although several factors are responsible for implant failure or of poorly peri-implant tissue integration, a critical role is played by the quality and the quantity of existing or augmented peri-implant mucosa. Several works report that the soft tissue integration is essential to improve implant graft and final clinical success (Artzi et al., 1993; Chiu et al., 2015; Esfahanizadeh et al. 2016). In particular, a contextual soft tissue graft is recommended when the keratinized oral epithelium on the apical free gingiva is limited, or the space between the apical sulcus and the junctional epithelium is lower than 2 mm. However, this solution is not always applicable due to the lower availability of tissue for the allograft and the morbidity associated with the autograft (Artzi et al., 1993).

Therefore, new strategies to improve soft tissue recovering and integration with implants should be developed. However, the literature still lacks clear information regarding the molecular mechanism driven the keratinocytes to differentiate towards a keratinized on the non-keratinized epithelium. To overtake this limitation, the first part of this thesis was focused on the evaluation of this phenomenon.

As shown by several studies, keratinocytes can be chemically induced toward keratinized fate by chemical factors such as Calcium ions (Ca^{2+}), glycerol, 12-O-tetradecanoylphorbol-13-acetate (TPA) and vitamin D3. Glycerol and Calcium Chloride ($CaCl_2$) are often used to improve the formation of the *stratum corneum* in skin 3D models. However,

despite those factors induce the Ck10 expression in monolayered cells, they are not able to induce it in 3D models (Lamber et al., 2006; Pol et al., 2002).

Sonkoly et al. (2010) and You et al. (2007) showed, in two independent studies, that the pathways dependent by protein-kinase C (PKC) can be activated by TSG101, a protein implicated in multiple biological functions including regulation of gene transcription, vesicular trafficking, cellular growth and differentiation. TSG101-PKC signaling activates the miR-203, which induce CK10 expression and keratinocytes differentiation. However, those studies were conducted on skin models and the mechanism troughs the activities of TSG101 is upregulated remain unclear.

Like other researchers, Neupane et al. (2018) focused their research on the connective tissue underlying the epithelia. In particular, they focused on the anteroposterior axis of hard-soft palate development in a mouse model. They conducted a tissue recombination assay of the embryos palate at (E16) for 2 days they demonstrated the role of Meox2 to induce the non-keratinized fate during the soft palate development.

Since the sulcular epithelia follow a similar trend, in the first part of this thesis, the effect of stromal cells on keratinocytes differentiation was evaluated using a custom-made 3D organotypic mucosa model.

We demonstrated that stromal compartment affects the epithelial stratification. In particular, the fibroblast subtype and the concentration of glycerol, $CaCl_2$ and FBS influenced the stratum spinosum appearance and, consequently, the differentiation grade and keratin production of the stratum corneum (fig. X-1). This finding reinforced the idea that the mesenchyme substrate strongly influences keratinocytes behaviour. However, this observed phenomena cannot explain what happens *in vivo* since there are not evidences, until now, of different gingival fibroblast subset. Thus, we hypothesised that cells other than fibroblasts might influence the epithelia stratification: i) mesenchymal stem cells, present in the periosteum and ii) osteoblasts which are nearby located in the alveolar bone. Due to the potential of hMSC to migrate toward the damaged site and differentiate in loco, we decide to evaluate the effect of hMSC onto keratinization not only in the undifferentiated condition but also during the differentiation.

The first parameter taking into the account was the paracrine effect of hMSC secretome in undifferentiated condition and during the differentiation. Interestingly, the hMSC_CM have a negative effect towards keratinocytes stratification. Indeed, the keratinization was induced during the proliferative stage of the basal layer with the consequent impairment of the spinosum layer.

The effect of secretome derived from hMSC grown in pro-osteogenic condition was also evaluated. As expected, the full differentiation of hMSCs into osteoblasts (OB) occured in 28 days. During this period, according to the literature, mineralization (Iwamoto et al., 2016; Kulterer et al., 2007), gene expression (with downregulation of pro-proliferation genes such as TGF-β2, and upregulation of pro-mineralization gene such osteopontin, osteocalcein and osteonectin), and secretome composition changed and promoted the bone matrix formation.

During our experiments, the differentiative state of hMSC was weekly checked by specific stain, and the media collect. OB_CM effect was visually assessed by haematoxylin and eosin staining (Fig. X-2) which revealed a huge increase of the keratinized layer in all tested conditions and the impairment of the spinosum layer in contrast with that observed when hMSC_CM was used. Actually, the latter did not affect the stratum spinosum, which was well represented, and neither the epithelium thickness that was comparable with the control.

Intriguingly, studying the specimens treated with OB_CM with immunohistochemical analysis, we observed that thi effect corresponds to an up-regulation of the CK10 induced by the CM (fig. X-3) and that the OB14_CM more induced in a statistically significative manner the expression of CK10 than any other condition. Our results suggest that keratinized gingival formation is mediated by MSC which migrated toward the healing bone around the implant during the differentiation so inducing keratinization.

To elucidate which secretome factor mediates this effect, a protein array was performed. Among the 55 evaluated proteins, 15 of them (Serpin E1, Serpin F1, VEGF, FGF-1, IGFBP-3, Pentraxin-3, Persephin, CD26, Angiopoietin-2, TIMP-1, Thrombospindin-1, Thrombospindin-2, Coagulation Factor 3, uPA and Vasohibin) were down-regulated, 8 (CXCL16, IGFBP-1, Angiopoietin-1, Angiogenin, PK-1, TIMP-4, KGF, and EG-VEGF) up-regulated, 8 (Amphiregulin, Artemin, GDNF, IGFBP-2, CXCL8, MCP-1, MMP-9, and PIGF) showed an irregular trend during the hMSC differentiation in vitro, 5 (VEGF-C, IL-1β, HGF, GM-CSF, CD105, and ADAMTS-1) were expressed only by hMSCs, 4 (CXCL4, Leptin, TGF-β1, and HB-EGF) were expressed only during the differentiation, and the basic FGF was expressed only by OB14 (fig. X-4).

Among the possible factors, KGF was selected to be quantified by the ELISA technique since it has been previously showed that KGF is a critical mediator in keratinocytes proliferation and it acts directly on keratinocytes without influence fibroblast. ELISA test mainly confirmed the data obtained by the proteomic array. Indeed, KGF resulted secreted only by OB, and its secretion increased during the differentiation in a statistically significant way. Interestingly, this trend was also observed when hMSCs were grown and differentiated in three-dimensional condition. KGH was not detected in oral mucosa treated with the conditioned media. This data suggests that KGF available might be quickly metabolized by keratinocytes.

To confirm the above described results, two cocultures systems were developed. One defined indirect, in which the oral mucosa and the MSCs were grown in the same system but without contact, and one defined direct, in which the three cell types (HGF and HOK of the oral mucosa and the MSC) were grown in contact.

In the indirect co-culture, mucosae moved to the air-liquid interface were grown in transwell positioned onto repopulated deep well. Histological analysis revealed that the co-cultivation of OM with hMSC improve the cells differentiation and stratification since the 4 layers seems to better resemble the native tissue. In particular, the basal layer resulted well-formed with the presence of firmly attached, compact and cuboidal keratinocytes at the interface with the connective tissue. However, the spinosum layer of OM grown on co-culture with hMSC in the absence of osteogenic factor presented more prickle cells in comparison with the OM grown in the presence of the osteogenic factors.

The described effect is bi-directional; our results demonstrated that hMSCs differentiation was speeded up by the presence of OM. Indeed, after the 12 days of co-cultivation in the presence of osteogenic factors, hMSCs resulted positive both to Von Kossa and Alizarin red staining while, in the other condition, staining was negative (figure X-7). Our results showed, for the first time, that oral mucosa play a role in MSC differentiation even if the crosstalk between keratinocytes and MSC are well known. For instance, Sevamani et al. (2015) observed that hMSC differentiate toward myofibroblast in transwell co-cultivation with keratinocytes.

We also tested the effect of direct co-cultivation of hMSC with the oral mucosa by embedding the MSC themselves within the collagen matrix with the HGF (hMSC:HGF 1:10). The histological analysis showed that despite hMSC were able to improve keratinocytes proliferation (indeed, a fully stratified epithelium was observed after only six days of cultivation. After one more week of cultivation, the basal keratinocytes retain their proliferative state, and keratinocytes lose their organized structure.

Finally, to conclude this work, the knowledge acquired during the other experiments were used to develop an innovative mucoperiosteum model mimicking the anatomical association between oral mucosal tissue and the underlying bone. This new engineer tissue equivalent is designed to be a valuable tool in testing new material intended to be implanted near the hard-soft tissue interface. The main advantages of this model, in comparison with the others presented in the introduction (Almeda et al., 2016, 2018 a and b) is that the mucosal model and the bone model are let growth together, allowing the cross-talk between the three cell-type involved.

The bone counterpart was accurately selected accordingly to the literature analysis. Firstly, we considered that most of the newly implanted materials are developed to face different challenges. Implanted material, indeed, must be able to counteract, or at least reduce, bacteria adhesion while improving the tissue regeneration around the implant itself. Indeed, we excluded bone scaffolds with intrinsic immunomodulatory or antibacterial properties or unsuitable for further improvements such as the vascularization. Next, we considered bone physiological composition.

Since calcium phosphate is the main element of the bone ECM, a basic bovine tendon collagen (BTC) based sponge enriched with nano-hydroxyapatite (nHA) was selected. The BTC/nHA model was subsequently improved with the fibrin gel to increase the stiffness and improve hMSC proliferation and differentiation. The advantage of this collagen-based model in comparison with the printed ceramic-based scaffold used by Almeda et al. (2018) is that the hydrogel allows nutriment passage between medium and the mucosal model and the fibrin gel expand this effect. This characteristic allowed the keratinocytes growth at air-liquid directly on the top of the bone matrix.

Indeed, the mucoperiosteum model was successfully developed, as showed by the histological analysis (fig X-9 a). Regarding the mechanical evaluation (fig. X-9 b and c), the “full model” storage modulus curve resembles the one obtained with the empty scaffold. This result suggest that OM improved the osteoblast secretion of ECM components and ECM mineralization and, taken together with the effect observed with the indirect co-cultures, confirms that in a pro-osteogenic microenvironment, OM induces the hMSC towards the osteogenic fate.

Even though the present models do not represent the full complexity of the mucoperiosteum model due to the missing of blood vessels or immune system model, they still represent a huge enhancement in the oro-facial model development. Indeed, to our knowledge, this is the first innervated mucoperiosteal model in which oral keratinocytes are able to stratify on the repopulated collagen matrix in direct contact with a repopulated bone substitute.

XII. Bibliography

- Adams D. Keratinization of the oral epithelium. Ann R Coll Surg Engl. 58(5):351-8. (1976)
- Almela T, Al-Sahaf S, Bolt R, Brook IM, Moharamzadeh K. Characterization of Multilayered Tissue-Engineered Human Alveolar Bone and Gingival Mucosa. Tissue Eng Part C Methods. 24(2):99-107. (2018) doi: 10.1089/ten.TEC.2017.0370.
- Almela T, Al-Sahaf S, Brook IM, Khoshroo K, Rasoulianboroujeni M, Fahimipour F, Tahriri M, Dashtimoghadam E, Bolt R, Tayebi L, Moharamzadeh K. 3D printed tissue engineered model for bone invasion of oral cancer. Tissue Cell. 52:71-77. (2018) doi: 10.1016/j.tice.2018.03.009.
- Almela T, Brook IM, Moharamzadeh K. Development of three-dimensional tissue engineered bone-oral mucosal composite models. J Mater Sci Mater Med. 27(4):65. (2016) doi: 10.1007/s10856-016-5676-7.
- Artzi Z, Tal H, Moses O, Kozlovsky A. Mucosal considerations for osseointegrated implants J Prosthet Dent. 70(5):427-32. (1993)
- Atsuta I, Ayukawa Y, Kondo R, Oshiro W, Matsuura Y, Furuhashi A, Tsukiyama Y, Koyano K. Soft tissue sealing around dental implants based on histological interpretation. J Prosthodont Res. 60(1):3-11. (2015) doi:10.1016/j.jpor.2015.07.001.
- Berkovitz BK, Barrett AW. Cytokeratin intermediate filaments in oral and odontogenic epithelia. Bull Group Int Rech Sci Stomatol Odontol. 40(1):4-23. (1998)
- Blumenberg M, Connolly DM, Freedberg IM. Regulation of keratin gene expression: the role of the nuclear receptors for retinoic acid, thyroid hormone, and vitamin D3. J Invest Dermatol. 98(6 Suppl):42S-49S. (1992)
- Blumenberg M, Savtchenko ES. Linkage of human keratin genes. Cytogenet Cell Genet. 42(1-2):65-71. (1986)
- Blumenberg M, Tomić-Canić M. Human epidermal keratinocyte: keratinization processes. EXS. 78:1-29. (1997)
- Boukamp P, Petrussevska RT, Breitkreutz D, Hornung J, Markham A, Fusenig NE. Normal keratinization in a spontaneously immortalized aneuploid human keratinocyte cell line J Cell Biol. 106(3):761-71 (1988)
- Calenic B, Greabu M, Caruntu C, Tanase C, Battino M. Oral keratinocyte stem/progenitor cells: specific markers, molecular signaling pathways and potential uses. Periodontol 2000. 69(1):68-82. doi: 10.1111/prd.12097.
- Ceccarelli S, Romano F, Angeloni A, Marchese C. Potential dual role of KGF/KGFR as a target option in novel therapeutic strategies for the treatment of cancers and mucosal damages. Expert Opin Ther Targets. 16(4):377-93. (2012) doi: 10.1517/14728222.2012.671813.
- Chen J, Li Y, Hao H, Li C, Du Y, Hu Y, Li J, Liang Z, Li C, Liu J, Chen L. Mesenchymal Stem Cell Conditioned Medium Promotes Proliferation and Migration of Alveolar Epithelial Cells under Septic Conditions In Vitro via the JNK-P38 Signaling Pathway. Cell Physiol Biochem. 37(5):1830-46. (2015) doi: 10.1159/000438545.
- Chiu YW, Lee SY, Lin YC, Lai YL. Significance of the width of keratinized mucosa on peri-implant health. Journal of the Chinese Medical Association; Volume 78, Issue 7, Pages 389-394. (2015). doi.org/10.1016/j.jcma.2015.05.001
- Del Angel-Mosqueda C, Gutiérrez-Puente Y, López-Lozano AP, Romero-Zavaleta RE, Mendiola-Jiménez A, Medina-De la Garza CE, Márquez-M M, De la Garza-Ramos MA. Epidermal growth factor enhances osteogenic differentiation of dental pulp stem cells in vitro. Head Face Med. 11:29. (2015) doi: 10.1186/s13005-015-0086-5.
- Deo PN, Deshmukh R. Pathophysiology of keratinization. J Oral Maxillofac Pathol. 22(1):86-91. (2018) doi: 10.4103/jomfp.JOMFP_195_16.
- Dongari-Bagtzoglou A. and Kashleva H. Development of a highly reproducible three-dimensional organotypic model of the oral mucosa. Nat Protoc. 1: 20128 (2006)
- Edmondson R, Broglie JJ, Adcock AF, Yang L. Three-dimensional cell culture systems and their applications in drug discovery and cell-based biosensors. Assay Drug Dev Technol12(4):207-18. doi: 10.1089/adt.2014.573.
- El-Ghalbzouri A, Lamme EN, van Blitterswijk C, Koopman J, Ponec M. The use of PEGT/PBT as a dermal scaffold for skin tissue engineering. Biomaterials. 25:2987-2996. (2004)
- Esfahanizadeh N, Daneshparvar N, Motallebi S, Akhondi N, Askarpour F, Davaie S. Do we need keratinized mucosa for a healthy peri-implant soft tissue? General dentistry 64(4):51-55. (2016)
- Evans EW. Treating Scars on the Oral Mucosa. Facial Plast Surg Clin North Am. 25(1):89-97. (2017) doi: 10.1016/j.fsc.2016.08.008.

- Finch PW, Rubin JS. Keratinocyte growth factor/fibroblast growth factor 7, a homeostatic factor with therapeutic potential for epithelial protection and repair. Adv Cancer Res. 91:69-136. (2004)
- Gartner LP. Oral anatomy and tissue types. Semin Dermatol. 13(2):68-73. (1994). Review.
- Hassan NT, Abdel Aziz NA. Oral Mucosal Stem Cells, Human Immature Dental Pulp Stem Cells and Hair Follicle Bulge Stem Cells as Adult Stem Cells Able to Correct Limbal Stem Cell Deficiency. Curr Stem Cell Res Ther. 13(5):356-361. (2018) doi: 10.2174/1574888X13666180223124936.
- Herson MR, Mathor MB, Altran S, Capelozzi VL, Ferreira MC. In vitro construction of a potential skin substitute through direct human keratinocyte plating onto decellularized glycerol-preserved allodermis. Artif Organs. 25:901-906 (2001)
- Hildebrand HC, Hakkinen L, Wiebe CB, Larjava HS. Characterization of organotypic keratinocyte cultures on deepithelialized bovine tongue mucosa. Histol Histopathol. 17:151-163. (2002).
- Iwamoto Y, Nishikawa, Imai R, Furuya M, Uenaka M, Ohta Y, Morihana T, Itoi-Ochi S, Penninger JM, Katayama I, Inohara H and Ishii M. Intercellular Communication between Keratinocytes and Fibroblasts Induces Local Osteoclast Differentiation: a Mechanism Underlying Cholesteatoma-Induced Bone Destruction. Mol. Cell. Biol. vol. 36 no. 11 1610-1620 (2016)
- Izumi K., Feinberg S.E., Iida A., Yoshizawa M. Intraoral grafting of an ex vivo produced oral mucosa equivalent: a preliminary report. Int J Oral Maxillofac Surg. 32: 188-97 (2003)
- Izumi K., Takacs G., Terashi H., Feinberg S.E. Ex vivo development of a composite human oral mucosal equivalent. J Oral Maxillofac Surg. 57: 571-.7(1999)
- Izumi K., Terashi H., Marcelo C.L., Feinberg S.E. Development and characterization of a tissue-engineered human oral mucosa equivalent produced in a serum-free culture system. J Dent Res. 79: 798-805 (2000)
- Izumi K., Tobita T., Feinberg S.E. Isolation of human oral keratinocyte progenitor/stem cells. J Dent Res. 86: 341-6 (2007)
- Lee DY, Ahn HT, Cho KH. A new skin equivalent model: dermal substrate that combines de-epidermized dermis with fibroblast populated collagen matrix. J Dermatol Sci. 23:132-137. (2000)
- Lee KH. Tissue-engineered human living skin substitutes: development and clinical application. Yonsei Med J. 41:774-779. (2000).
- Li M, Zhao Y, Hao H, Dai H, Han Q, Tong C, Liu J, Han W, Fu X. Mesenchymal stem cell-conditioned medium improves the proliferation and migration of keratinocytes in a diabetes-like microenvironment. Int J Low Extrem Wounds. 14(1):73-86. (2015) doi: 10.1177/1534734615569053.
- Ma L, Gao C, Mao Z, Zhou J, Shen J, Hu X, et al. Collagen/chitosan porous scaffolds with improved biostability for skin tissue engineering. Biomaterials. 24:4833-4841. (2003).
- Masuda I. An in vitro oral mucosal model reconstructed from human normal gingival cells. Kokubyo Gakkai Zasshi. 63:334-353. (1996)
- Moriyama T, Asahina I, Ishii M, Oda M, Ishii Y, Enomoto S. Development of composite cultured oral mucosa utilizing collagen sponge matrix and contracted collagen gel: a preliminary study for clinical applications. Tissue Eng. 7:415-427. (2001)
- Müller T, Bain G, Wang X, Papkoff J. Regulation of epithelial cell migration and tumor formation by beta-catenin signaling. Exp Cell Res. 280(1):119-33. (2002)
- Neupane S, Adhikari N, Jung JK, An CH, Lee S, Jun JH, Kim JY, Lee Y, Sohn WJ, Kim JY. Regulation of mesenchymal signaling in palatal mucosa differentiation. Histochem Cell Biol. 149(2):143-152. (2018) doi: 10.1007/s00418-017-1620-2.
- Okazaki M, Yoshimura K, Suzuki Y, Harii K. Effects of subepithelial fibroblasts on epithelial differentiation in human skin and oral mucosa: heterotypically recombined organotypic culture model. Plast Reconstr Surg. 112:784-792. (2003)
- Peehl DM, Rubin JS. Keratinocyte growth factor: an androgen-regulated mediator of stromal-epithelial interactions in the prostate. World J Urol. 13(5):312-7. (1995)
- Pol A, Bergers M, van Ruissen F, Pfundt R, Schalkwijk J. A simple technique for high-throughput screening of drugs that modulate normal and psoriasis-like differentiation in cultured human keratinocytes. Skin Pharmacol Appl Skin Physiol. 15(4):252-61. (2002)
- Rakhorst HA, Tra WM, Posthumus-van Sluijs SJ, de Groot E, van Osch GJ, van Neck JW, Hofer SO. Mucosal keratinocyte isolation: a short comparative study on thermolysin and dispase. Int J Oral Maxillofac Surg. 35(10):935-40. (2006).

- Rouabhia M, Deslauriers N. Production and characterization of an in vitro engineered human oral mucosa. Biochem Cell Biol. 80:189-195. (2002)
- Saintigny G, Bonnard M, Damour O, Collombel C. Reconstruction of epidermis on a chitosan cross-linked collagen-GAG lattice: effect of fibroblasts. Acta Derm Venereol. 73:175-180 (1993)
- Schroeder HE, Listgarten MA. The gingival tissues: the architecture of periodontal protection. Periodontol 2000. 13:91-120. (1997)
- Sculean A, Gruber R, Bosshardt DD. Soft tissue wound healing around teeth and dental implants. J Clin Periodontol. 41 Suppl. 15:S6-22. (2014) doi:10.1111/jcpe.12206.
- Shetty S; Gokul S. Keratinization and its disorders. Oman Med J. 27(5):348-57. (2012) doi: 10.5001/omj.2012.90.
- Sonkoly E, Wei T, Pavez Loriè E, Suzuki H, Kato M, Törmä H, Ståhle M, Pivarcsi A. Protein kinase C-dependent upregulation of miR-203 induces the differentiation of human keratinocytes. J Invest Dermatol. 130(1):124-34. (2010) doi: 10.1038/jid.2009.294.
- Squier CA. Keratinization of the sulcular epithelium--a pointless pursuit? J Periodontol. 52(8):426-9. (1981)
- Tamama K, Kawasaki H, Wells A. Epidermal growth factor (EGF) treatment on multipotential stromal cells (MSCs). Possible enhancement of therapeutic potential of MSC. J Biomed Biotechnol. 795385. (2010) doi: 10.1155/2010/795385
- Velasco MA, Narváez-Tovar CA, Garzón-Alvarado DA. Design, materials, and mechanobiology of biodegradable scaffolds for bone tissue engineering. Biomed Res Int. 729076. (2015) doi: 10.1155/2015/729076.
- Wang H, Pieper J, Peters F, van Blitterswijk CA, Lamme EN. Synthetic scaffold morphology controls human dermal connective tissue formation. J Biomed Mater Res A 74:523-532. (2005)
- Westerhof W, Dingemans KP. The morphological details of globular keratohyalin granules. J Cutan Pathol. 13(5):375-82. (1986)
- Westerhof W, Dingemans KP. The morphology of keratohyalin granules in orthokeratotic and parakeratotic skin and oral mucosa. Int J Dermatol. 26(5):308-13. (1987)
- You HL, Eng HL, Hsu SF, Chen CM, Ye TC, Liao WT, Huang MY, Baer R, Cheng JT. A PKC-Sp1 signaling pathway induces early differentiation of human keratinocytes through upregulation of TSG101. Cell Signal. 19(6):1201-11. (2007)
- Yu X, Tang X, Gohil SV, Laurencin CT. Biomaterials for Bone Regenerative Engineering. Adv Healthc Mater. 4(9): 1268–1285. (2015) doi: 10.1002/adhm.201400760

Chapter 4

Innervated Mucoperiosteal model development

XIII. Introduction

13.1. Periodontium innervation

The innervation is a crucial factor during embryogenesis and tissue regeneration. Indeed, both sensory and motor neurons are indispensables for correct organ functions. Recently, the theory that innervation is not only essential for organs functions but also for organs and tissue development acquired more consideration. For instance, the Möbius syndrome is a congenital syndrome characterized by hypoplastic abducens of facial nerves that have been related to a defective formation of the orofacial portions (i.e., teeth or palate) (Kandel et al.,2000). Also, the potential of neurons to interact with stem cell niches and their capability to mediates the environmental soluble factors to regulate stem cells fate remain an unexplored but still fascinating process (Jimenez-Rojo et al., 2012; Pagella et al., 2014).

Like all the other organs, orofacial structures are innervated by specific neuronal subtypes that are responsible for organs motility and sensitivity. The mechanisms which regulate the axonal growth and innervation are similar between each organ; indeed, the innervation starts with the secretion of specific soluble proteins, which binds the nerve branches and allows or inhibits the migration and elongation of axons through long distances (Kandel et al.,2000). During the axon elongation, several tropic guidance molecules are secreted or exposed on the cell membrane by different tissue types to drive the correct branches toward the correct tissue target.

The most known axon guidance proteins are the membrane-associated inhibitory proteins Semaphorins and ephrins, the laminin-related secreted Netrins (with the capability to binds both pro-innervation and anti-innervation receptors) and the Neurotrophins (NTs), the most studied trophic molecules with the capability to chemoattract neurons and support the axonal outgrowth. Nowadays, four mammalian NTs are well studied, and they are the nerve growth factor (NGF), the brain-derived neurotrophic factor (BDNF), the neurotrophin-3 (NT-3), and the neurotrophin-4 (NT-4). All NTs act trough the bindings of specific receptors: p75 neurotrophin receptor (p75NTR), TrkA, TrkB, and TrkC. Each NT binds to these receptors with different affinities (Reichardt et al., 2006; Egea et al., 2007; Raper et al., 2010; Lai Wing Sun et al., 2011).

Axons secrete the neurotransmitters once they reach their target tissue or organs to regulate the production of guidance molecules. Neurotransmitters can act both as inhibitory or activator factors accordingly to the receptors they bind, and different classes of them are secreted accordingly to the neuron types. The most important neurons type for the periodontium are the: *i)* motor neurons that innervate the muscles via neuromuscular junctions controlling the buccal movements and secrete acetylcholine and the *ii)* sensory neurons with the capability to convert external stimuli

into electric stimuli that are processed by the central nervous system and secrete various neuropeptides such as substance P, neurokinines, and CGRP onto the innervated organs (Kandel et al., 2000).

Interestingly, Blais et al. (2014) demonstrated in an innervated 3D skin model that Substance P improves skin reepithelialisation. This finding suggests that substance P can also act onto other epithelial tissues such as gingiva and cornea that are well innervated by sensory neurons. Moreover, it is well-known that both gingiva and bone structures are full of the neurokinin-1 receptors (NK1-Rs) that bind with high specificity the Substance P, the NK1-Rs receptor is present on osteoclast, osteoblast, and keratinocytes of the junctional epithelial surface.

In general, the periodontal membrane innervation depends on dental and interalveolar nerves, branches of the alveolar nerves. The nerve ending in the periodontal membrane is divided into non-medullated nerve fibres (small fibrils which innervate stromal cells, cementoblasts, and cementum) and the unmyelinated naked fibrils.

Part of the fibres from the periodontal membrane innervates the gingival tissue through lamina propria. Most of them innervate the attached gingiva.

13.2. Innervated epithelial model

Nowadays, there are not available innervated oral mucosa models even if some authors have developed innervated 3D epithelial models mainly focused on ophthalmology. In 2017 Wang et al. present a complex corneal model composed by epithelium, stroma, and nerve based on a repopulated thin silk protein film (which composes the epithelial and stromal part) supported by a porous silk sponge that supports the neuronal growth. In this model, dorsal root ganglia were used and drove towards the other compartments using a collagen-based hydrogel loaded with NGF. Due to the use of NGF, this model is not suitable to evaluate corneal keratinocytes capability to drive DRGs outgrowth.

In 2012, Lebonvallet et al. produced the first innervated skin model by using a decellularized dermal substitute repopulated with rat-DRGs, but the authors did not observe any differences in keratinocytes behaviour. On the opposite, in 2013, Roggenkamp et al. produced a similar model, and they observed that the inhibition of calcitonin gene-related peptide (CGRP), but not substance P (SP) signaling, decrease the epidermal growth. As previously described, in a 3D wounded skin model, Blais et al. proved the role of the substance P in the re-epithelialization process. These last two works suggest that the different neuropeptides are involved and regulated by different processes; GPCR is produced during the epithelial stratification while substance P activation occurs after damage.

Finally, Kuchler-Bopp et al. (2016) described an innervated tooth by a mixture, composed of epithelial and mesenchymal cells and trigeminal ganglia dispersed in a semi-solid media, implanted under mice skin.

13.3. Aims

The following part of this Ph.D. thesis was aimed to the advancement of the previously described epithelial 3D models. In particular, this study focused on the effect of 3D mucosal models onto axonal outgrowth and on the optimization of an innervated bone-mucosa model.

XIV. Materials and methods

14.1. Mucosa model effect on the nervous system

14.1.1. Axonal outgrowth evaluation

In order to evaluate if the osteomucosa model can be innervated, ND7/23 were incubated with all OM_CM collected, and the axonal outgrowth assessed. Briefly, 96 well-plate were coated with poly-D-Lysin and laminin in sterile condition. Afterward, ND7/23 cells were detached and diluted to 10^4 cell/ml in DMEM high glucose complemented with 0.5% FBS and 25 µM FDU (5-fluoro-2'-deoxy-uridine) and seeded in pre-coated well in 100 µl. After 6 hours of adhesion, cells were incubated with pre-warmed conditioned media for 24 hours. Finally, after the incubation time, ND7/23 cells were fixed, stained with DAPI, ad photographed using the In Cell Analyzer 2000.

14.1.2. DRG Isolation

Embryonic lumbar (L1-L6) dorsal root ganglia (DRGs) were gained from 16 to 18 days-old (E16-18) C57BL/6 embryos. After decapitation, embryos were conserved in ice-cold Hank's balanced salt solution (HBSS, Invitrogen) for the DRGs collection. Under a stereomicroscope, the spines were detached from the whole body and opened using a scissor to expose the DRGs. The meninges were removed while the isolated DRG roots were cut. Finally, DRGs were seeded into the lower wells of a 15-well µ-Slide Angiogenesis plate from Ibidi (Cat. No. 81506) embedded in the fibrin solution. The fibrin gel was obtained by mixing a 12 mg/ml plasminogen-free fibrinogen with an equal volume of solution concentrated 4 NIH U/mL thrombin activated by 5 mM of CaCl2 and 20µg/mL of aprotinin. The fibrin gel polymerized for 30 min at 37˚C in a 5% CO2 humidified incubator, before the addition of culture media. DRGs were cultured with neurobasal medium supplemented with 2% v/v B-27 Serum-Free Supplement 1 (B-27, Invitrogen), FDU (Sigma-Aldrich), 25 mM glucose (Glu, Sigma-Aldrich), 1 mM pyruvate (Sigma-Aldrich), 50 ng/ml 7S Nerve Growth Factor (NGF, Calbiochem), 2 mM glutamine (Q, BioWitacker) and 1% penicillin/streptomycin (P/S) and left adhere for 24 hr before treatments.

14.1.3. Quantification of axonal growth

Axonal outgrowth was quantified after 72 hr of treatment with different conditioned media derived from oral mucosa (OM), human mesenchymal stem cells (hMSCs), hMSCs under osteogenic condition for 14 days (OB14) and hMSCs under the osteogenic condition for 28 days (OB28). FAD media, with or without osteoblast differentiation factors, were used as control. After the treatments, DRGs were fixed for 10 minutes in a 4% PFA solution implemented with 4% sucrose, blocked and permeabilised with a 1% BSA solution implemented with 0,2% Triton incubated over-night with the mouse anti-β-Tubulin III (1:2000) at 4°. The day after, the signal was developed by using an AlexaFluo488-conjugated goat anti-mouse antibody (1:400) and nuclear stain DAPI for 1 hr at room temperature. Finally, images were acquired using IN Cell Analyzer 2000 equipped with IN Cell Investigator software (GE Healthcare, United Kingdom). To quantify the differences between the treatment, the radial outgrowth, defined as the area comprised between the ganglion edge and the outgrowth front, was automatically calculated, and the outgrowth area quantified according to Bessa et al. (2013), using a validated MatLAB algorithm.

14.2. Mucoperiosteum model

The mucoperiosteum model was prepared following the scheme below (fig. XIV-1). Briefly, hMSCs were trypsinized, count by trypan blue stain, and resuspend $2x10^6$ cell/ml in 1:1 fibrinogen (12 mg/ml) and complete medium. Next, 30 mU/ml thrombin were added immediately before seeding, and 10^5 cells were seeded for in each scaffold. Subsequently, the fibrin gel formation was fastened by mechanical stimulation, and hMSCs were let adhere in the incubator. After 2 hours of incubation, scaffolds were submersed with 1.5 ml of DMEM 10% FBS and let it grow for one week before preparing the connective tissue substitute. The connective substitute solution (1.65 ml Rat tail collagen type I 6.6 mg/ml, 105 µL 10x F12, 105 µL FBS, 10.5 µL PEN/Strep 100x, 2.5 µl NaOH 1 M) was prepared, filled with $3,3x10^5$ HGF/ml, pour in 48 well plate pre-coated 10^5 collagen embedded ND7/23 and let solidify for 2 days in incubator. Then, 50 µl of fibrin glue (10 mg/ml fibrin mixed with 0,5 NIH U thrombin and activated with 2,4 mM $CaCl_2$) were used to coat the upper surface of the repopulated BTC/nHA scaffold and the connective layer was moved with a sterile spoon-like spatula on the top of the fibrin glue and left untouched for 30 minutes. Later, $2,5x10^5$ HOKs were seeded in 20 µl on each model, left adhere for 2 hours in the incubator and submerged in FAD medium for 4 days. Finally, the system was cultivated for 12 days with the bone part submerged and the mucosa counterpart at the air-liquid interface.

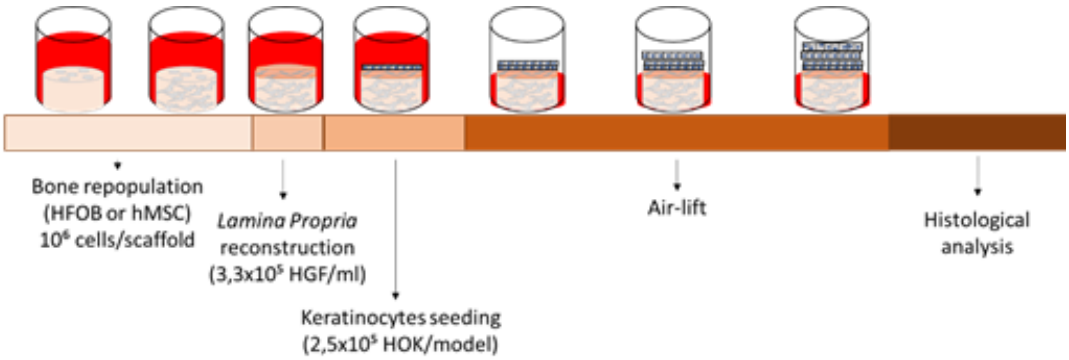

Figure XIV-1 *Schematic representation of the mucoperiosteum setting methods*

14.2.1. Masson Trichrome assay

The histological analysis was carried out on, at least, three tissue sections obtained from formalin-fixed paraffin-embedded 3D epithelial tissue cultures. Briefly, slides were deparaffinized and re-hydrated with sequential passages in xylene and descending concentrations of ethanol (100, 95, 90, 70, and 50%). Once rinsed, slides were stained with the Bio-Optica kit 04-010802 and following the manufacturer instructions. Briefly, slides were incubated for 10 minutes with the Weigert's iron hematoxylin, drained out and re-incubated with the Picric acid alcoholic solution; after that, slides were rapidly washed and incubated for other 4 minutes in the Mallory's Ponceau acid fuchsin, washed and reintubated in a Phosphomolybdic acid solution for other 10 minutes. Finally, slides were counterstain for 5 minutes in Masson aniline blue and mounted with a water-based mounting media (Bio-Optica).

14.2.2. Immunofluorescence analysis

Immunofluorescent staining was carried out on, at least, three tissue sections obtained from formalin-fixed paraffin-embedded 3D epithelial tissue cultures. Briefly, slides were deparaffinized and re-hydrated with sequential passages in xylene and descending concentrations of ethanol (100, 95, 90, 70 and 70%); once rinsed, slides were unmasked in citrate buffer (1 M, pH 6) for 15 at 500 W in a microwave, saturated for 1 hour in PBG (0,5% BSA and 0,2% gelatine in PBS) and incubated overnight with the primary mouse antibodies against β-tubulin III (1:2000; Sigma-Aldrich), rabbit antibody against TBR1 (1:250; GeneTex) and sheep antibody against NGF (1:300; Thermofisher). Signals were developed by using a corresponding AlexaFluo-conjugated secondary antibody. Finally, nuclei were counterstained with DAPI for 10 minutes at room temperature (RT) and mounted in an aqueous mounting medium. Image were acquired under an Inverted Fluorescence Microscope (Zaiss).

XV. Results

15.1. Effect of oral mucosa on the neuronal compart

15.1.1. ND7/23

The pro-innervation potential of OM was evaluated with the immortalized cell line ND7/23. ND7/23 were incubated for 24 hours with CM from different OM models, NGF enriched medium and FAD were used as control. As shown in figure XV-1, most of OM models have a positive effect on axonal outgrowth; however, any statistically significant difference ($p>0,05$) was detected. Despite this positive trend, OM_hMSC CM showed a negative effect on axonal outgrowth.

Interestingly, the CM derived by indirect co-cultures of OM with hMSC under osteoblastic differentiation condition showed a positive effect on axonal elongation. This effect is particularly relevant since it has been showed that the positive effect of hMSC on axonal outgrowth decrease during the osteoblastic differentiation until to become negative when hMSC are fully osteogenically differentiated. These results support that the crosstalk between the OM and hMSC mutually modified the behaviour of both components, inducing the production of more neuroprotective factors to the detriment of anti-innervation factors.

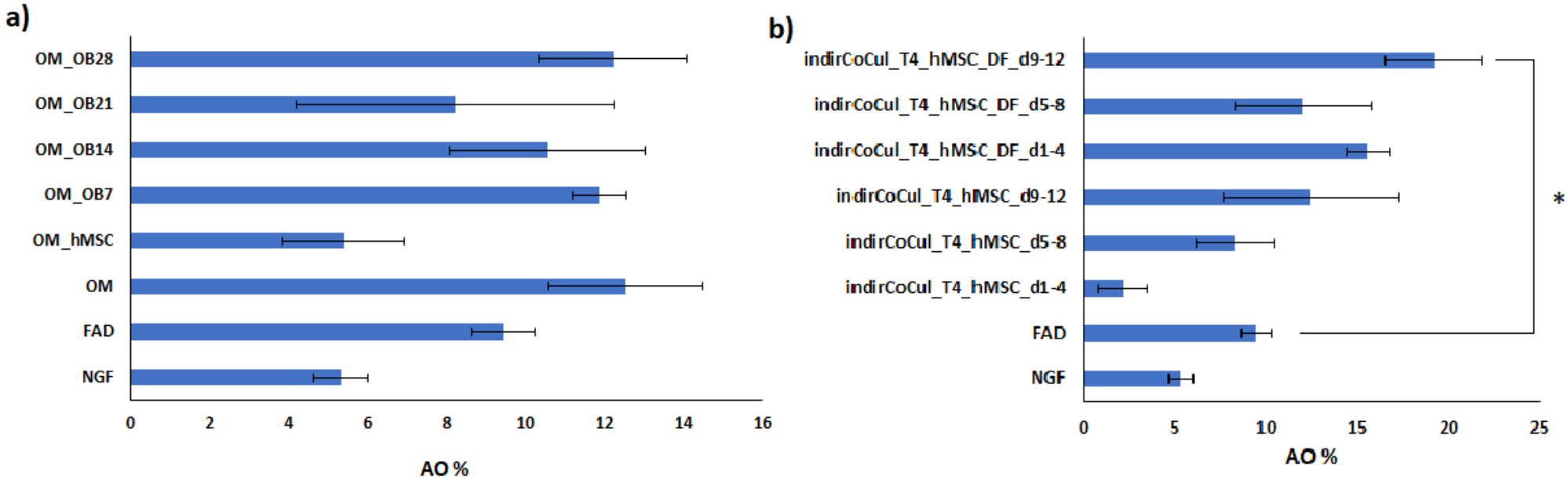

Figure XV-1 *The histograms represent the axonal outgrowth (AO) among different conditions. Bars represent the means of the percentage of axon-presenting cells on the total cell amount, error bars represent the standard deviation, and * represent the statistically significant result (p<0,05). In the histogram a is represented the effect of complete OM models on ND7/23 cells; NGF 100 ng/ml) and FAD media were used as control. In the histogram b is represented the effect of OM Co-cultivated with hMSC, with or without differentiation factors (DF) during keratinocytes differentiation; NGF 100 ng/ml) and FAD media were used as controls.*

15.1.2. Dorsal Root Ganglia

The pro-innervation potential of OM was also evaluated with primary DRGs. DRGs 23 were incubated for 72 hours with CM collected by OM models growth with or without CM derived by hMSCs, OB14, and OB28, FAD with or without differentiation factors (DF) were used as control.

Surprisingly, results were opposed to ones obtained with the immortalized cell line ND7/23. In particular, as shown by immunofluorescence images (fig XV-2 a), in which the neuronal marker β-Tubulin III is stained in red, all conditions showed a well-formed, dense and homogeneously neurite network emerging from DRG.

However, when conditions are compared with controls, a decrease raging between 2-3-fold is observed. The higher difference is noted when OM and OM_hMSC are compared with their controls FAD. These results suggest a negative effect of OM on axonal outgrowth. Nevertheless, it must be minded that innervation is a complex process regulated by a plethora of positive and negative signals. Images suggest that OM produces not only factors that inhibit the axonal outgrowth but also molecules that induce the neurite network formation (fig XV-2 b).

DRGs are not supposed to innervate the oral mucosa and this, unexpected results could support previous work (Joacher et al. 2018), which suggests the capability of the specific neuronal branches to recognise and migrate only toward the body area that they must innervate.

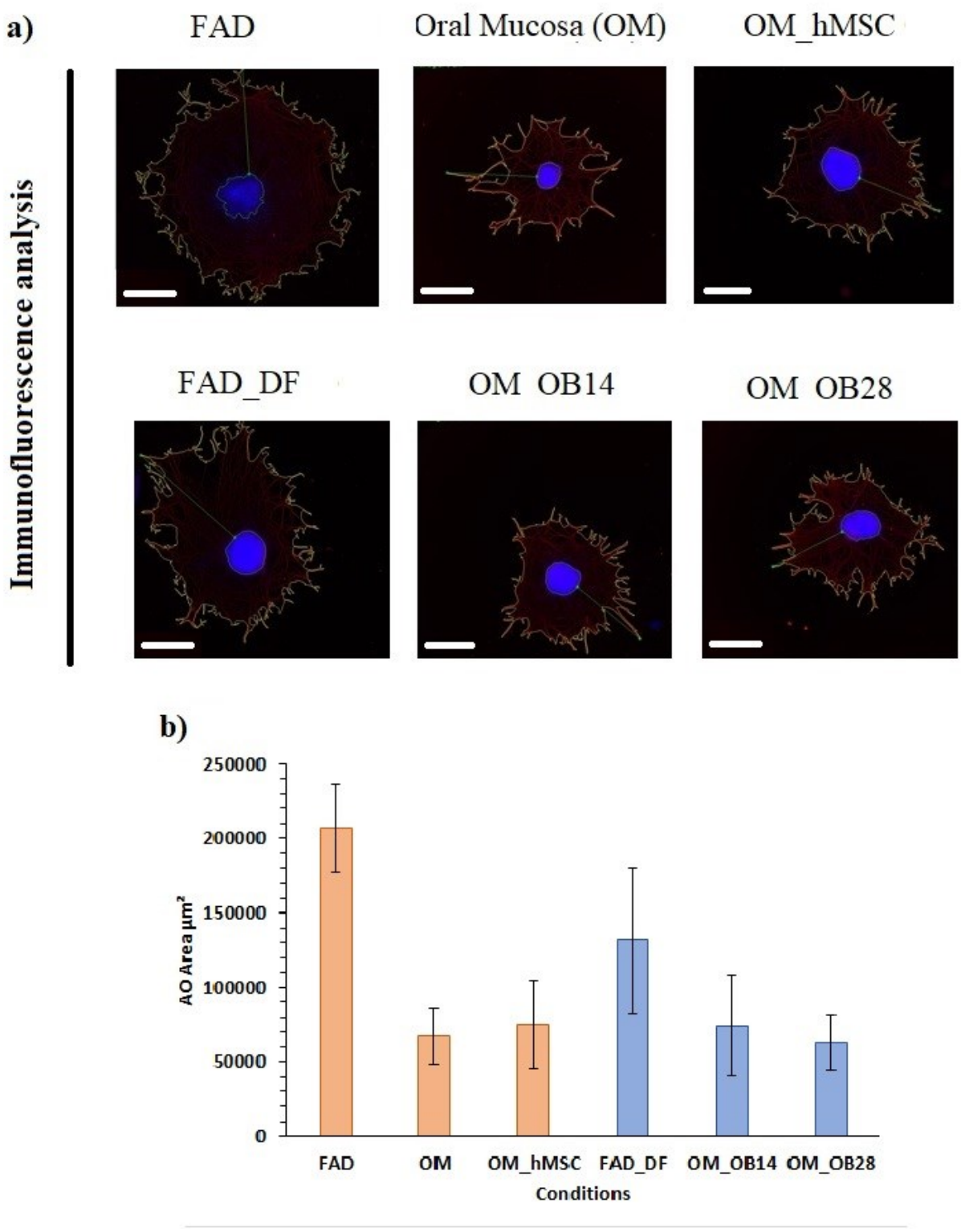

Figure XV-2 *Axonal growth quantification of embryonic dorsal root ganglion (DRG) treated with OM conditioned media or control (FAD media). The fluorescence images were acquired after staining with the antibody against β-tubulin III (red) and nuclear DAPI stain (blue). Magnification 4x, bar scale 100 µm (a). Images were quantified using Bessa et al. (2013) algorithm developed for quantification of axonal outgrowth (b).*

15.2. 3D composite model

15.2.1. Scaffold suitability:

15.2.1.1. Histological analysis

Masson Trichrome stain was used (fig XV-3 a and c) to evaluate the mucoperiosteum model morphology. As shown by the histological sections, the connective tissue adapts to the scaffold surface following the porous structures of the scaffold itself. The keratinocytes layers are less in comparison with the base models and the basal cells appear flatter than their usual morphology. However, the spinosum layer is well-formed with and thick. The keratinization was not observed.

Moreover, in the innervated model, it is possible to observe several cells migrating within the bone counterpart (fig XV-3 c and f). The migrating cells were characterized by immunofluorescence analysis and, at the interface between bone and oral mucosa, several TBR1/β-tubulin type III positive cells identified as ND7/23. However, any axonal prolongations were found despite the presence of secreted NGF within the model (fig XV-3 e)

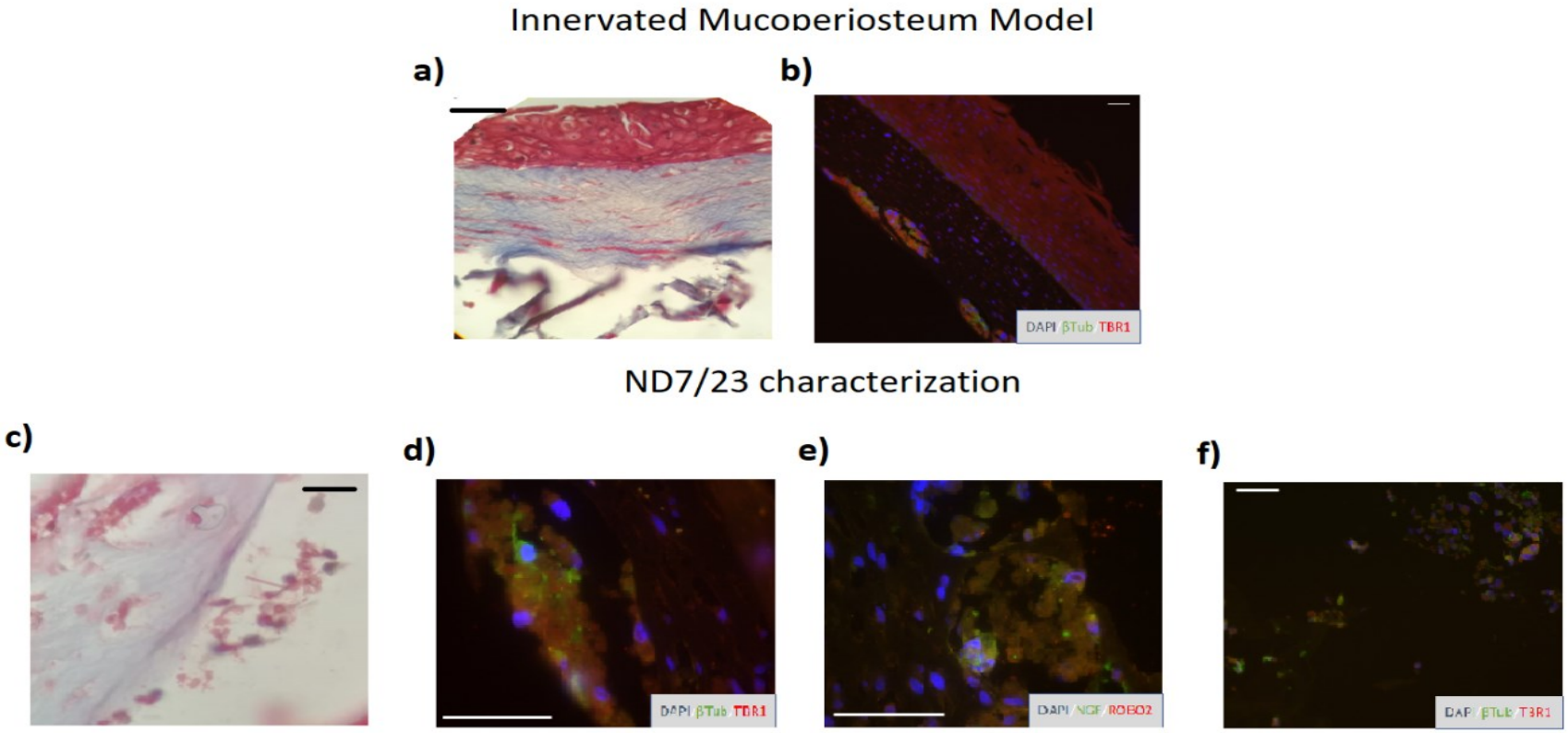

Figure XV-3 Histologies show the development of a mucoperiosteum model and an innervated mucoperiosteum model. 50 µm bar scale. a) Histological image of the mucosal counterpart of the mucoperiosteum stained with Masson Trichrome; Magnification 20x, bar scale 50 µm. b) Immunofluorescence (IF) stain of the mucosal counterpart of the mucoperiosteum stained with the fluorescent nuclear stain DAPI (blue), the neuronal transcription factor 1 (TBR1; red) and the neuronal microtubule element (β-tubulin III; green), Magnification 10x, bar scale 50 µm. c) Masson Trichrome staining ND7/23 at the hard-soft tissue interface, Magnification 20x, bar scale 50 µm. d) IF stain of ND7/23 at the hard-soft tissue interface with nuclear stain DAPI (blue), the neuronal transcription factor 1 (TBR1; red) and the neuronal microtubule element (β-tubulin III; green). e) IF of ND7/23 at the hard-soft tissue interface with the nuclear stain DAPI (blue), the neuronal guidance receptor (ROBO2; red), and neuronal growth factor (NGF; green). f) IF of ND7/23 migrated within the bone scaffold stained with the fluorescent nuclear stain DAPI (blue), the neuronal transcription factor 1 (TBR1; red) and the neuronal microtubule element (β-tubulin III; green), Magnification 40x, bar scale 50 µm.

XVI. Discussion

Oral cavity is a complex anatomical structure composed of many tissues finely interacting with each other. Mimicking this complexity remains an important challenge in tissue engineering where true biomimetic mucoperiosteum model characterized by the alveolar bone covered by the stromal tissue lined by a squamous pluristratified epithelium, has not been engineered yet as well as organotypic mucosal model including innervation.

To overcome these limitations, in the present work *i*) the behaviour of 2 different neuronal type, the immortalized ND7/23 and the primary dorsal root ganglia (DRGs) were evaluated; *ii*) a human 3D mucoperiosteum model innervated with the ND7/23.

First of all, the indirect effect of our custom-made OMs on neuronal cell types was assessed.

When applied onto the immortalized neuronal murine model, ND7/23, OM secretomes demonstrated a slight induction of axonal outgrowth. This effect was enhanced when OMs were grown in the presence of differentiated hMSC (15% axon elongation increasing) or OB28 secretome (20% axon elongation increasing). This phenomenon is particularly fascinating because, on the contrary, osteoblast conditioned media decreased axonal outgrowths.

Nevertheless, when the assay was performed onto primary dorsal root ganglia, the results obtained were controversial since OMs secretomes reduced axons elongation. As shown in figure XV-2, OM_CM and OM_hMSC_CM decrease the AO of 3,5 times in comparison with the control (FAD media).

Regarding these latter results, some considerations should be made. OM is innervated by the trigeminal ganglia (TGs) and not by the DRGs and, despite both ganglia arise from the same embryological compartment, a different behaviour between TGs and DRGs has been observed. For instance, Joacher et al. (2018) compared the response of both TGs and DRGs to typical neuronal growth factors, in presence or absence of mechanical injury; they observed differences between the two subpopulations in terms of viability and comparing the mean number of processes per neuron. Probably, this means that after axon elongation, the two subpopulations retain different receptor types and topography, which could explain a different behaviour. Considering that, is it possible that OMs showed a negative effect on DRGs but still may be innervated by specific trigeminal ganglia.

Subsequently, to conclude this analysis, the mucoperiosteum model (chapter 3) was improved with ND7/23 cells and the expression of NGF by the model itself (fig XV-3 e) suggested that the model could be fully innervated. However, the innervation protocol must be furtherly development since, despite ND7/23 appeared able to migrate in the bone counterpart (fig XV-3 d and f) and to express neuronal marker (fig. XV-3 d), the axon elongation was not observed.

Finally, to evaluate bone matrix formation, the dynamic compression test was performed on the complete model. According to the literature, osteoblasts increase the degradation rate of the fibrin gel (Noori et al., 2017); indeed, the storage modulus of the repopulated scaffold was 3 times lower than the FG coated sponge.

XVII. Bibliography

- Almela T, Al-Sahaf S, Bolt R, Brook IM, Moharamzadeh K. Characterization of Multilayered Tissue-Engineered Human Alveolar Bone and Gingival Mucosa. Tissue Eng Part C Methods. 24(2):99-107. (2018) doi: 10.1089/ten.TEC.2017.0370.
- Almela T, Al-Sahaf S, Brook IM, Khoshroo K, Rasoulianboroujeni M, Fahimipour F, Tahriri M, Dashtimoghadam E, Bolt R, Tayebi L, Moharamzadeh K. 3D printed tissue engineered model for bone invasion of oral cancer. Tissue Cell. 52:71-77. (2018) doi: 10.1016/j.tice.2018.03.009.
- Almela T, Brook IM, Moharamzadeh K. Development of three-dimensional tissue engineered bone-oral mucosal composite models. J Mater Sci Mater Med. 27(4):65. (2016) doi: 10.1007/s10856-016-5676-7.
- Bernick S. Innervation of teeth and periodontium after enzymatic removal of collagenous elements. Oral Surg Oral Med Oral Pathol. 10(3):323-32. (1957)
- Bessa S, Quelhas P, Amaral IF, Sanches JM, Mico ´ L, Cardoso JS. Automatic Quantification of Cell Outgrowth from Neurospheres. Pattern Recognition and Image Analysis: 6th Iberian Conference, IbPRIA Springer Berlin Heidelberg; 141–8. (2013) doi: 10.1007/ 978-3-642-38628-2_16
- Blais M, Mottier L, Germain MA, Bellenfant S, Cadau S, Berthod F. Sensory neurons accelerate skin reepithelialization via substance P in an innervated tissue-engineered wound healing model. Tissue Eng Part A. 20(15-16):2180-8. (2014) doi: 10.1089/ten.tea.2013.0535.
- Egea J, Klein R. Bidirectional eph-ephrin signaling during axon guidance. Trends Cell Biol. 17(5):230–238. (2007) doi:10.1016/j.tcb.2007.03.004
- Goto T, Kido MA, Yamaza T, Tanaka T. Substance P and substance P receptors in bone and gingival tissues. Med Electron Microsc. 34(2):77-85. (2001)
- Jimenez-Rojo L, Granchi Z, Graf D, Mitsiadis TA. Stem cell fate determination during development and regeneration of ectodermal organs. Front Physiol. 3:107. (2012) doi:10.3389/fp hys.2012.00107
- Jocher G, Mannschatz SH, Offterdinger M, Schweigreiter R. Microfluidics of Small-Population Neurons Allows for a Precise Quantification of the Peripheral Axonal Growth State. Front Cell Neurosci. 15;12:166. (2018) doi: 10.3389/fncel.2018.00166
- Kandel R, Schwartz JH, Jessell TM Principles of neural science, 4th edn. McGraw-Hill, New York. (2000)
- Kuchler-Bopp S, Bécavin T, Kökten T, Weickert JL, Keller L, Lesot H, Deveaux, E, Benkirane-Jessel N. Three-dimensional Micro-culture System for Tooth Tissue Engineering. J Dent Res. 95(6):657-64. (2016) doi: 10.1177/0022034516634334.
- Kulterer B, Friedl G, Jandrositz A, Sanchez-Cabo F, Prokesch A, Paar C, Scheideler M, Windhager R, Preisegger KH, Trajanoski Z. Gene expression profiling of human mesenchymal stem cells derived from bone marrow during expansion and osteoblast differentiation. BMC Genomic. 8:70. (2007). doi: 10.1186/1471-2164-8-70
- Lai wing Sun K, Correia JP, Kennedy Te. Netrins: versatile extracellular cues with diverse functions. Development. 138(11):2153–2169. (2011) doi:10.1242/dev.044529 9.
- Lebonvallet N, Boulais N, Le Gall C, Pereira U, Gauché D, Gobin E, Pers JO, Jeanmaire C, Danoux L, Pauly G, Misery L. Effects of the re-innervation of organotypic skin explants on the epidermis. Exp Dermatol. 21(2):156-8 (2012) doi: 10.1111/j.1600-0625.2011.01421.
- Lebonvallet N, Pennec JP, Le Gall-Ianotto C, Chéret J, Jeanmaire C, Carré JL, Pauly G, Misery L. Activation of primary sensory neurons by the topical application of capsaicin on the epidermis of a re-innervated organotypic human skin model. Exp Dermatol. 23(1):73-5. (2014). doi: 10.1111/exd.12294.
- Noori A,Ashrafi SJ, Vaez-Ghaemi R, Hatamian-Zaremi A, Webster TJ. A review of fibrin and fibrin composites for bone tissue engineering. Int J Nanomedicine. 12: 4937–4961. (2017). doi: 10.2147/IJN.S124671
- Pagella P, Jimenez-Rojo L, Mitsiadis TA. Roles of innervation in developing and regenerating orofacial tissues. Cell. Mol. Life Sci. 71(12):2241-51. (2014). doi 10.1007/s00018-013-1549-0
- Raper J, Mason C. Cellular strategies of axonal pathfinding. Cold Spring Harb Perspect Biol. 2(9):a001933. (2010) doi:10.1101/cshperspect.a001933
- Reichardt LF. Neurotrophin-regulated signalling pathways. Philos Trans R Soc Lond B Biol Sci. 361(1473):1545– 1564. (2006). doi:10.1098/rstb 2006.1894

- Roggenkamp D, Köpnick S, Stäb F, Wenck H, Schmelz M, Neufang G. Epidermal nerve fibers modulate keratinocyte growth via neuropeptide signaling in an innervated skin model. J Invest Dermatol. 133(6):1620-8. (2013). doi:10.1038/jid.2012.464.
- Wang S, Ghezzi CE, Gomes R, Pollard RE, Funderburgh JL, Kaplan DL. In vitro 3D corneal tissue model with epithelium, stroma, and innervation. Biomaterials. 112:1-9. (2017). doi: 10.1016/j.biomaterials.2016.09.030.

XVIII. Conclusion and future perspective

In the present work, the regulatory role of the mesenchymal tissue onto epithelial was evaluated. Indeed, from the literature, it is well known that, accordingly to the position, keratinocytes follow different differentiative fates. Still, the microenvironment is not enough to induce the specific keratinized fate and the correct gene expression.

Moreover, accordingly to 3Rs law, to limits the use of animal models for implant validation, a better knowledge of the relationship between hard and soft tissue and a new model able to mimic this interaction was needed.

To assess the role of mesenchymal stem cells hMSCs in an undifferentiated condition and under osteogenic toward keratinocytes behaviour, we developed a home-made organotypic 3D oral mucosa (OM) cultures. The 3D model was treated with the conditioned media (CM) of hMSC, and hMSC derived osteoblast (OB) at for stage of differentiation (OB7, OB14, OB21, OB28) and the first results showed that during the differentiation hMSC produce and secrete factors that induce the keratinization and the expression of the marker of differentiation CK10; in particular in the middle stage of differentiation (OB14). This finding may impact the design of new implantable devices able to induce, alone, the epithelial growth and keratinization to improve implant graft avoiding epithelial graft linked to the morbidity of another zone.

This effect was also confirmed in the indirect co-cultivation of hMSC and OM in the presence or absence of the osteogenic condition. Indeed, the osteogenic stains showed that OM mediates and improve the effect of pro-osteogenic factors, inducing the bone phenotype within 12 days of cocultivation (instead of 28) and that, this phenotype, upregulate the CK10 expression by OM.

To elucidate the mechanism that may drive this effect, we investigated 55 proteins that were found in the secretomes, and we found differences trough the hMSC differentiation in 40 of them. One of them was already showed to be important in skin re-epithelialization and, in general, in keratinocytes proliferation and migration. Indeed, this factor secretion increase during the differentiation in a statistically significant way ($p<0,001$). Remarkably, this increase is retained when the hMSC are differentiated within a 3D porous scaffold. However, further studies with a purified protein are needed to confirm the role of KGF in the observed phenotype.

In the present work, we also showed that OM might have a pro-innervation effect, at least during the last stages of keratinocytes stratification. However, the correct primary models, the Trigeminal ganglia (TGs), was not yet available. Another interesting perspective in this work would be the evaluation of OM effect onto different TG branches.

This data offers the evidence that OM model may also be used as valuable tools to analyse the mechanism which drove specific ganglion branches toward the correct body site.

Finally, an innovative tool for biomaterial evaluation was produced. Indeed, a mucoperiosteum model, able to mimic the features of the bone-mucosa structures and with an integrative and functional cross-talk, confirmed by the

improvement of the mechanical properties of the bone growth in direct co-cultures with the OM in comparison with the bone model alone, is presented for the first time. This model, which already present unique features, have been studied to allow further development, such as vascularization or integration with the immune system since the porous structures is suitable to sustain vessel formation and the absence of elements, such the chitosan, known to modulate immune system behaviour, would allow a physiological behaviour of both innate (i.e., monocytes or macrophages) or adaptative (i.e., lymphocytes) immune cells. This latter characteristic makes this model suitable for co-cultures with both commensal and pathogenic bacteria allowing the studies onto the antibacterial properties of studied materials.

XIX. Abbreviation list

ALP: alkaline phosphatase

AR: Alizarine Red

B-27: B27 Serum-Free Supplement 1

BM: bone marrow

BMPs: bone morphogenetic proteins

BTC/nHA: bovine tendon collagen/nano-hydroxyapatite

CK: cytokeratin

CM: conditioned medium

DED: De-epidermalized dermis

DFs: osteogenic/differentiation factors

DMA: Dynamical mechanical analysis

DMEM: Dulbecco's modified Eagle medium

DPMSCs: dental pulp hMSC

DRG: dorsal root ganglia

E': Storage modulus

EC: European Commission

ECM: extracellular matrix

EDC: 1-Ethyl-3-(3-dimethylaminopropyl) carbodiimide

EGF: epidermal growth factor

EMILIN: fibulins and elastin microfibril Interface Located Protein

F12: Ham's F-12 medium

FAD: DMEM/F12

FBS: foetal bovine serum

FCS: foetal calf serum

FDU: 5-fluoro-2'-deoxy- uridine

FG: fibrin gel

FGF-7 or KGF: fibroblast growth factor-7

FN: fibronectin

GVHD): graft versus host disease

HB-EGF: heparin-binding EGF-like growth factor

HBSS: Hank's balanced salt solution

HDF: human dermal fibroblast

HE: Haematoxylin and eosin stain

HGF: human gingival fibroblast

HLA (human leucocyte antigen)

HOK: Human Oral Keratinocytes

IL-1: interleukin-1

ITGβ1: integrin β1

JE: junctional epithelium

KGF: keratinocytes growth factor

KHG: keratohyalin granules

MAGPs: microfibril associated glycoproteins

MMPs: metalloproteinase

MSC-derived osteoblast (OB)

MSCs: mesenchymal stem cells

NGFR: Nerve growth factor receptor

NHS: N-Hydroxysuccinimide

OB7: hMSCs under osteogenic condition for 7 days

OB14: hMSCs under osteogenic condition for 14 days

OB21: hMSCs under osteogenic condition for 21 days

OB28: hMSCs under osteogenic condition for 28 days

OE: oral epithelium

OM: oral mucosa

O-MSCs: oral mesenchymal stem cells

OSE: oral sulcular epithelium

PDL1: programmed death ligand 1

PEN/Strep: penicillin and streptomycin

PF: pulp fibroblasts

PIE: peri implant epithelium

PISE: peri-implant sulcular epithelium

PKC: protein-kinase C

PPAR-γ: peroxisome proliferator-activated receptor-gamma

RT: room temperature

RTC: rat tail collagen

SAMs: substrate adhesion molecules

SEM: scanning electron microscopy

TAF: tumour-associated fibroblast

Tan delta: loss factor

TE: tissue engineering

TGF: Tansforming growth factors

Th17: T regulatory cells

VK: Von Kossa

XX. Figure Index

XXI. Table Index

XXII. Acknowledgement

Firstly, I would like to express my sincere gratitude to my advisor Prof. Lia Rimondini for the support of my Ph.D study and her guidance during the writing of this thesis.

My sincere thanks also go to Prof. Meriem Lamghari and to her group (Luis, Estrela, Francisco, Teresa, Juliana, Daniela, Ines and Catarina) who welcomed me in their lab and provided me the opportunity to improve as a person and as a researcher. Without their precious support and advices most results of the present work would not exist.

I am grateful to prof. Barbara Azzimonti who introduced me to the "magic world of science" and kept supporting me during my research, despite everything.

I thank my fellow labmates (Manuela, Diletta, Giulia, Vera, Alessia, Andrea, Soni and Gaia) and for sharing with me the lowest and the high of the last four years.

Also, I thank my friends within the department, and in particular the immunology lab (Nausicaa, Luca and Elena) who always gave me a place to hide and exchange joke and gossip when needed and the physiology/dermatology lab (Serena, Lara and Patrizia) who were always ready to offer tea, biscuits and laughs.

Last but not the least, I would like to thank my family (my parents and my brothers) and my friends (Mariangela, Hanka and Alice) for supporting (and put up with) me throughout the craziness of the (lab) life.